

University of Groningen

## Chemical analysis of the Fornax dwarf galaxy

Letarte, Bruno

**IMPORTANT NOTE:** You are advised to consult the publisher's version (publisher's PDF) if you wish to cite from it. Please check the document version below.

*Document Version*

Publisher's PDF, also known as Version of record

*Publication date:*

2007

[Link to publication in University of Groningen/UMCG research database](#)

*Citation for published version (APA):*

Letarte, B. (2007). *Chemical analysis of the Fornax dwarf galaxy*. [Thesis fully internal (DIV), University of Groningen]. [s.n.].

### Copyright

Other than for strictly personal use, it is not permitted to download or to forward/distribute the text or part of it without the consent of the author(s) and/or copyright holder(s), unless the work is under an open content license (like Creative Commons).

The publication may also be distributed here under the terms of Article 25fa of the Dutch Copyright Act, indicated by the "Taverne" license. More information can be found on the University of Groningen website: <https://www.rug.nl/library/open-access/self-archiving-pure/taverne-amendment>.

### Take-down policy

If you believe that this document breaches copyright please contact us providing details, and we will remove access to the work immediately and investigate your claim.

Downloaded from the University of Groningen/UMCG research database (Pure): <http://www.rug.nl/research/portal>. For technical reasons the number of authors shown on this cover page is limited to 10 maximum.

# Chapter 6

## A high resolution spectroscopic study of Fornax Field Stars

paper in preparation\*

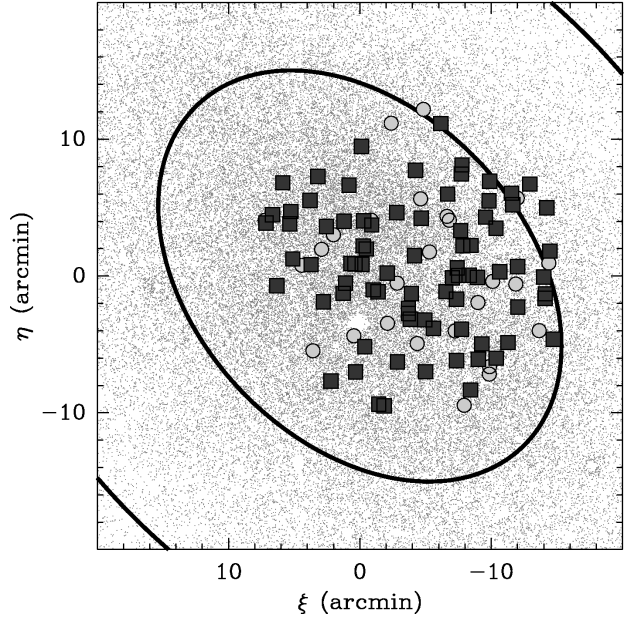
**B. Letarte, V. Hill, E. Tolstoy, and DART**

**ABSTRACT**— In this chapter, we present the results of our high resolution abundance analysis of 81 individual stars in the central region of Fornax. Using the FLAMES/GIRAFFE spectrograph on the VLT, we obtained high resolution ( $R \sim 20\,000$ ) spectra for 81 Red Giant Branch stars in the central  $25'$  of the Fornax dSph (see chapter 4 and Table 4.3 for a description of the observations). Chapters 3 and 4 describe the methods we used to determine abundances, and in this chapter we present the sample selection and discuss the abundances that we have obtained, including  $\alpha$ -elements (Mg and Ca, Si, Ti, O), iron-peak (Fe, Ni and Cr) and heavy (Y, Ba, Eu, La and Nd) elements. This is consistent with the fact that we randomly selected our sample from the RGB and that the more metal rich stars are centrally concentrated (e.g. Battaglia et al. 2006). We compare our results with Milky Way (MW) studies, and to recent VLT/UVES abundance determinations of nine individual stars in Fornax globular clusters (chapter 5 and Letarte et al. 2006) and to the Sculptor dSph (Hill et al. in prep). Fornax stars are found to have unusually low  $\alpha$ -elements ratios, as well as Ni and Na abundances. The role of metal poor AGB in the creation of  $s$ -process elements is clearly seen by our high  $[\text{Ba}/\text{Y}]$  compared to the Milky Way.

---

\* Based on FLAMES observations collected at the European Southern Observatory, proposal number 171.B-0588

**Figure 6.1:** The spatial distribution of the HR spectroscopic targets in the central region of Fornax. The squares are stars for which we have successfully derived abundances and circles for those that were rejected during our analysis. The ellipses represent  $R_c$ , the core radius and  $2 R_c$  (Battaglia et al. 2006).



## 6.1 Sample selection

As first illustrated in Figure 1.3 in chapter 1, our FLAMES HR survey covers the central  $25'$  region, see Figure 6.1. The radial velocities of our targets are presented in chapter 4, Table 4.4, and the coordinates and photometrically determined  $T_{\text{eff}}$  of individual stars are presented in Table 4.A3. Our 107 spectroscopic targets are represented by squares and circles; the squares for stars for which we obtained reliable abundances and the circles for those that were rejected during our analysis. Stars were rejected for various reasons: their  $V_{\text{rad}}$  suggested that they are not members of Fornax (1 star); velocity offsets in spectra taken at different times making it impossible to stack the different exposures (possibly these are binary stars, 8 stars); or the  $[\text{Fe}/\text{H}]$  coming from different lines were too scattered to perform a conclusive analysis because they are not RGB stars (possibly foreground dwarfs) and/or have a too low signal to noise (17 stars).

Figure 6.2 shows a Colour Magnitude Diagram of a circular region of  $10'$  radius in the centre of Fornax, matching the FLAMES field of view, on which we identify our targets, including the rejected ones. As can be seen, we selected our stars to include the entire RGB colour range, going as far to the blue and red side as possible and thus (hopefully) the entire age and metallicity range. We cross-correlated our potential target list with known carbon stars\* in Fornax so we could minimise the number of AGB stars that we would observe. Still, we were expecting that the bluest and reddest stars might be foreground dwarf or AGB stars but we are confident we didn't exclude extremely metal poor stars through our sample selection and subsequent analysis. This is supported by our single metal poor star BL085 at  $[\text{Fe}/\text{H}] = -2.58$  which was analysed without any problems.

\* We are grateful to Serge Demers for providing us with his list

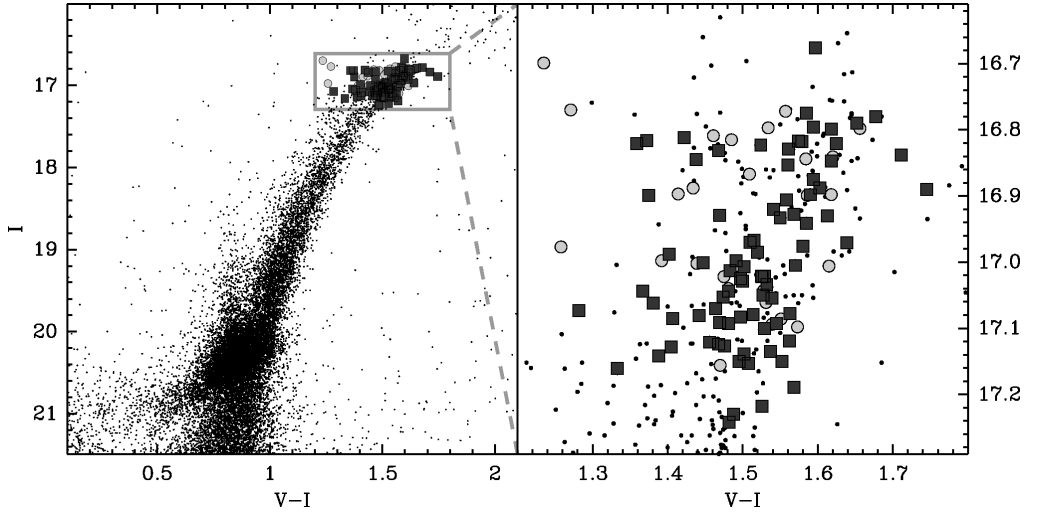


**Figure 6.2:** A CMD of the FLAMES field of view in the centre of Fornax coming from our WFI data. Our spectroscopic targets are represented by squares for stars for which we were able to determine abundances and circles for those that were rejected during our analysis.

## 6.2 Results

In this section, we present the abundance ratios for the 81 stars which survived the selection process described in section 6.1. The stellar parameters we assigned to each star, following the method presented in chapter 4 can be found in Table 6.A1. The line list used, along with the measured *EW*s for each star (for every element) can be found in Table 6.A2 and all the abundance ratios used throughout this chapter are listed in Table 6.A3.

### 6.2.1 Iron abundance

One of the most straightforward results is an accurate determination of the iron abundance,  $[\text{Fe}/\text{H}]$ , which in our case is derived from  $\sim 40+$  lines per star. We present our  $[\text{Fe}/\text{H}]$  distribution in Figure 6.3 and compare it to the distribution of Battaglia et al. (2006), where they used low resolution ( $R = 6500$ ) Ca II triplet measurements to determine  $[\text{Fe}/\text{H}]$ . Our distribution peaks sharply at  $[\text{Fe}/\text{H}] \simeq -0.8$  and is clearly skewed towards more metal rich stars. There are a few stars outside the main distribution (on the metal poor side) but the centre of Fornax is clearly dominated by stars with  $[\text{Fe}/\text{H}] > -1$ . However, we still sample two orders of magnitude in  $[\text{Fe}/\text{H}]$ , from  $-2.5 \lesssim [\text{Fe}/\text{H}] \lesssim -0.5$ .

As seen in Figure 1.3 (chapter 1), our FLAMES field included Fornax globular cluster 4 but there is no sign that our field sample includes any star from GC 4. This can be seen from the spatial distribution and abundance measurements. The single, really metal poor star we have in our sample ( $[\text{Fe}/\text{H}] \simeq -2.5$ ) is the only star to overlap with Fornax

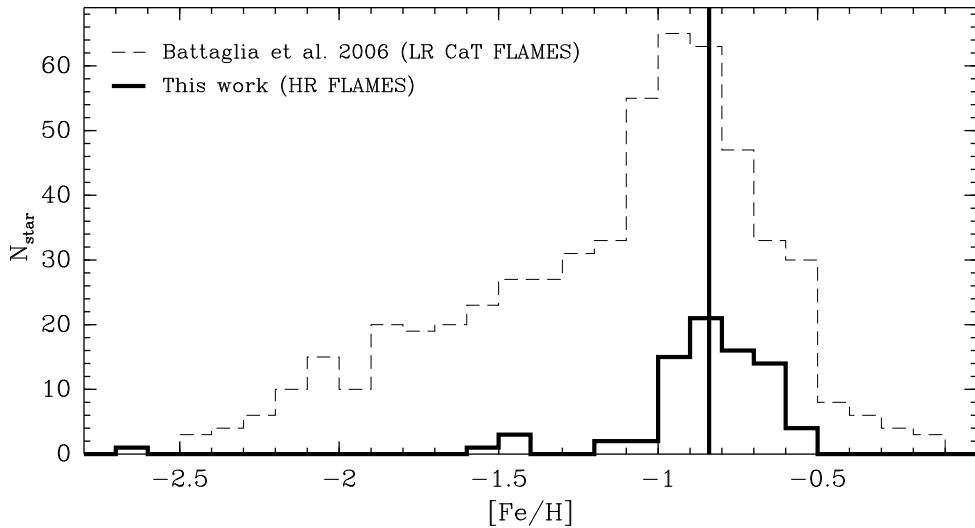


**Figure 6.3:** The  $[\text{Fe}/\text{H}]$  distribution of our Fornax sample (solid line) of stars, with a peak at  $[\text{Fe}/\text{H}] \approx -0.8$ , richer than the sample of Battaglia et al. (2006) (dashed line).

GCs metallicity range and it is not spatially close to GC 4. Therefore, it seems likely that it is a metal poor field star, the only representative of Fornax oldest population in our field star sample.

### 6.2.2 Alpha Elements

The evolution of chemical abundances in a galaxy is linked to its star formation history, SFH, (e.g. Tinsley 1979; Pagel 1997) and the  $[\alpha/\text{Fe}]$  ratio is a useful tool to study this evolution. Alpha elements, which include Calcium (Ca), Magnesium (Mg), Titanium (Ti) Oxygen (O) and Silicon (Si) are predominantly produced by high mass, ( $> 8 \mathcal{M}_{\odot}$ ) short lifetime Type II supernovae explosions (SNe II). The ratio  $[\alpha/\text{Fe}]$  is a way of tracing the relative contribution of SN II and SN Ia products that were available when the star formed. Lower mass SNe II ( $8-12 \mathcal{M}_{\odot}$ ) result in lower yields than more massive SNe II (Woosley & Weaver 1995). The stars that form after the ISM has been enriched by a SNe II event should have an enhanced  $[\alpha/\text{Fe}]$  while those that form after the SNe Ia have started to contribute significant amounts of Fe to the ISM should have a lower  $[\alpha/\text{Fe}]$ .

The  $[\text{Fe}/\text{H}]$  at which the  $[\alpha/\text{Fe}]$  ratio starts decreasing (the “knee”) in a galaxy depends on several factors: the SFH; the initial mass function (IMF); the time it takes for the first SN Ia to explode and the time it takes for the mixing of SNe Ia and SNe II products back into the ISM (e.g. Matteucci 2003). The arrival of the first SN Ia should be *constant in age* (commonly believed to happen after  $\sim 1$  Gyr) for all galaxies since it’s the result of the binary interaction between two *evolved* stars. The higher in  $[\text{Fe}/\text{H}]$  this “knee” occurs, the more efficient the system was at enriching its gas before the arrival of the first SNe Ia. A plateau is reached when (presumably) there is balance between the contribution of SNe II and SNe Ia.

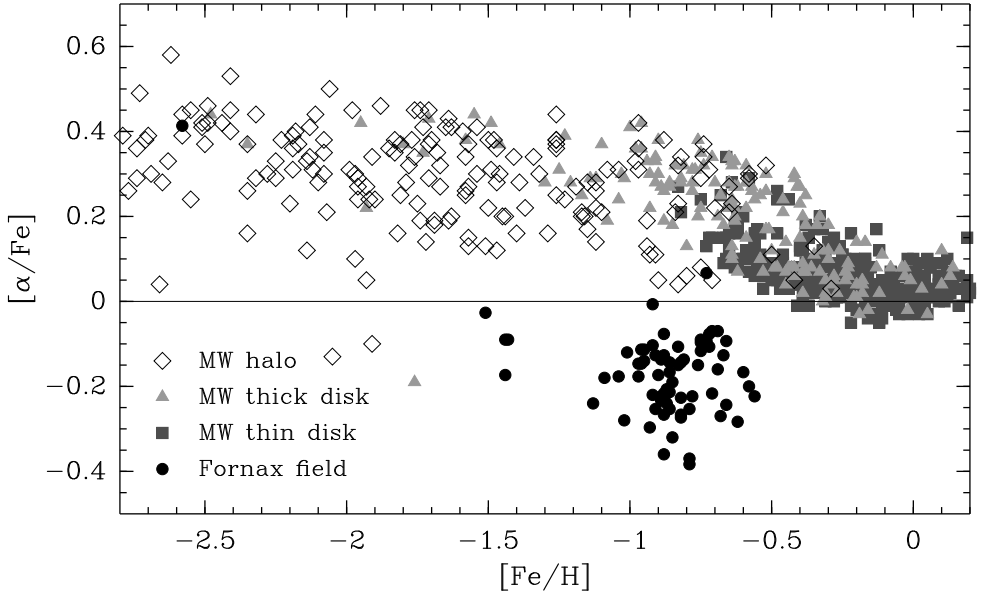


**Figure 6.4:**  $[\alpha/\text{Fe}]$  as a function of  $[\text{Fe}/\text{H}]$ . We computed  $\alpha$  as the average of Mg, Ca and TiI abundances. The Milky Way points were taken from the compilation of Venn et al. (2004), with different symbols for thin disk (dark grey squares), thick disk (light grey triangles), halo (empty diamonds) stars and our Fornax Field star results (black circles). In subsequent plots in this chapter, there will be no distinction between the MW components, for clarity.

In the Milky Way,  $\alpha$ -elements are typically overabundant in GCs and metal poor halo stars relative to disk stars. To obtain an average measure of  $\alpha$ -element abundance, the average of Mg, Ca and Ti is taken and is shown in Figure 6.4, where we compare MW halo, thin and thick disk stars to Fornax Field stars. It is obvious from Figure 6.4 that our  $[\alpha/\text{Fe}]$  are significantly underabundant compared to the MW at the same  $[\text{Fe}/\text{H}]$ , a sign that the evolutionary history of is Fornax is significantly different from the MW. Note that the Milky Way stars in the  $[\text{Fe}/\text{H}]$  range of Fornax are a mix of halo, thin and thick disk stars, a population possibly not as uniform as what we might expect from the centre of a dwarf galaxy like Fornax. A simple comparison in  $[\text{Fe}/\text{H}]$  of Fornax versus the MW does not take into account the different evolutionary processes in the MW different components, but it is obvious that Fornax does not overlap with any part of the MW.

Individual  $[\alpha/\text{Fe}]$  ratios are presented in Figure 6.5 ( $[\text{Mg}/\text{Fe}]$ ,  $[\text{Si}/\text{Fe}]$  and  $[\text{Ca}/\text{Fe}]$ ) and Figure 6.6 ( $[\text{Ti I}/\text{Fe}]$  and  $[\text{Ti II}/\text{Fe}]$ ). Along with our Fornax GC and MW points, we introduce the eight peculiar\* halo stars observed by Nissen & Schuster (1997) (NS97). These stars were found to display low  $[\alpha/\text{Fe}]$  and  $[\text{Ni}/\text{Fe}]$  (along with other chemical peculiarities) when compared to normal MW halo stars, and this has been suggested that they might have been accreted by the MW from a dwarf galaxy.

\* These stars have unusual kinematics and orbital parameters: large maximum distance from the Galactic centre ( $R_{\text{max}}$ ) and large distance from the Galactic plane ( $z_{\text{max}}$ ).

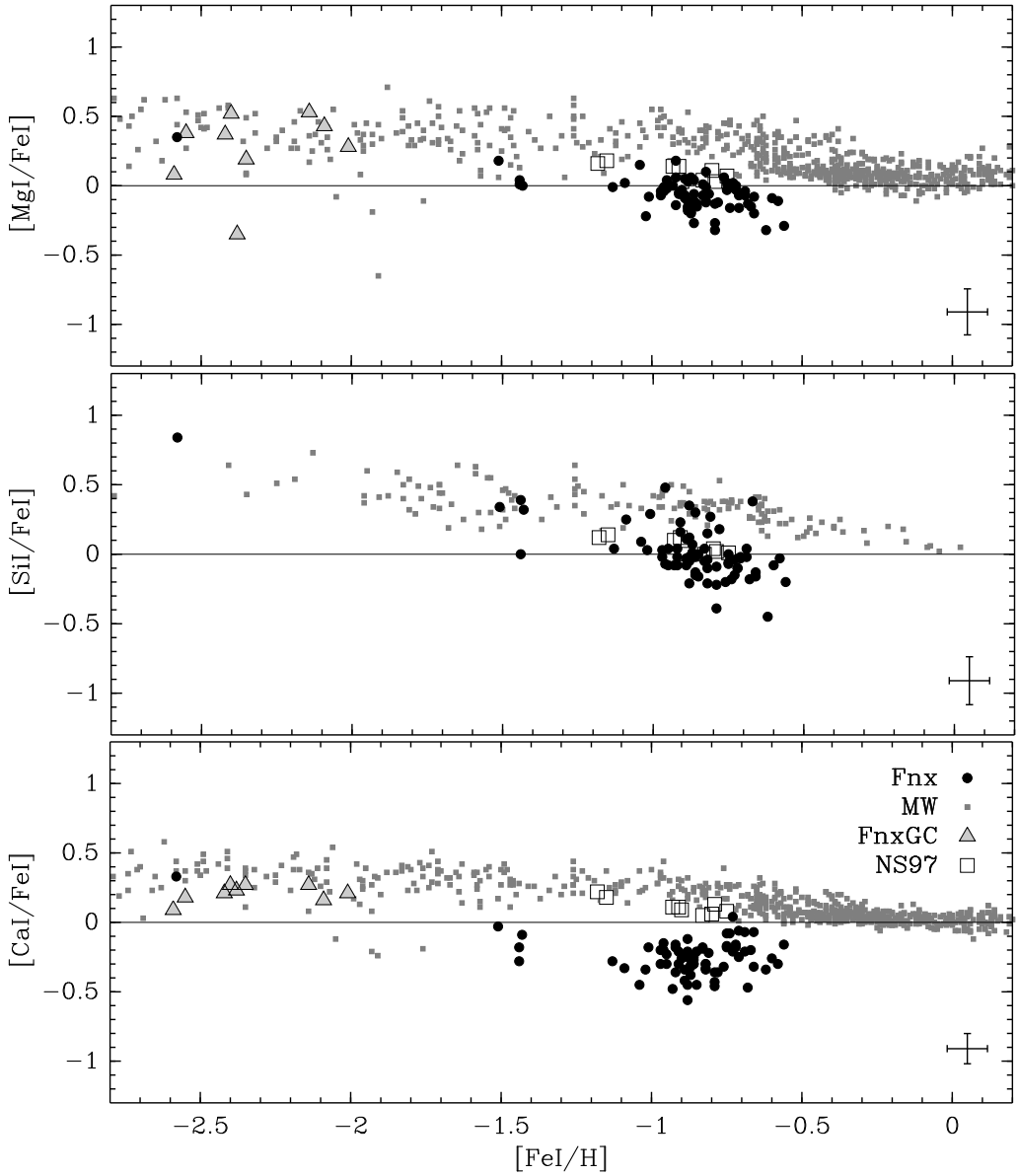


**Figure 6.5:**  $[\text{Mg}/\text{Fe}]$ ,  $[\text{Si}/\text{Fe}]$  and  $[\text{Ca}/\text{Fe}]$  as a function of  $[\text{Fe}/\text{H}]$ . The Fornax field stars are plotted as solid circles, the galactic stars of Venn et al. (2004) as small grey squares, the Fornax globular clusters of chapter 5 as triangles and the eight peculiar halo stars from Nissen & Schuster (1997) as empty squares. There is a representative (average) error bar for the Fornax field star abundances in the bottom right corner of each panel. This is the quadratic sum of  $[\text{element}/\text{H}] + [\text{Fe}/\text{H}]$ , (measurement errors) taken from Table 6.A3. The same axis scale will be used for every  $[\text{element}/\text{Fe}]$  vs  $[\text{Fe}/\text{H}]$  plots presented in this chapter, for easy comparison.

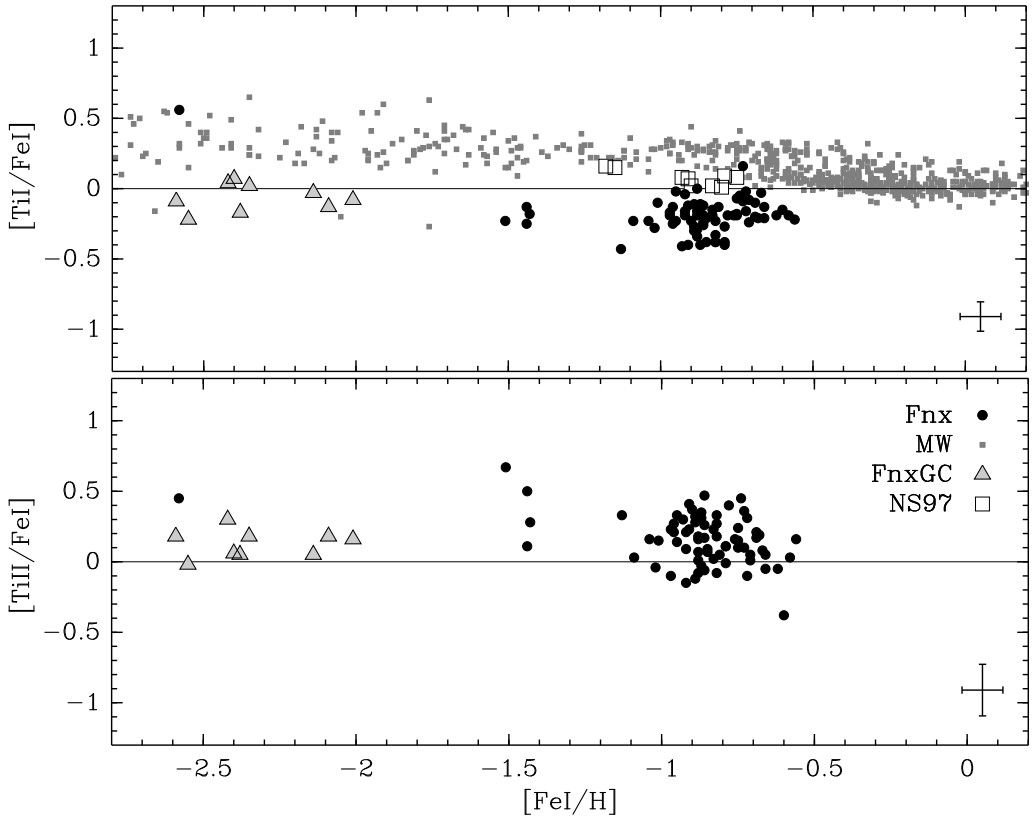


**Figure 6.6:**  $[\text{Ti I}/\text{Fe I}]$  and  $[\text{Ti II}/\text{Fe I}]$  as a function of  $[\text{Fe I}/\text{H}]$ . Symbols are defined in Figure 6.5.

It can be seen from Figure 6.5 that globally, the metal poor star and the GCs of Fornax show a typical overabundance in  $\alpha$ -elements but as the  $[\text{Fe}/\text{H}]$  increases,  $[\alpha/\text{Fe}]$  decreases, reaching a significant underabundance for the highest metallicities. The  $[\text{Mg}/\text{Fe}]$  are typically close to zero, lower than Galactic stars by at least 0.2 to 0.5 dex and the highest values just overlap NS97. The  $[\text{Ca}/\text{Fe}]$  ratios are globally lower than other  $\alpha$ -elements, especially for the handful of stars close to  $[\text{Fe}/\text{H}] = -1.5$ . At higher metallicity ( $[\text{Fe}/\text{H}] \gtrsim -0.7$ ), our  $[\text{Ca}/\text{Fe}]$  ratios seems to increase, as if the balance in SN II/SN Ia has been broken and suddenly there was less contribution from SN II, which seems unlikely, since Ca is the only element for which we notice such behaviour. The  $[\text{Si}/\text{Fe}]$  ratios are the highest for the  $\alpha$ -elements (if we do not consider Ti II, which will be discussed later), with a mean value close to zero. The  $[\text{Si}/\text{Fe}]$  in Fornax agree with the eight peculiar halo stars of NS97, the only  $\alpha$ -element for which this is clearly the case.

In our  $T_{\text{eff}}$  range, ( $\lesssim 4400$  K) atoms of Ti and O can be trapped in molecules, like TiO and CO, artificially lowering our derived abundances. This is not a problem in hotter atmospheres, where the the molecules will always be broken up into their atomic form. We have tested the influence of molecules on atomic abundances by using a line forma-



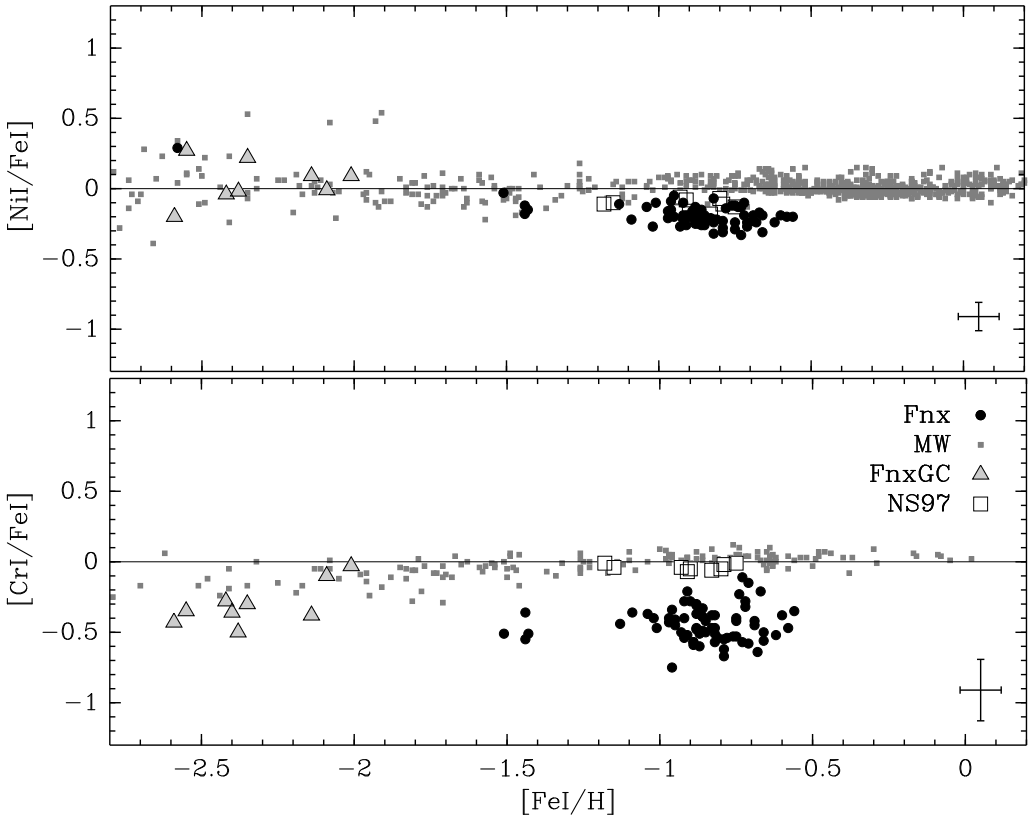


**Figure 6.7:** Iron peak elements in Fornax,  $[\text{Ni}/\text{Fe}]$  and  $[\text{Cr}/\text{Fe}]$  as a function of  $[\text{Fe}/\text{H}]$ . Symbols are defined in Figure 6.5.

tion code that takes molecules into account\* to derive our abundances and compare these with our standard analysis. We chose stars to cover the  $T_{\text{eff}}$  range of the Fornax field stars.

We observed a significant difference ( $\sim 0.3$  dex) in our O/H ratios, confirming that at this  $T_{\text{eff}}$ , there is a significant fraction of oxygen locked in the form of CO. The O abundance is not only affected by molecules, but it also has a problem with the lines used for this analysis. They are two O lines in our wavelength range, the forbidden line at  $6300 \text{ \AA}$  and another one at  $6363 \text{ \AA}$ . The more reliable line at  $6300 \text{ \AA}$  is not suitable for Fornax stars as the typical  $V_{\text{rad}}$  means this matches a telluric absorption line, rendering it unusable for most of our stars. The second one is a very weak line, falling in a region that is affected by a Ca I auto-ionisation broad feature at  $6362 \text{ \AA}$ , and would deserve much more attention than could be awarded in the course of this thesis, to provide an accurate O abundance indicator.

\* TURBOSPECTRUM (Alvarez & Plez 1998), used in the plane-parallel approximation

In contrast to oxygen, we found that Ti abundances are typically *not* affected by the amount of Ti locked in the form of TiO. However, it can be seen from Figure 6.6 that  $[\text{Ti I}/\text{Fe}]$  is quite different from  $[\text{Ti II}/\text{Fe}]$ , a sign that there are significant non-LTE effects, affecting more Ti I abundances (since most of the Ti I lines have a low  $\chi_{\text{ex}}$ ) than Ti II. However, our Ti I abundances are statistically more reliable than Ti II, since Ti I was calculated using on average  $\sim 8$ -9 lines compared to only  $\sim 2$ -3 lines for Ti II. This is reflected in the much larger error bars on Ti II. If we consider only Ti I, its behaviour is similar to a typical  $\alpha$ -element like Ca or Mg.

### 6.2.3 Iron peak elements

According to nucleosynthetic predictions, iron peak elements like Iron (Fe), Chromium (Cr), and Nickel (Ni) are believed to be formed predominantly from explosive nucleosynthesis, in SN Ia (Iwamoto et al. 1999; Travaglio et al. 2005). In Figure 6.7, we present the  $[\text{Ni}/\text{Fe}]$  and  $[\text{Cr}/\text{Fe}]$  abundance ratios for Fornax stars as a function of  $[\text{Fe}/\text{H}]$ . Both ratios behave in more or less the same way, but Ni has much smaller error bars due to the larger number of lines available; we have  $\sim 15$  lines of Ni per star, compared to only 1 line of Cr.  $[\text{Cr}/\text{Fe}]$  seems to be more scattered than  $[\text{Ni}/\text{Fe}]$  but consistent with the larger error bars.

Our metal poor star (BL085,  $[\text{Fe}/\text{H}] = -2.58$ ) has a significantly higher  $[\text{Ni}/\text{Fe}]$  than the other Fornax field stars, comparable to MW halo stars and Fornax GC stars. At this low metallicity, we do not detect as many Ni lines as for the more metal rich stars, only 4 instead of  $\sim 15$  lines, giving it a much larger error bar than the average shown in the bottom corner of the plot as can be seen in Table 6.A3.

For  $[\text{Cr}/\text{Fe}]$ , we performed the abundance determination on an Arcturus spectrum, known to have  $[\text{Cr}/\text{Fe}] \simeq 0.0$ , similar to other MW stars with  $[\text{Fe}/\text{H}] \simeq -0.5$ , and with the same line, we obtain  $[\text{Cr}/\text{Fe}] = -0.2$ . The same analysis was done for the Ni lines and we obtained the expected  $[\text{Ni}/\text{Fe}] = 0.0$  for Arcturus. This is a sign that the Cr line could have an erroneous  $\log gf$ , leading to lower a abundance. We therefore expect that the true  $[\text{Cr}/\text{Fe}]$  could be some  $\sim 0.2$  higher than what is currently displayed in Figure 6.7, with an average closer to the  $[\text{Ni}/\text{Fe}]$  value.

At  $[\text{Fe}/\text{H}] \lesssim -1.5$ ,  $[\text{Ni}/\text{Fe}]$  appears to be Galactic halo-like, while near  $[\text{Fe}/\text{H}] \simeq -1.0$ , it decreases. This  $[\text{Ni}/\text{Fe}]$  underabundance has also been observed in the eight peculiar halo stars of Nissen & Schuster (1997) (but not for  $[\text{Cr}/\text{Fe}]$ ). Similar to the NS97 stars, our  $[\text{Ni}/\text{Fe}]$  underabundance in Fornax is also accompanied by a moderate decrease in  $[\text{Na}/\text{Fe}]$  and  $[\alpha/\text{Fe}]$  in this metallicity range. These low values of  $[\text{Ni}/\text{Fe}]$  and  $[\text{Cr}/\text{Fe}]$  cannot be easily explained with our current understanding of nucleosynthesis. The  $[\text{Ni}/\text{Fe}]$  ratios should be zero and constant for all  $[\text{Fe}/\text{H}]$  since the two elements are believed to be predominantly created in the same production site, SN Ia (Travaglio et al. 2005). To witness this different behaviour is an indication that the production factors for each iron-peak element are not the same and depend on the evolutionary history of the parent population. Maybe the SNe Ia Ni yields are linearly dependant on the original metallicity of the white dwarf progenitor, as suggested by Timmes et al. (2003), or some elements (like Ni but not Fe) are more affected by winds, causing preferential metal loss in the ISM. This result is surprising and will need to be investigated further, as Fornax is not

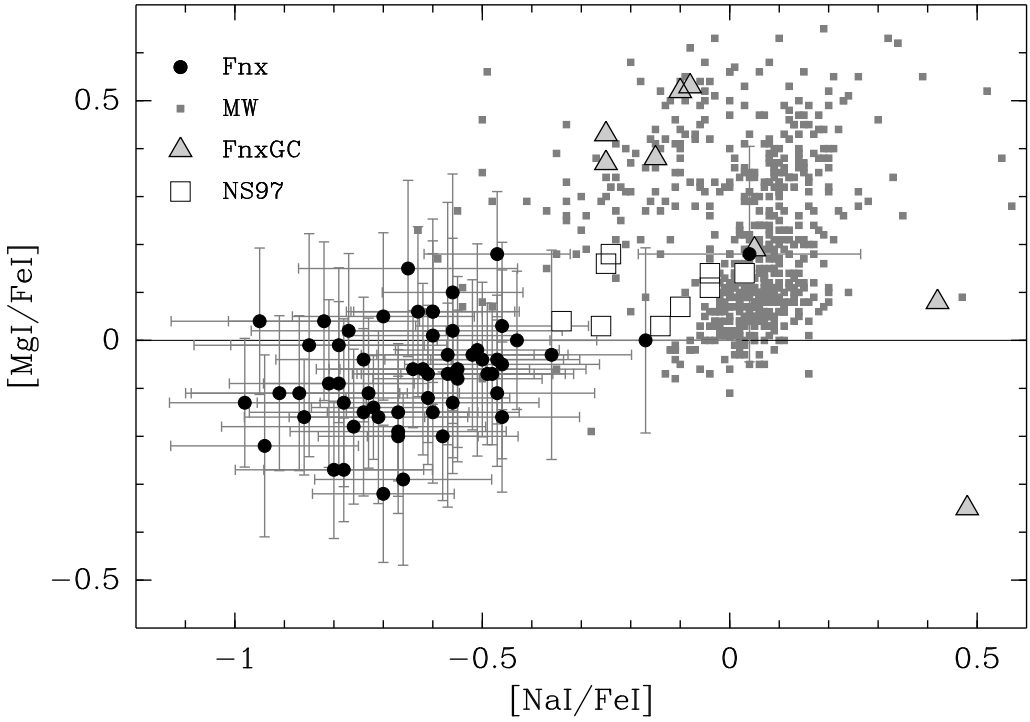


**Figure 6.8:**  $[\text{Mg}/\text{Fe}]$  plotted against  $[\text{Na}/\text{Fe}]$ . Unlike two of the Fornax GC stars, there is no sign deep mixing pattern in the field.

the only galaxy in which this behaviour is observed. This under-abundance patterns in  $[\text{Ni}/\text{Fe}]$  and  $[\text{Cr}/\text{Fe}]$  have been observed in the Large Magellanic Cloud (LMC) disk stars by Pompeia et al. (2006).

This under-abundance of Ni and Cr was *not* observed by Shetrone et al. (2003), with which we have three stars in common. We attribute this difference to a combination of systematic effects, where the most important one is the use of a different line list. See section 4.4.1 and Figure 4.16 for more detail on the systematics in abundance determination.

### 6.2.4 Deep-mixing pattern

The so-called deep mixing pattern is believed to be caused by self pollution in a star that modifies the upper atmosphere abundances. Proton-capture nucleosynthesis can convert O, N and Ne to Na, and Mg to Al in the H fusion layer of evolved RGB stars. A deep-mixing pattern can thus cause a decrease in O associated to an increase in Na and a decrease in Mg with an increase in Al. This has only been observed in stars belonging to globular clusters, in a range of different galaxies, like the Milky Way, the LMC and Fornax (see chapter 5).

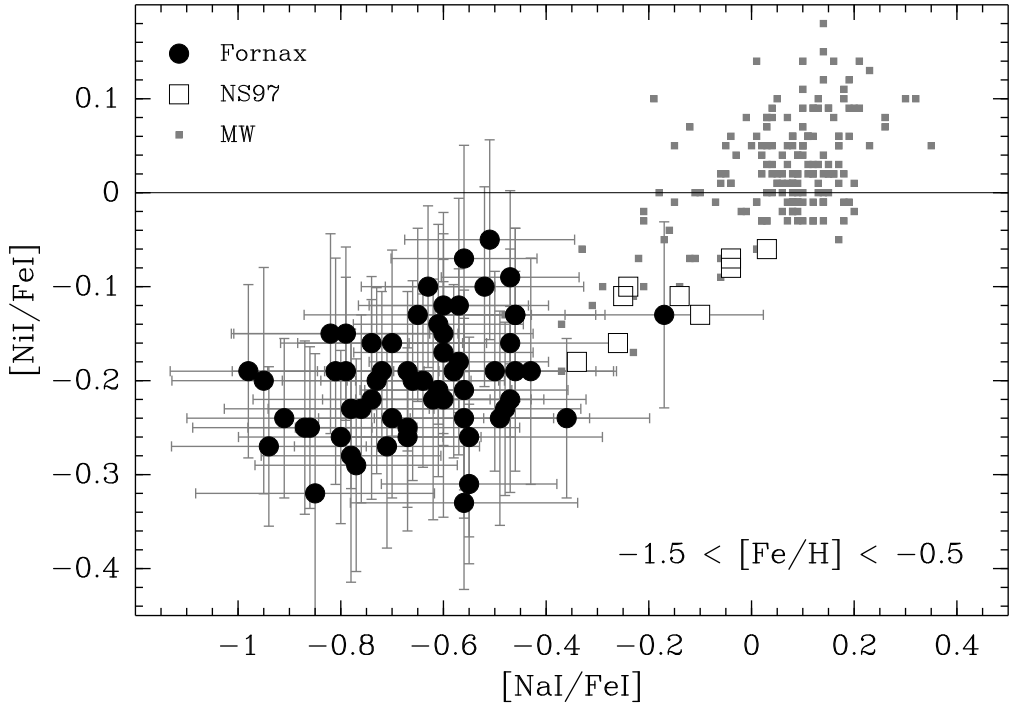


**Figure 6.9:** The Na-Ni relationship. Symbols are defined in Figure 6.5.

In the Fornax field stars, we do not find evidence of deep mixing pattern, see Figure 6.8. Unfortunately, our FLAMES observation wavelength coverage (usable) stops at  $\lambda \simeq 6690 \text{ \AA}$ , just missing two Al lines at  $6696.03 \text{ \AA}$  and  $6698.67 \text{ \AA}$ . It is therefore not possible to say anything about Al. Also, as mentioned in section 6.2.2, we do not yet have a reliable O abundance for our Fornax stars. However, it is clear from Figure 6.8 that there is no enhanced Na. All  $[\text{Na}/\text{Fe}]$  values show a significant underabundance, much lower than MW stars of similar metallicity, going as low as  $[\text{Na}/\text{Fe}] = -1.0$  in the extreme cases. There are only two outliers that have higher  $[\text{Na}/\text{Fe}]$  but these are compatible with *normal* MW stars, showing no hints of deep mixing. There are some low  $[\text{Mg}/\text{Fe}]$  values in Fornax, but without a high  $[\text{Na}/\text{Fe}]$ , this is not deep-mixing. In Fornax only the GC stars show deep mixing pattern.

### 6.2.5 The Na-Ni relationship

Where does Ni come from? As mentioned in section 6.2.3, Ni comes predominantly from SN Ia, but at earlier times, before the first SN Ia start to enrich the ISM, it is linked to the Na production in SNe II. As explained in section 5.6 of Clayton (1983), a correlation between Na and Ni is a natural result of nucleosynthesis in massive stars. Timmes et al. (1995) suggest that Na is delivered to the ISM when massive stars explode as SNe II and the amount of Na produced is controlled by the neutron excess, where  $^{23}\text{Na}$  is the only stable neutron-rich isotope produced in significant quantity during C and O burning stage.

During the SN II event, the elements are photodissociated to protons and neutrons, which will recombine to form  $^{56}\text{Ni}$ , which  $\beta$  decays to  $^{56}\text{Fe}$ , the dominant isotope of iron.  $^{54}\text{Fe}$  and/or  $^{58}\text{Ni}$  can also be produced at this stage, depending on the abundance of the neutron-rich elements (e.g.  $^{23}\text{Na}$ ). The amount of  $^{54}\text{Fe}$  made is small compared with the total yield of iron (dominated by the  $^{56}\text{Fe}$  production), but this is the main source for  $^{58}\text{Ni}$ , the stable isotope of nickel. In summary, the Ni production depends on the neutron excess during the photodissociation of the core during the SN II event, and the neutron excess will depend primarily on the amount of  $^{23}\text{Na}$  produced earlier. So the Na-Ni relationship is expected when SN II enrichment dominates. The arrival of SN Ia can break (or flatten) this relationship, as Ni is produced without Na in the standard model of SNe Ia (Tsujimoto et al. 1995). But the Na yields are still a matter of discussion, because SN Ia involve binary star interactions, and the outcome is dependent on the accreted star. So it is hard to accurately predict the SNe Ia contribution to the Na-Ni correlation.

This has two implications of interest to us: i) In SNe II, the dominant source of Ni is independent of the dominant source of Fe, possibly allowing an underabundance in  $[\text{Ni}/\text{Fe}]$  at low metallicities, before the SN Ia start to enrich the ISM. ii) If the first SNe II were not neutron rich, then there will be a lack of Na (therefore also Ni) created. The next generation of stars that will be formed *could* carry this signature, even at higher metallicity. Our low Ni at high metallicity is possibly the consequence of low Na in earlier generations, caused by neutron-poor SNe II.

For Galactic stars, it has been observed that stars with low  $[\alpha/\text{Fe}]$  also have low  $[\text{Na}/\text{Fe}]$  and low  $[\text{Ni}/\text{Fe}]$ . Nissen & Schuster (1997) first found this behaviour for eight peculiar halo stars. They suggested that these stars might have been accreted from a nearby dwarf galaxy (their abundance patterns show that they are chemically different from the MW). Other studies, by Fulbright (2002), suggested something similar for stars at large galactocentric distances. Stephens & Boesgaard (2002) suggest that there might be a gradient (0.1 dex over 10 kpc) in our galaxy, reflecting the different *local* conditions where the stars form.

If we look at Figure 6.9, our extremely low  $[\text{Na}/\text{Fe}]$  values go beyond the previous gradient (to lower  $[\text{Na}/\text{Fe}]$ ) observed by Venn et al. (2004) (their Figure 5). As they have done, we have restricted the iron abundance of the stars plotted to  $-1.5 < [\text{Fe}/\text{H}] < -0.5$ , where the Na-Ni relation can be seen. This suggests that the chemical evolution of this metal rich sub-sample of Fornax stars is *relatively similar* to the MW, at least in how Na is linked to Ni in this  $[\text{Fe}/\text{H}]$  range, with the NS97 points filling the gap between Fornax and the MW.

### 6.2.6 Heavy elements

Heavy elements are those with atomic number  $Z > 30$ , like Yttrium (Y), Barium (Ba), Europium (Eu), Lanthanum (La) and Neodymium (Nd). They are neutron capture elements built from elements that are exposed to the high neutron flux. Iron peak elements, like  $^{56}\text{Fe}$ , are the most efficient seeds to capture neutrons to create heavier elements. There are two main types of neutron capture, the *s*-process (or slow process)

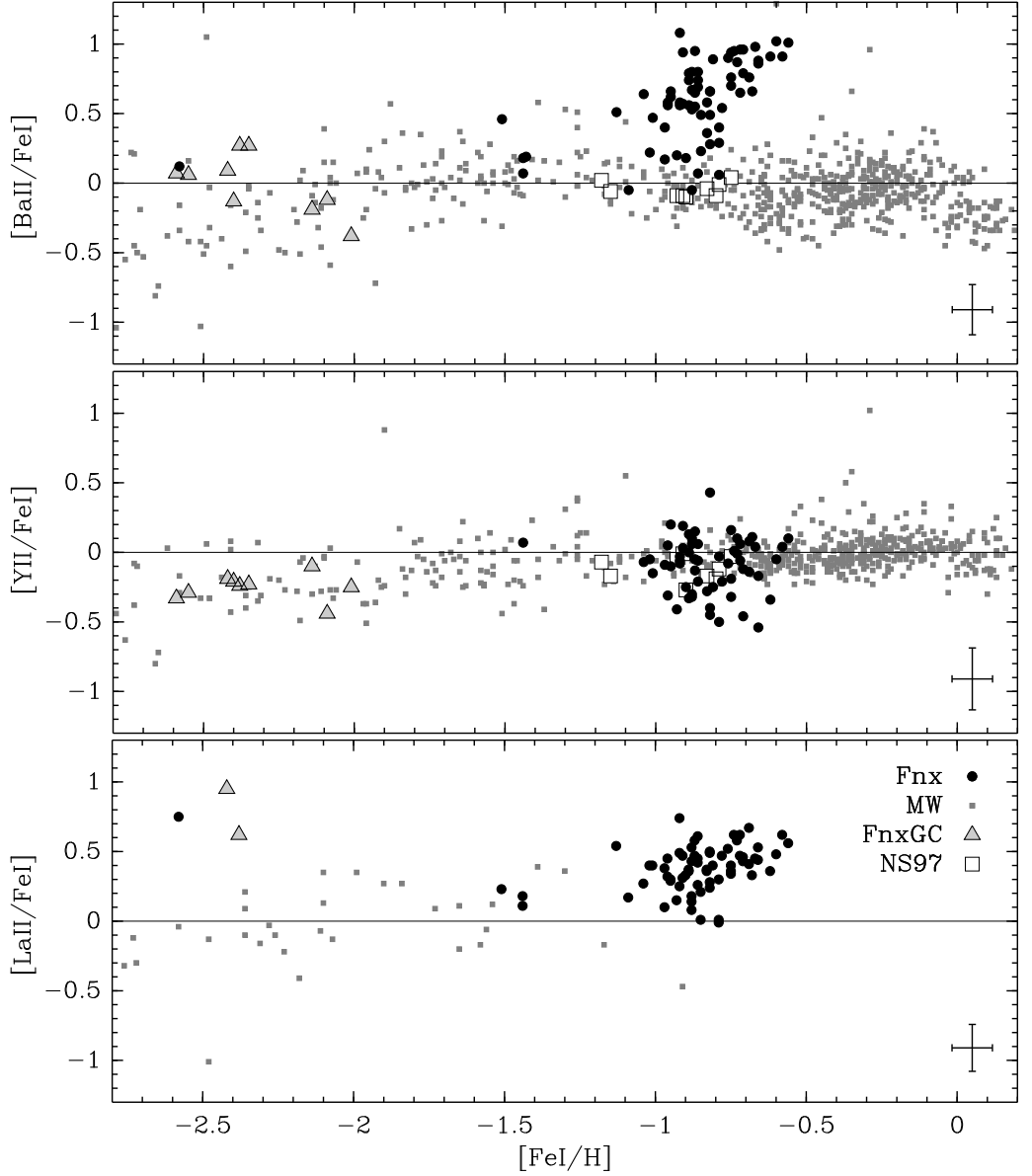


**Figure 6.10:** Heavy elements:  $[\text{Ba}/\text{Fe}]$ ,  $[\text{Y}/\text{Fe}]$  and  $[\text{La}/\text{Fe}]$  as a function of  $[\text{Fe}/\text{H}]$ . Symbols are defined in Figure 6.5.

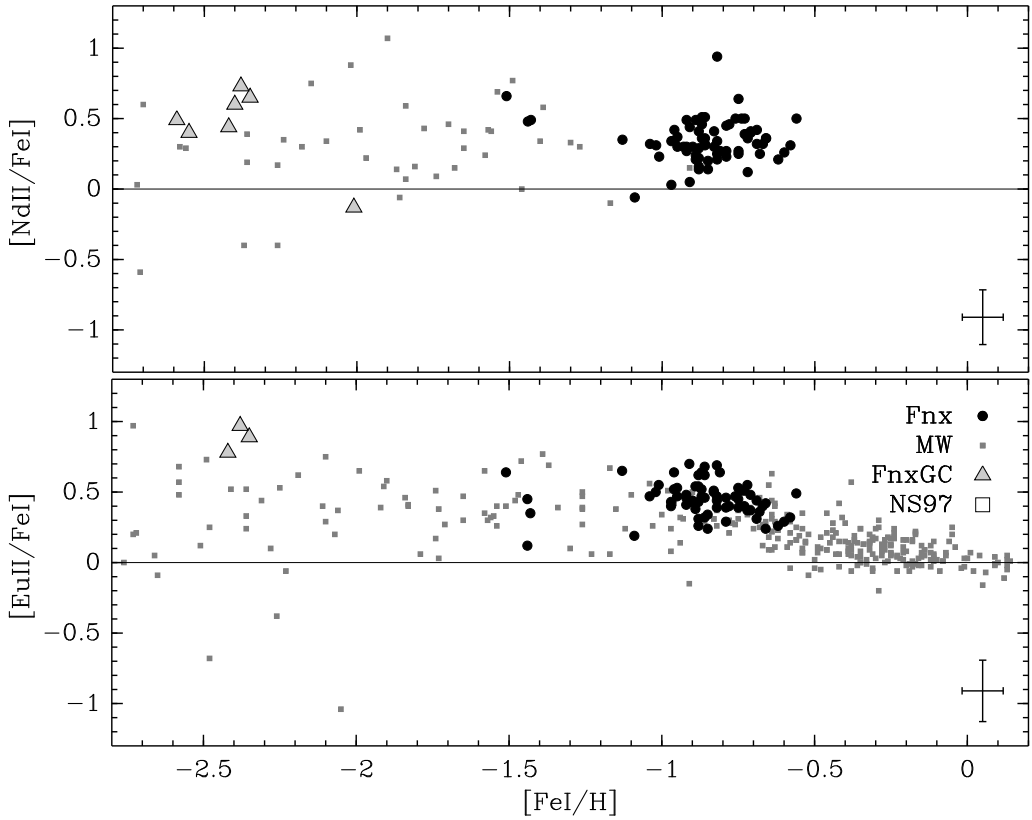


**Figure 6.11:** Heavy elements in Fornax:  $[\text{Nd}/\text{Fe}]$  and  $[\text{Eu}/\text{Fe}]$  as a function of  $[\text{Fe}/\text{H}]$ . Symbols are defined in Figure 6.5. The  $[\text{Nd}/\text{Fe}]$  points are from Burris et al. (2000).

and the  $r$ -process (rapid process). When a seed accumulates neutrons and leads to the production of a  $\beta$ -unstable nucleus, like  $^{59}\text{Fe}$ , the outcome will depend on neutron-capture timescales. In the  $s$ -process, most of the unstable nuclei will have time to undergo  $\beta$ -decay before capturing other neutrons and building up heavier elements (Pagel 1997). The main contribution of the  $s$ -process is believed to be from thermal pulses in 2-4  $\mathcal{M}_{\odot}$  AGB (cool giants) stars (Truran 1981). The  $r$ -process by contrast usually involves more extreme conditions, very high temperature and neutron densities, possibly found in low mass (8-12  $\mathcal{M}_{\odot}$ ) SN II explosions.

### Tracing the $s$ -process and $r$ -process contribution

We present the abundance ratios of  $[\text{Ba}/\text{Fe}]$ ,  $[\text{Y}/\text{Fe}]$ ,  $[\text{La}/\text{Fe}]$ ,  $[\text{Nd}/\text{Fe}]$  and  $[\text{Eu}/\text{Fe}]$  as a function of  $[\text{Fe}/\text{H}]$  in Figures 6.10 and 6.11 in decreasing order of  $s$ -process contribution. Ba is the element with the larger  $s$ -process contribution (for the *main\**  $s$ -process) in the Sun, with a fraction of 88%  $s$ -process (Kappeler et al. 1989). Then, Y has an  $s$ -process

\* Contribution from the *weak*  $s$ -process (helium burning in massive star) is 4% for Y, 1% for Ba, La, Nd and 0% for Eu.

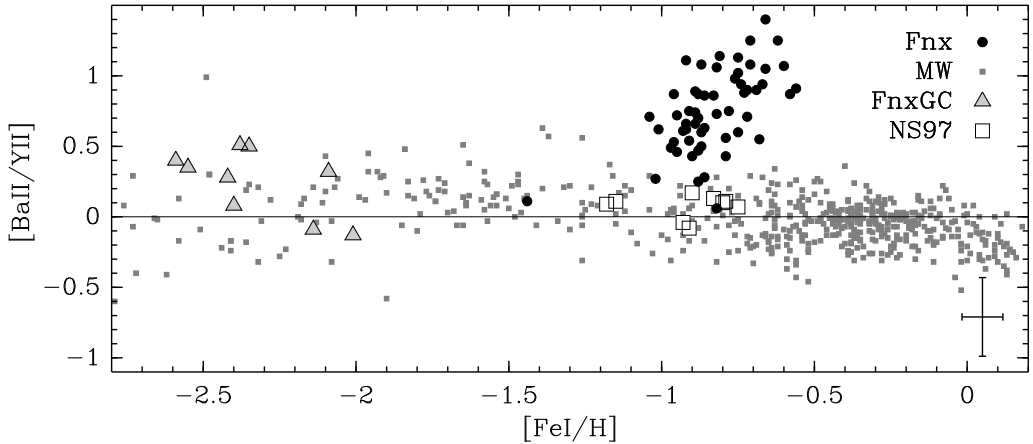


**Figure 6.12:**  $[\text{Ba}/\text{Y}]$  as a function of  $[\text{Fe}/\text{H}]$ . Symbols are defined in Figure 6.5.

contribution of 85% (Raiteri et al. 1992), The La  $s$ -process fraction is 75%, Nd 46% (Kappeler et al. 1989) and only  $\lesssim 5\%$  for Eu, as it is 95%  $r$ -process (Burris et al. 2000). Their relative abundance is thus a good discriminant of the dominant neutron capture processes in Fornax stars.

According to nucleosynthesis calculations based on hydrodynamical simulations, the  $s$ -process does not occur before  $[\text{Fe}/\text{H}] \gtrsim -2.0$  and is not significant before  $[\text{Fe}/\text{H}] \simeq -1.0$  (Travaglio et al. 1999, 2004). This is consistent with what we observe in Fornax, where  $[\text{Ba}/\text{Fe}]$  increases significantly only at  $[\text{Fe}/\text{H}] \gtrsim -1.0$ . This is different than what we observe for  $[\text{Y}/\text{Fe}]$ , also a  $s$ -process-dominated element. From Figure 6.10, we see that the  $[\text{Y}/\text{Fe}]$  ratio distribution is flat, scattered around zero in almost the same way as MW stars. This means that the  $s$ -process-enrichment does not uniformly contribute to the creation of different  $s$ -process-elements which, in the Sun, have the same  $s$ -process contribution. The behaviour of  $[\text{La}/\text{Fe}]$  is similar to  $[\text{Ba}/\text{Fe}]$ , except that the rise in  $[\text{La}/\text{Fe}]$  with increasing  $[\text{Fe}/\text{H}]$  is not as prominent, probably due to the smaller contribution from  $s$ -process to La. The same reasoning goes for  $[\text{Nd}/\text{Fe}]$  in Figure 6.11: with a smaller  $s$ -process contribution comes a smaller increase (barely noticeable) with increasing  $[\text{Fe}/\text{H}]$ . And finally,  $[\text{Eu}/\text{Fe}]$  shows no increase at all with  $[\text{Fe}/\text{H}]$ , confirming that Eu is  $r$ -process dominated. In summary, from Figures 6.10 and 6.11, we observe that the  $s$ -process becomes clearly dominant at  $[\text{Fe}/\text{H}] \gtrsim -1.0$ .

### Dominant role of metal poor AGB

$[\text{Ba}/\text{Y}]$  behaves quite differently in Fornax than in the MW, as can be seen in Figure 6.12, which clearly shows that Fornax favoured the creation of Ba over Y compared to the MW. Both elements are supposed to be  $s$ -process dominated from our knowledge of  $s$ -process contribution in the Sun. Ba ( $Z=56$ ) belongs to the 2<sup>nd</sup> peak in the distribution of neutron magic numbers and Y ( $Z=39$ ) belongs to the 1<sup>st</sup> peak. These magic numbers are related to low neutron-capture cross-sections which lead to abundance peaks close to Sr ( $Z=38$ , next to Y), Ba and Pb ( $Z=82$ ).



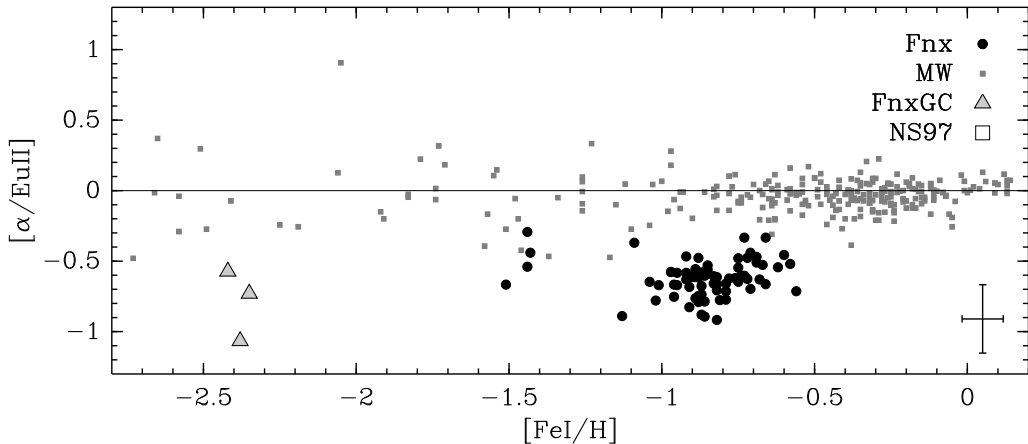


**Figure 6.13:**  $[\alpha/\text{Eu}]$  as a function of  $[\text{Fe}/\text{H}]$ . Symbols are defined in Figure 6.5.

The high  $[\text{Ba}/\text{Y}]$  in Fornax could be explained in a scenario where Fornax has a larger contribution from metal poor AGB stars compared to the MW. This would mean that the AGB that created the  $s$ -process elements were more metal poor in Fornax, favouring the creation of heavier elements, bypassing first peak elements (Y) in favour of second peak elements (Ba). A more metal poor environment has fewer nuclei (seeds) to absorb the neutrons available from the AGB envelop so they have to accumulate on fewer targets (creating more high- $Z$  elements). In a more metal rich environment, the neutrons will have more targets on which to distribute, creating more low- $Z$  elements.

### 6.3 Discussion

In summary, because it reached low  $[\alpha/\text{Fe}]$  values at much lower  $[\text{Fe}/\text{H}]$  than the MW, Fornax was most likely less efficient in enriching its gas, possibly due to galactic winds. The lack of Fornax stars (in our sample) with  $-2.5 < [\text{Fe}/\text{H}] < -1.0$  prevents us from making a more conclusive statement, as we cannot trace the decline (the knee) from high to low  $[\alpha/\text{Fe}]$ . The  $[\alpha/\text{Fe}]$  deficiency at  $[\text{Fe}/\text{H}] \gtrsim -1.0$  could be explained as the result of an early burst of star formation in the evolutionary history of Fornax followed by a dormant period with predominantly SN Ia enrichment before the relatively recent star formation episode that formed most of the stars in our sample (1-3 Gyr ago).

The underabundance of  $[\alpha/\text{Fe}]$  in Fornax with respect to the MW could be attributed SNe Ia starting to contribute Fe at lower metallicities in Fornax, resulting in a lower ratio. Also, perhaps because Fornax is a small galaxy with a low average star formation rate,  $\alpha$ -elements were most likely only produced by low-mass SNe II ( $8-12 M_{\odot}$ ) which result in lower yields than more massive SNe II (Woosley & Weaver 1995). This suggests an “effectively” truncated IMF. This is *plausible* since intuitively, a small system like Fornax is less likely to form giant molecular clouds (that are believed to be required to obtain massive stars) than a much larger system like the MW.

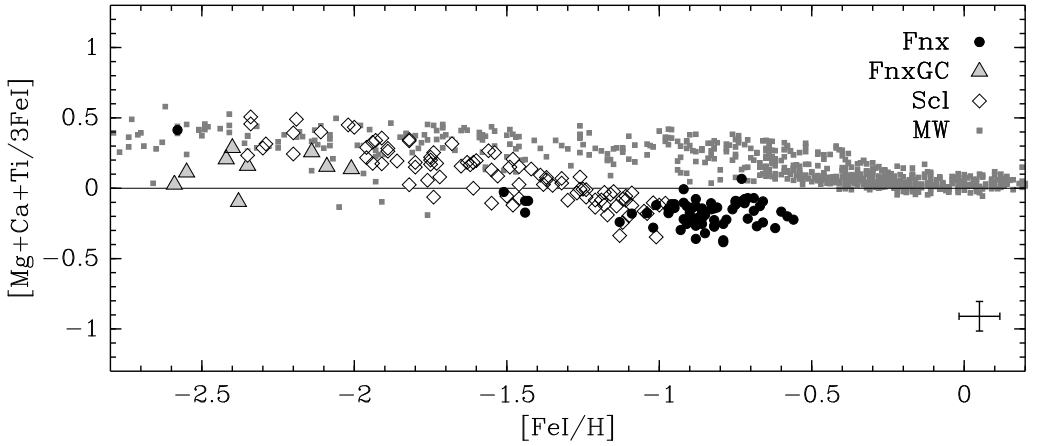


**Figure 6.14:**  $[\alpha/\text{Fe}]$  ratio as a function of  $[\text{Fe}/\text{H}]$ , including points for the Sculptor dSph (Hill et al. in prep.).

It has been argued that the  $r$ -process production occurs in low mass SNe II (Mathews et al. 1992). The high  $[\text{Eu}/\text{Fe}]$  ratios in Fornax (reaching slightly higher than the MW) suggest an important contribution of these low mass SNe II in the enrichment of Fornax. This is compatible with low  $[\alpha/\text{Fe}]$ , for which we also need low mass SNe II. When we plot  $[\text{Eu}/\alpha]$  ratios (Figure 6.13), it is clear that the sites and relative contribution of  $\alpha$ - and  $r$ -process-elements creation differ in Fornax and the (average) MW, where the Fornax values are  $\simeq 0.7$  dex lower than the MW. If both  $r$ -process and  $\alpha$ -elements were created in the same way in every galaxy, the ratio of  $[\text{Eu}/\alpha]$ , should be the same in every system. But we know this is not the case, as shown in chapter 5, the stars of Fornax cluster 3 are  $r$ -process enhanced, (Eu-rich) something not common but still seen in many M15 stars (Snedden et al. 1997). The reason why all Fornax stars have low  $[\alpha/\text{Eu}]$  is not the same for the field stars and the GC. The stars of Cluster 3 are Eu-rich and the field stars are  $\alpha$ -low.

### 6.3.1 Comparison of Fornax and Sculptor

In Figure 6.14 we compare the average  $\alpha$ -element abundance in Fornax with those found in a similar FLAMES study of the Sculptor dSph (Hill et al., in prep). Sculptor is a faint dSph galaxy ( $L_{\text{Fnx}} \simeq 7 \times L_{\text{Scl}}$ ) dominated by old (10-12 Gyr) stars. Using the combined data set we clearly see a decline in  $[\alpha/\text{Fe}]$  as SN Ia become more important. It appears that the stars observed in Fornax (except for the single metal poor star) are all lying in the “plateau” where a balance has been achieved between SN Ia and SN II element production. To understand if this is a recent minimum or the end product of the entire evolutionary history of Fornax we need to observe more stars in Fornax in the metallicity range  $-2.0 < [\text{Fe}/\text{H}] < -1.0$ . This would also allow us to make a more detailed comparison between the metal enrichment history of Scl and Fnx, which are two galaxies with very different star formation histories (cf. Tolstoy et al. 2003).

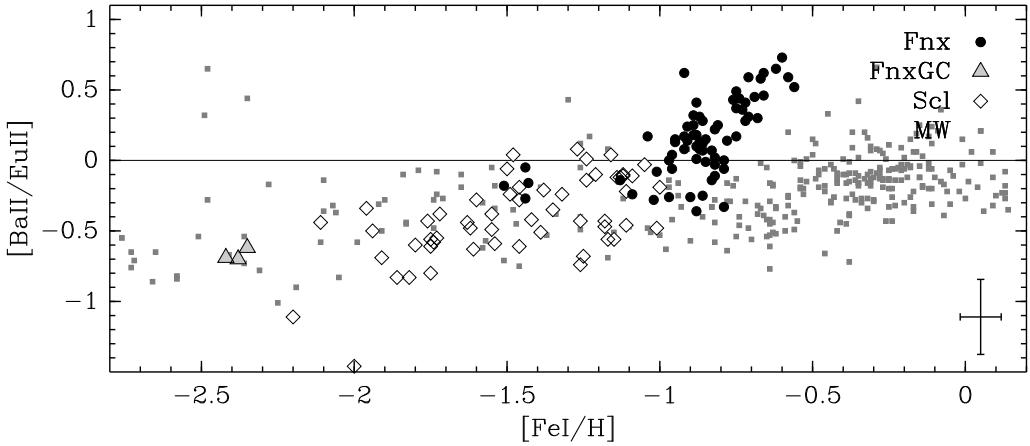


**Figure 6.15:**  $[\text{Ba}/\text{Eu}]$  ratio as a function of  $[\text{Fe}/\text{H}]$ , including points for the Sculptor dSph (Hill et al. in prep.).

In Figure 6.15, we compare  $[\text{Ba}/\text{Eu}]$  in Fornax to the same Sculptor results. Using  $[\text{Ba}/\text{Eu}]$  we track the slow increase in the  $s$ -process contribution with increasing  $[\text{Fe}/\text{H}]$ . As the stellar population becomes more metal rich there is a steady rise in the Ba abundance. In Figure 6.15 we also show the Galactic measurements, and it can be seen that the  $s$ -process is a much stronger contribution to chemical evolution of Fornax than it is to the MW, with a startling divergence at  $[\text{Fe}/\text{H}] \simeq -1.0$ . This suggests that stellar winds (e.g., from AGB stars) have played a uniquely important role in the (recent, 2-4 Gyr ago) enrichment history of Fornax. It is also clear that Sculptor with its much shorter star formation history never reached this stage where stellar winds from evolved stars had a strong effect on the enrichment of the ISM.

### 6.3.2 Age and $[\text{Fe}/\text{H}]$

In Figure 6.16 we show a Colour-Magnitude diagram where we have colour-coded the stars depending upon their spectroscopically determined  $[\text{Fe}/\text{H}]$ . From this plot we can see that the metallicity distribution is strongly peaked, with most stars in a relatively small metallicity range which are quite spread out in colour over the RGB. Broadly speaking the high metallicity stars (the darker points) are redder than the low metallicity stars (lighter points). However, it is clear that there are exceptions, and that it can be risky to use the RGB to determine the metallicity of a complex stellar population.

Using isochrones of the appropriate metallicity we can determine ages for each star (see Battaglia et al. 2006, for details). In Figure 6.17 we plot the ages and metallicities for both the HR (this work) and the LR (Battaglia et al.)  $[\text{Fe}/\text{H}]$  measurements of Fornax field stars, including the age-metallicity relation (dashed line) determined by Battaglia et al.. We compare our observations to the age-metallicity relation of Gallart et al. (2005), which is determined from a detailed Colour-Magnitude Diagram analysis. It is not easy to make strong conclusions on the basis of this comparison, as the spectroscopic samples consist of only RGB stars (which are thus always more than 1 Gyr old), whereas

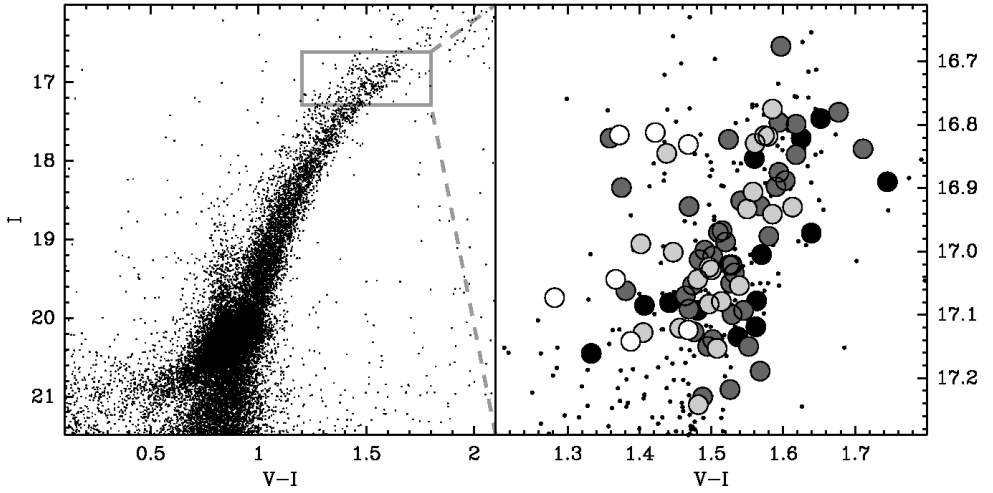


**Figure 6.16:** (*left*): Colour-Magnitude Diagram of the central ( $10'$  radius) region of Fornax, with a box around the area where we selected our targets. (*right*): Close-up of the CMD where our targets are colour coded (grey-scale) according to their metallicity in the following way. Black for stars of  $-0.5 > [\text{Fe}/\text{H}] > -0.7$ , dark grey for  $-0.7 > [\text{Fe}/\text{H}] > -0.9$ , light grey for  $-0.9 > [\text{Fe}/\text{H}] > -1.1$  and white for  $-1.1 > [\text{Fe}/\text{H}] > -2.6$ .

the CMD analysis also includes stars as young as  $\sim 200$  Myr old. However, it is clear that, although there is a large spread in  $[\text{Fe}/\text{H}]$  especially at relatively young ages, the spectroscopic measurements suggest that the majority of 1.5-2 Gyr old stars in Fornax are more metal rich than the chemical evolutionary history from CMD analysis suggests they should be. This discrepancy needs further detailed investigation to understand what is going on. It might be that this highlights a very complex metallicity distribution in the younger stars in Fornax, possibly as the result of a recent merger with a galaxy having quite a different (higher) average metallicity. This would likely confuse the determination of a chemical evolution history from CMD analysis.

## 6.4 Conclusions

The young metal poor stars of Fornax have low  $[\alpha/\text{Fe}]$  ratios associated to a sub-zero  $[\text{Ni}/\text{Fe}]$ . The  $[\alpha/\text{Fe}]$  dependence on  $[\text{Fe}/\text{H}]$  is different from the Milky Way, showing a different efficiency in gas enrichment. Fornax is dominated by  $s$ -process at high metallicity, showing the strong role of (metal poor) AGB in its evolution. The oldest most metal poor field star in Fornax is almost indistinguishable from the Galactic halo stars at the same  $[\text{Fe}/\text{H}]$ , except in the case of  $[\text{La}/\text{Fe}]$  which may indicate a problem in our La measurements rather than anything more fundamental. We expect that the hyperfine structure correction (which we have not applied yet) for La will not lower it enough to be compatible with MW stars. There is also a near perfect agreement between the abundance ratios observed in individual stars in Galactic globular clusters and in the Fornax globular clusters. However, observations of more low metallicity stars will be needed to better understand the full chemical evolution history of Fornax dSph.

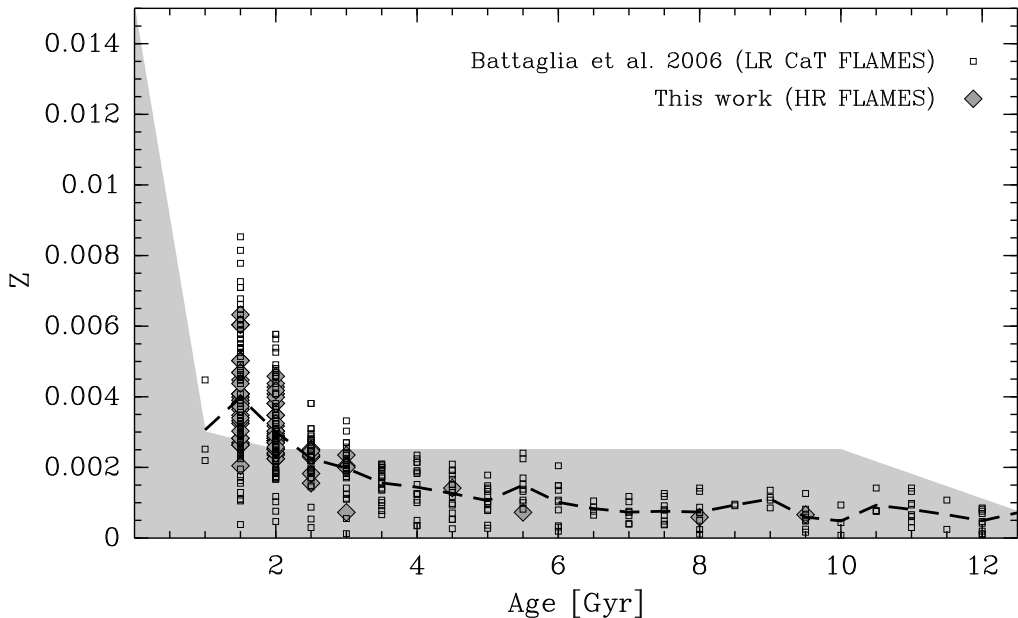


**Figure 6.17:** Age and metallicity ( $Z = 10^{[\text{Fe}/\text{H}]} \times 0.02$ ) of the 81 stars from the HR sample (diamonds), and the LR sample of Battaglia et al. (2006) (empty squares) with the average value for each age bin (dashed line). The age-metallicity relation (filled gray section) was taken from Gallart et al. (2005),

An interesting next step is to link the stellar abundances in the nearby dwarf galaxies, especially the old, low metallicity stars to studies carried out at high redshift. For example the damped  $\text{Ly}\alpha$  systems (DLAs) give us similar information about chemical abundances of the gas in distant systems. These objects are potentially the precursors of what we observe in the Local Group today.

Further work on Fornax will be to investigate the different regions of this surprisingly complex dwarf galaxy in more detail. We would benefit from obtaining more resolution high abundances of individual stars. Although 81 stars is a dramatic improvement on the previous high resolution study (of 3 field stars) it also leaves several intriguing questions unanswered. Specifically we would like to study more metal poor field stars in this galaxy in both the central region and the outskirts. It would also be interesting to continue our detailed abundance studies of the globular clusters, obtaining high resolution spectra for stars in GC 4 & 5. Another intriguing open question is the nature of the “shell-like” structures found in and around Fornax, and high resolution abundances of individual stars may shed some light on their origins.

## Appendix 6.A Large tables

**Table 6.A1:** Stellar parameters of the model used for our sample of 81 stars, along with the minimum  $EW$  used for each star.

Star	$T_{\text{eff}}$	$\log g$	[Fe/H]	$v_t$	$EW_{\text{min}}$	Star	$T_{\text{eff}}$	$\log g$	[Fe/H]	$v_t$	$EW_{\text{min}}$	Star	$T_{\text{eff}}$	$\log g$	[Fe/H]	$v_t$	$EW_{\text{min}}$
BL038	3980	0.69	-0.88	2.2	14.24	BL148	4023	0.72	-0.62	2.2	20.62	BL218	3939	0.67	-0.62	2.0	16.17
BL045	4122	0.85	-1.09	2.1	12.15	BL149	4100	0.88	-0.91	2.2	14.30	BL221	4056	0.81	-0.86	2.1	13.80
BL052	3997	0.72	-1.02	2.4	14.24	BL150	4025	0.80	-0.83	2.2	15.29	BL227	4046	0.84	-0.87	2.0	15.40
BL065	4330	0.97	-1.43	1.9	11.33	BL151	4024	0.81	-0.86	2.1	13.37	BL228	3992	0.71	-0.88	2.3	13.31
BL076	4065	0.83	-0.86	2.2	13.04	BL155	4060	0.90	-0.74	2.3	17.21	BL229	4014	0.80	-0.71	2.3	15.73
BL077	4026	0.80	-0.79	2.2	12.71	BL156	4099	0.89	-1.14	2.2	13.48	BL233	4048	0.83	-0.68	2.2	14.52
BL079	4036	0.76	-0.56	2.1	17.98	BL158	4078	0.87	-0.87	2.0	15.79	BL239	4123	0.89	-0.88	2.1	13.80
BL081	4062	0.82	-0.62	2.1	14.08	BL160	4027	0.84	-0.87	2.2	14.30	BL242	4063	0.85	-1.04	2.1	12.98
BL084	3968	0.72	-0.82	2.1	12.10	BL163	4124	0.88	-0.73	2.3	15.62	BL247	4032	0.85	-0.82	2.3	18.64
BL085	4291	0.87	-2.58	2.2	9.18	BL166	4086	0.84	-0.89	2.3	14.24	BL250	3944	0.65	-0.67	2.2	19.14
BL091	4162	0.86	-0.96	2.1	11.99	BL168	4113	0.83	-0.88	2.1	15.40	BL253	4003	0.82	-0.66	2.3	14.46
BL092	3961	0.74	-0.95	2.0	15.23	BL171	4048	0.87	-0.90	2.4	15.79	BL257	3994	0.78	-0.58	2.3	16.77
BL096	4010	0.75	-0.75	2.1	17.98	BL173	3988	0.85	-0.78	2.3	17.77	BL258	4030	0.85	-0.56	2.2	16.88
BL097	4060	0.82	-0.92	2.3	12.98	BL180	4114	0.77	-0.90	2.2	13.09	BL260	4009	0.79	-0.85	2.4	14.90
BL100	4044	0.84	-0.92	2.1	12.04	BL185	4098	0.69	-0.73	2.1	15.84	BL261	4046	0.82	-0.79	2.0	16.99
BL104	4013	0.77	-0.96	2.2	13.37	BL190	3979	0.82	-0.79	2.3	13.37	BL262	4130	0.84	-0.78	2.1	15.68
BL113	4187	0.83	-0.75	2.2	13.91	BL195	4261	0.91	-1.00	2.1	11.99	BL266	4212	0.83	-1.44	2.0	12.10
BL115	4116	0.79	-1.44	2.0	11.77	BL196	4015	0.76	-1.02	2.4	11.93	BL267	4201	0.80	-0.72	2.1	15.62
BL123	3993	0.71	-0.97	2.3	11.66	BL197	3956	0.68	-0.89	2.2	14.19	BL269	3990	0.75	-0.81	2.0	13.86
BL125	4080	0.79	-0.73	2.1	13.64	BL203	4037	0.79	-0.83	2.1	15.07	BL278	4072	0.64	-0.72	2.3	15.51
BL132	3909	0.65	-0.85	2.1	13.75	BL204	4139	0.97	-1.00	2.4	17.54	BL279	4272	0.95	-1.52	1.6	13.31
BL135	4058	0.83	-0.95	2.2	16.28	BL205	4243	0.96	-0.69	2.2	14.13	BL295	3980	0.70	-0.70	2.3	17.38
BL138	3939	0.71	-1.01	2.3	14.85	BL208	4159	0.89	-0.66	2.1	13.59	BL300	3990	0.71	-0.92	2.2	15.68
BL140	3992	0.75	-0.86	2.1	14.52	BL210	4062	0.81	-0.76	2.2	15.62	BL304	3950	0.70	-0.89	2.3	14.41
BL141	4078	0.84	-0.82	2.1	13.64	BL211	4058	0.69	-0.65	2.1	14.13	BL311	4027	0.79	-0.78	2.2	16.94
BL146	4076	0.84	-0.92	2.3	12.98	BL213	4032	0.78	-0.86	2.2	13.53	BL315	4139	0.86	-0.81	1.8	16.72
BL147	4194	0.94	-1.38	1.8	12.21	BL216	3998	0.75	-0.72	2.2	14.08	BL323	3881	0.66	-0.88	2.3	14.46

Table 6.A2: Complete line list with parameters and associated  $EW$ 's (in mÅ, measured by DAOSPEC) for all the stars. Part 1/5.

$\lambda$ (Å)	elem	$\chi$	$gf$	038	045	052	065	076	077	079	081	084	085	091	092	096	097	100	104
6141.73	Ba II	0.70	-0.08	265.7	182.3	227.5	174.2	236.8	226.5	290.2	267.4	238.8	141.6	226.5	224.8	248.4	247.7	197.9	238.5
6496.91	Ba II	0.60	-0.38	259.7	204.4	278.5	161.6	257.9	244.2	...	287.1	272.3	134.5	231.4	246.9	260.8	274.8	228.3	252.4
6122.23	Ca I	1.89	-0.32	243.6	219.3	218.2	176.0	242.1	237.9	277.5	265.2	239.3	116.5	214.9	...	261.2	...	213.9	236.9
6156.03	Ca I	2.52	-2.39	37.9	...	23.5	...	28.3	19.7	52.0	27.6	17.0	...	...	24.2	36.5	25.5	...	22.9
6161.30	Ca I	2.52	-1.27	144.3	97.1	106.5	44.0	112.7	121.4	167.2	142.5	130.2	17.2	119.5	117.6	141.9	123.9	103.5	131.9
6162.17	Ca I	1.90	-0.32	271.8	248.2	249.9	200.2	266.1	252.9	295.7	293.0	260.4	135.6	243.2	262.4	284.8	267.7	235.3	260.8
6166.44	Ca I	2.52	-1.14	141.2	97.5	107.2	51.6	126.1	114.7	134.7	132.2	122.5	...	105.6	121.1	123.3	119.1	99.9	122.5
6169.04	Ca I	2.52	-0.80	125.4	121.0	120.8	91.9	146.0	143.9	128.0	151.6	144.6	...	...	134.4	130.2	...	146.3	115.4
6169.56	Ca I	2.52	-0.48	149.8	131.0	135.8	112.8	145.6	164.6	160.8	174.6	158.9	35.6	153.7	156.5	...	161.8	138.9	166.0
6439.08	Ca I	2.52	0.39	234.7	199.4	229.8	167.9	228.2	227.2	258.3	237.6	219.9	105.8	205.8	215.8	...	228.6	201.2	217.9
6455.60	Ca I	2.52	-1.29	146.3	102.4	31.4	117.2	76.1	...	40.6	148.5	134.7	...	123.3	85.0	126.2	154.5	48.1	127.3
6471.67	Ca I	2.52	-0.76	...	...	...	...	...	...	...	...	...	20.7	...	...	...	...	...	...
6493.79	Ca I	2.52	-0.32	117.7	166.2	194.6	143.0	177.2	189.8	239.5	195.4	186.5	78.3	169.0	177.1	181.6	174.1	175.1	179.1
6499.65	Ca I	2.52	-0.82	237.9	101.5	130.4	59.6	142.0	117.8	165.6	136.4	137.1	25.3	118.4	133.8	153.3	118.0	124.2	127.4
6508.84	Ca I	2.52	-2.41	38.6	...	24.6	...	33.7	22.4	67.9	43.1	26.6	...	...	37.0	...	37.3	23.1	38.8
6303.09	Cr I	0.94	-2.92	152.6	108.7	130.8	35.1	133.9	128.0	164.9	139.9	134.6	...	115.6	131.3	137.0	122.6	120.7	106.4
6645.13	Eu II	1.37	0.20	85.0	27.3	81.5	23.3	50.9	50.7	90.1	59.0	65.4	...	57.9	62.2	79.0	60.7	...	76.0
5399.96	Fe I	4.37	0.54	146.2	154.2	125.0	...	175.2	177.0	...	180.7	173.9	41.0	159.5	147.4	162.6	145.3	163.9	143.0
5383.37	Fe I	4.31	0.50	165.1	143.0	158.5	126.9	162.0	157.5	154.3	163.4	153.7	68.1	164.4	141.6	166.2	167.7	150.0	158.5
5386.34	Fe I	4.16	-1.74	37.7	62.7	30.2	31.0	...	54.6	...	33.9	66.2	...	32.3	45.6	...	45.1	39.1	...
5393.17	Fe I	3.24	-0.92	191.0	191.9	173.7	149.5	196.3	202.0	210.3	208.5	206.8	77.1	205.9	175.9	189.2	206.5	176.0	195.2
5395.22	Fe I	4.45	-1.73	...	22.3	...	...	...	...	...	41.1	...	...	21.4	...	...	23.4	16.7	...
5405.79	Fe I	0.99	-1.85	...	...	...	268.7	...	...	...	...	...	205.0	...	...	...	...	...	...
5415.19	Fe I	4.39	0.51	115.7	155.6	119.1	137.7	158.7	166.2	148.2	165.9	161.9	71.0	164.8	142.3	149.4	163.3	154.7	145.3
5417.04	Fe I	4.42	-1.42	31.2	27.9	27.6	...	33.1	40.6	31.0	63.1	37.8	24.9	49.4	33.9	28.8	37.1	32.1	46.6
5434.53	Fe I	1.01	-2.12	...	...	...	261.2	...	...	...	...	...	206.0	...	...	...	...	...	...
5436.30	Fe I	4.39	-1.35	...	...	...	...	...	...	...	...	...	...	...	...	...	...	...	...
5464.29	Fe I	4.14	-1.62	74.9	41.2	52.9	...	51.1	57.9	86.4	72.4	73.4	...	48.5	54.0	55.0	59.4	57.9	56.7
5470.09	Fe I	4.45	-1.60	43.2	21.8	26.7	...	29.5	...	34.9	41.2	...	...	18.7	30.8	27.0	25.6	20.8	22.2
5501.48	Fe I	0.96	-0.35	258.9	236.3	239.1	193.2	247.9	269.1	265.1	276.3	273.9	159.8	241.3	254.3	253.3	267.3	243.0	254.7
5506.79	Fe I	0.99	-2.79	...	273.2	294.2	203.6	...	...	...	...	...	158.7	290.6	...	...	...	272.1	...
5539.29	Fe I	3.64	-2.59	47.1	41.0	27.4	31.9	57.1	67.1	62.0	82.3	65.6	...	56.6	42.3	53.9	63.5	54.8	54.8
5586.77	Fe I	3.37	-0.10	194.0	203.2	141.5	175.9	211.2	232.9	175.6	238.8	226.1	108.8	215.9	207.6	214.7	228.6	221.2	229.2
6120.26	Fe I	0.91	-5.94	70.3	67.7	92.1	33.9	87.0	85.8	87.4	106.2	83.2	...	57.9	92.5	94.9	96.2	67.6	91.0
6136.62	Fe I	2.45	-1.50	178.0	...	261.1	209.1	...	...	...	...	...	118.1	...	...	268.1	...	...	...
6137.00	Fe I	2.20	-2.95	...	...	181.4	...	...	...	...	...	...	...	...	...	165.2	...	...	...
6151.62	Fe I	2.18	-3.37	132.7	122.7	137.3	93.6	125.6	148.1	128.0	150.7	126.3	21.4	136.7	133.4	154.4	130.7	126.1	133.9
6157.75	Fe I	4.07	-1.26	125.5	94.5	102.3	51.0	110.7	107.7	137.9	122.8	112.6	...	94.7	103.1	120.9	113.0	95.4	115.7
6159.38	Fe I	4.61	-1.97	47.8	...	...	...	...	...	...	28.9	...	...	...	...	27.8	...	...	25.2
6165.36	Fe I	4.14	-1.47	64.4	56.4	66.5	37.2	65.2	74.7	88.5	63.9	60.9	...	66.1	62.7	73.7	68.4	68.0	50.6
6173.34	Fe I	2.22	-2.85	169.3	150.5	169.6	102.5	160.9	166.9	176.6	176.2	169.7	33.9	148.4	164.9	167.7	164.6	155.9	161.5
6180.20	Fe I	2.73	-2.78	49.8	119.4	93.6	79.4	119.5	131.8	112.9	...	134.2	34.7	130.9	116.4	144.3	123.9	112.0	123.5
6187.99	Fe I	3.94	-1.58	81.4	65.1	72.7	32.1	76.7	81.8	90.9	96.2	78.7	...	77.9	71.1	76.7	87.8	67.2	79.2
6200.31	Fe I	2.61	-2.44	138.8	138.5	151.4	114.0	151.2	151.5	147.9	164.4	150.6	39.3	144.0	145.4	157.9	152.0	140.0	158.7
6213.43	Fe I	2.22	-2.66	188.6	170.0	195.5	143.4	183.2	203.7	207.2	200.8	200.5	72.5	165.1	178.5	185.4	182.4	175.7	180.6
6219.29	Fe I	2.20	-2.44	199.9	185.7	209.7	135.0	187.8	199.5	203.6	210.5	206.1	68.3	190.2	195.3	205.4	191.4	179.8	190.3
6226.74	Fe I	3.88	-2.20	60.2	41.4	62.4	21.0	59.3	57.1	74.1	48.4	51.9	...	58.8	70.3	72.2	55.6	57.4	61.7
6252.57	Fe I	2.40	-1.76	219.9	193.7	200.3	154.7	207.4	218.5	203.1	214.9	203.2	115.3	187.0	198.0	216.1	205.6	190.3	205.3
6265.13	Fe I	2.18	-2.55	178.1	167.1	180.8	113.5	179.0	194.9	190.2	186.1	183.0	66.5	170.4	190.9	192.1	196.7	181.2	171.2
6271.28	Fe I	3.32	-2.96	49.7	46.8	59.8	21.5	59.2	63.2	65.5	72.3	56.8	...	53.4	49.4	67.4	65.0	44.8	49.2
6297.80	Fe I	2.22	-2.74	...	...	...	...	...	...	...	...	...	42.0	...	...	...	...	...	...
6301.50	Fe I	3.65	-0.72	...	144.9	...	...	...	...	...	...	...	40.0	...	...	...	...	...	...
6307.85	Fe I	3.64	-3.27	...	...	...	...	...	...	33.6	26.1	...	...	...	...	...	...	15.8	...
6322.69	Fe I	2.59	-2.43	163.0	140.4	158.5	116.1	160.4	174.6	169.0	170.1	155.4	36.1	146.2	146.2	150.4	159.7	153.5	165.0
6330.85	Fe I	4.73	-1.22	37.8	26.3	35.3	17.3	42.6	38.5	41.3	50.7	31.4	...	34.7	44.3	34.0	35.6	36.5	17.1
6335.33	Fe I	2.20	-2.23	214.5	198.2	250.2	151.0	224.3	209.1	234.5	220.8	206.2	83.2	197.4	191.7	207.9	213.3	201.1	212.5
6336.82	Fe I	3.69	-1.05	144.3	144.9	145.5	108.8	140.5	139.9	157.7	144.0	142.3	33.7	150.9	129.9	138.0	134.0	130.4	128.6
6344.15	Fe I	2.43	-2.92	169.6	165.4	165.2	100.0	170.3	181.3	196.6	189.3	168.3	20.7	149.4	...	180.6	170.0	143.6	165.7
6355.04	Fe I	2.84	-2.29	164.2	143.2	149.7	86.5	160.5	163.5	176.3	148.2	153.6	35.2	150.7	159.1	...	162.0	150.4	160.1
6380.75	Fe I	4.19	-1.50	79.5	49.9	74.2	30.1	76.5	79.5	88.1	87.6	73.3	...	72.3	78.5	66.7	73.8	63.3	88.9
6392.54	Fe I	2.28	-3.95	80.1	84.8	82.9	46.2	85.7	89.3	78.2	106.7	90.0	17.3	78.8	94.2	95.9	87.9	87.5	94.1
6393.61	Fe I	2.43	-1.63	236.5	228.0	221.5	194.6	241.1	248.4	249.6	260.1	236.6	120.8	240.5	204.9	240.4	251.8	223.3	251.5
6408.03	Fe I	3.69	-1.00	149.0	140.4	142.1	101.0	149.6	153.4	131.4	167.8	140.8	32.2	141.5	118.5	143.8	142.3	123.3	142.7
6419.96	Fe I	4.73	-0.24	112.8	91.1	115.3	61.7	99.9	115.5	132.5	118.3	105.1	...	96.8	76.4	115.4	110.0	109.5	97.1
6421.36	Fe I	2.28	-2.01	228.9	217.8	233.8	163.9	237.0	234.2	255.5	234.9	223.8	92.9	213.5	218.3	226.9	222.6	214.7	223.8
6430.86	Fe I	2.18	-1.95	256.5	215.3	282.6	174.9	256.8	269.1	...	272.7	244.7	111.1	222.4	241.4	276.1	263		

$\lambda(\text{\AA})$	elem	$\chi$	$g^f$	038	045	052	065	076	077	079	081	084	085	091	092	096	097	100	104
6318.72	Mg I	5.11	-1.97	43.6	...	...	...	34.9	24.6	...	...	...	...	31.1	38.9	52.2	...	17.7	34.0
6319.24	Mg I	5.11	-2.21	...	27.0	26.9	...	...	23.3	36.2	24.9	...	...	...	30.6	42.1	...	31.8	...
6319.49	Mg I	5.11	-2.43	...	...	...	...	...	...	...	...	...	...	...	...	...	...	...	...
5420.36	Mn I	2.14	-1.46	217.4	160.5	166.5	67.8	188.6	198.1	204.4	203.5	202.4	...	176.3	162.5	192.5	209.3	174.0	187.5
5432.55	Mn I	0.00	-3.80	287.6	247.7	275.0	120.2	280.9	272.6	...	291.3	252.2	...	215.8	251.6	289.0	271.4	249.7	264.5
5516.77	Mn I	2.18	-1.85	169.4	99.3	141.5	36.1	145.4	145.0	179.4	171.6	137.9	...	117.2	132.7	141.2	141.7	111.8	138.6
6154.23	Na I	2.10	-1.56	38.8	...	...	...	23.5	...	35.7	36.3	...	...	25.6	15.5	23.4	19.8	...	...
6160.75	Na I	2.10	-1.26	58.4	...	23.3	...	38.2	38.6	65.5	54.5	...	...	38.5	21.1	47.6	39.7	...	28.5
5416.38	Nd II	0.86	-0.98	17.2	...	...	17.1	27.5	20.6	18.5	34.1	29.3	...	32.0	25.3	27.5	28.5	16.3	40.0
5431.54	Nd II	1.12	-0.47	65.0	...	43.7	...	47.3	42.4	73.6	62.0	58.0	35.3	42.5	45.0	72.1	48.3	39.4	52.3
5485.71	Nd II	1.26	-0.12	40.7	19.3	25.6	...	27.4	25.2	48.2	34.7	30.1	...	45.2	39.3	37.3	39.4	...	35.9
5578.73	Ni I	1.68	-2.67	135.0	119.9	116.0	86.8	117.7	130.9	142.9	140.0	138.5	29.0	133.0	123.0	125.5	141.0	115.4	151.5
5587.87	Ni I	0.93	-2.37	147.1	119.4	121.6	83.3	147.5	159.3	150.8	183.1	157.3	30.6	158.0	129.2	146.5	176.0	135.9	158.7
5589.37	Ni I	3.90	-1.15	25.0	19.1	26.3	...	32.4	24.6	29.2	34.7	29.1	...	18.7	31.3	26.7	18.8	23.9	27.7
5593.75	Ni I	3.90	-0.79	41.1	31.2	33.4	21.8	34.5	47.1	43.5	57.6	31.9	...	35.1	40.6	34.2	30.7	24.5	31.1
6128.97	Ni I	1.68	-3.39	94.8	61.2	93.5	48.1	87.6	76.9	99.4	90.0	82.1	...	74.3	72.9	105.7	88.8	75.0	82.8
6130.14	Ni I	4.27	-0.98	17.1	...	...	...	...	...	...	...	...	...	...	17.9	...	...	17.1	...
6177.25	Ni I	1.83	-3.60	72.6	40.2	51.7	...	55.4	57.7	76.8	73.3	65.4	...	69.5	...	52.4	72.2	45.0	61.6
6186.72	Ni I	4.11	-0.90	40.7	28.3	22.8	...	...	41.8	32.9	43.6	31.0	...	...	...	...	30.2	26.9	...
6204.61	Ni I	4.09	-1.15	...	...	...	18.7	20.8	22.3	24.5	22.4	...	...	28.9	...	...	23.0	22.4	...
6223.99	Ni I	4.10	-0.97	24.2	...	...	24.5	...	30.3	37.9	24.2	...	...	...	43.0	37.4	30.9	29.2	...
6230.10	Ni I	4.11	-1.20	45.7	23.6	24.5	...	26.5	...	42.7	...	26.7	...	25.4	...	...	32.9	...	...
6322.17	Ni I	4.15	-1.21	21.0	...	...	...	27.0	...	20.4	...	...	...	...	...	24.8	19.2	...	...
6327.60	Ni I	1.68	-3.09	110.9	94.9	100.3	70.4	109.7	106.5	127.7	116.7	107.2	...	102.2	119.9	102.0	117.2	106.6	113.6
6378.26	Ni I	4.15	-0.82	29.4	...	...	...	25.9	30.9	...	34.2	32.7	...	24.2	19.5	34.5	25.8	43.7	...
6384.67	Ni I	4.15	-1.00	22.9	...	...	...	33.3	...	50.2	35.4	30.4	...	...	...	20.9	27.6	36.2	...
6482.80	Ni I	1.94	-2.85	110.5	96.8	141.8	48.7	113.0	108.0	147.1	123.6	107.3	16.2	92.5	104.6	115.4	109.2	106.7	107.7
6586.32	Ni I	1.95	-2.79	137.0	135.4	44.1	123.9	66.9	89.8	...	134.5	144.6	45.8	128.7	57.0	51.5	148.1	66.5	94.6
6598.61	Ni I	4.24	-0.93	...	...	...	...	...	...	...	...	...	17.7	...	...	...	34.9	24.2	...
6635.14	Ni I	4.42	-0.75	...	15.1	...	...	...	...	46.9	...	...	...	18.6	24.9	...	...	...	18.2
6300.31	O I	0.00	-9.75	...	...	...	...	...	...	...	...	...	...	...	...	...	...	...	...
6363.79	O I	0.02	-10.25	53.3	26.8	39.1	28.4	37.2	45.8	53.3	45.0	34.4	...	24.6	33.5	57.3	39.5	30.7	46.3
5526.82	Sc II	1.77	0.03	118.4	113.7	124.9	104.2	109.3	107.1	116.3	114.5	119.4	74.4	121.6	110.8	114.1	120.8	107.5	115.4
6245.62	Sc II	1.51	-0.97	90.2	58.8	67.4	56.9	65.4	65.0	77.1	58.3	81.7	24.0	72.5	75.4	73.2	68.5	61.8	66.9
6309.90	Sc II	1.50	-1.52	...	33.4	...	26.3	...	...	47.8	...	38.3	...	...	27.7	42.5	...	41.7	...
6604.60	Sc II	1.36	-1.31	87.1	84.3	109.3	61.2	98.5	80.1	125.6	83.5	105.3	38.9	76.4	90.6	89.4	108.5	82.1	80.4
6125.03	Si I	5.62	-1.57	25.0	24.7	...	18.3	...	...	...	...	...	...	22.4	...	...	...	...	34.2
6142.48	Si I	5.62	-1.51	...	...	...	...	...	...	...	...	...	...	...	...	...	...	...	...
6145.02	Si I	5.61	-1.37	45.1	...	...	...	16.0	...	...	...	...	...	...	...	22.0	...	...	15.2
6155.14	Si I	5.62	-0.80	42.5	38.5	...	32.4	35.6	39.2	57.8	31.5	27.3	17.0	35.0	25.7	48.1	38.3	23.9	40.1
6237.33	Si I	5.61	-1.02	26.6	...	...	...	...	...	34.7	...	...	...	21.3	25.5	26.1	24.6	...	...
6243.82	Si I	5.61	-1.27	...	...	23.2	...	22.8	24.1	...	...	28.2	...	...	...	24.1	...	33.2	...
5490.16	Ti I	1.46	-0.93	121.8	83.7	104.4	34.0	109.1	102.3	142.0	125.3	112.4	...	84.4	103.8	109.5	98.8	84.1	116.1
5503.90	Ti I	2.58	-0.19	...	41.0	...	19.8	47.0	47.1	83.9	83.4	55.3	...	43.9	74.4	56.7	71.7	33.9	58.4
6126.22	Ti I	1.07	-1.42	149.2	110.7	119.7	48.9	131.6	130.4	167.1	150.6	142.1	20.0	113.5	107.1	158.2	135.5	113.3	140.1
6220.50	Ti I	2.68	-0.14	78.1	45.9	...	...	48.8	79.3	78.6	...	...	...	...	...	...	58.6	...	...
6258.10	Ti I	1.44	-0.35	208.0	139.2	...	77.3	176.3	159.6	231.6	191.6	195.5	...	143.9	192.0	...	182.0	...	194.3
6303.77	Ti I	1.44	-1.57	...	61.1	66.2	26.0	74.9	72.7	111.6	101.7	84.2	...	50.4	88.8	102.0	80.1	55.4	...
6312.24	Ti I	1.46	-1.55	...	...	66.8	...	63.2	66.9	115.9	97.8	79.9	...	51.4	88.8	...	80.6	54.5	88.2
6336.10	Ti I	1.44	-1.74	94.4	48.9	63.7	16.9	74.7	65.8	111.4	84.7	73.2	...	41.0	72.2	90.8	70.4	47.0	71.6
6508.12	Ti I	1.43	-2.05	64.6	27.1	...	...	62.0	40.6	105.0	61.9	50.3	...	28.1	58.9	59.3	37.8	30.2	58.8
6556.08	Ti I	1.46	-1.07	...	104.7	...	...	...	...	...	...	...	...	...	...	164.6	...	...	...
6599.13	Ti I	0.90	-2.09	151.6	81.6	128.0	35.6	141.1	128.7	179.9	146.9	149.8	...	87.8	109.4	141.6	130.8	105.4	120.1
6666.53	Ti I	1.46	-1.62	...	25.9	...	15.1	...	18.7	28.2	25.8	...	...	18.0	...	...	...	...	...
5418.77	Ti II	1.58	-2.11	111.6	107.9	73.6	89.0	94.6	98.7	97.3	91.1	103.5	69.1	96.9	94.9	108.1	108.4	104.0	103.0
6219.94	Ti II	2.06	-2.82	...	27.2	15.0	...	...	...	...	...	...	...	...	...	...	...	...	...
6559.58	Ti II	2.05	-2.02	...	48.3	...	45.2	...	...	...	...	...	16.4	...	...	81.2	...	...	...
6606.95	Ti II	2.06	-2.79	42.2	30.2	...	25.2	42.1	31.9	70.3	36.3	47.5	20.9	44.5	36.2	46.3	43.1	44.9	35.8
6680.13	Ti II	3.09	-1.86	...	...	23.9	18.9	22.7	...	...	19.0	...	16.6	32.6	27.0	...	16.8	...	16.3
6119.53	Vi I	1.06	-0.32	...	...	...	...	...	...	...	...	...	...	...	...	...	...	...	71.8
6128.33	Vi I	1.05	-2.30	...	...	...	...	...	...	30.3	...	...	...	...	...	...	...	...	...
6135.37	Vi I	1.05	-0.75	126.5	48.6	95.7	18.2	87.3	87.7	122.7	107.7	98.3	...	73.6	101.1	100.9	87.5	62.6	...
6150.15	Vi I	0.30	-1.79	156.7	98.6	118.7	18.7	125.6	129.4	186.0	154.2	146.0	17.3	99.4	124.1	156.0	135.7	91.4	150.5
6190.19	Vi I	0.29	-1.29	185.0	133.3	152.9	40.1	163.3	179.1	210.6	186.5	171.9	...	130.0	180.5	192.4	162.0	131.0	179.2
6216.36	Vi I	0.28	-0.81	217.5	141.6	169.3	41.8	176.7	173.2	211.0	184.0	184.0	21.2	136.6	168.0	198.2	165.7	142.7	185.6
6224.51	Vi I	0.29	-2.01	127.1	77.8	98.9	24.1	115.9	125.0	138.4	136.0	124.2	...	81.0	123.9	142.2	115.3	85.3	133.1
6233.20	Vi I	0.28	-2.07	102.1	64.1	92.4	...	95.4	89.7	128.6	96.4	90.2	...	61.2	106.5	108.4	85.4	53.3	97.8
6243.11	Vi I	0.30	-0.98	...	...	...	77.3	...	...	...	...	...	...	...	...	298.9	...	...	...
6251.82	Vi I	0.29	-1.30	163.8	100.2	140.9	36.0	137.2	137.9	174.9	157.7	158.0	...	115.9	137.2	158.8	139.1	109.5	149.0
6274.66	Vi I	0.27	-1.67	...	...	91.9	...	115.1	116.4	155.2	141.2	...	...	92.2	131.1	...	94.0	90.8	141.8
6357.29	Vi I	1.85	-0.91	38.3	...	...	...	...	17.8	43.7	25.7	...	15.5	...	23.8	50.3	...	15.4	21.2
6452.32	Vi I	1.19	-1.21	89.2	35.8	32.1	48.4	65.7	72.3	79.2	122.1	85.8	...	48.5	68.1	59.3	73.6	35.8	74.0
6504.19	Vi I	1.18	-1.23	60.0</															



Table 6.A2: Complete line list with parameters and associated  $EW$ 's (in mÅ, measured by DAOSPEC) for all the stars. Part 2/5.

				Equivalent width, one star per column, BLocx															
$\lambda(\text{\AA})$	elem	$\chi$	$gf$	113	115	123	125	132	135	138	140	141	146	147	148	149	150	151	155
6141.73	Ba II	0.70	-0.08	276.9	182.4	241.5	256.1	218.8	240.3	255.0	241.1	209.2	240.3	236.5	...	236.0	230.1	243.6	265.2
6496.91	Ba II	0.60	-0.38	...	...	171.9	235.9	277.9	248.3	255.0	227.5	257.0	227.5	266.2	244.7	227.2	257.8	236.3	253.6
6122.23	Ca I	1.89	-0.32	249.6	192.4	242.8	254.1	250.0	244.7	255.0	234.6	234.5	230.0	162.3	293.5	228.1	256.4	240.9	...
6156.03	Ca I	2.52	-2.39	43.4	...	...	...	40.5	28.5	...	24.2	34.5	...	...	70.9	18.7	36.6	22.4	27.6
6161.30	Ca I	2.52	-1.27	156.4	52.9	131.7	145.8	126.1	113.7	148.3	131.4	119.2	116.1	66.5	170.4	111.5	125.8	119.4	155.3
6162.17	Ca I	1.90	-0.32	264.2	204.5	262.9	284.9	261.6	266.1	279.5	254.3	247.1	265.4	194.6	...	244.5	268.6	265.7	277.2
6166.44	Ca I	2.52	-1.14	127.7	60.6	111.8	124.8	121.9	119.2	145.6	133.1	105.3	117.6	52.9	145.8	112.6	116.7	124.8	138.2
6169.04	Ca I	2.52	-0.80	145.9	87.2	141.7	139.1	135.1	129.7	153.1	148.0	149.2	139.0	59.7	143.1	116.5	155.5	148.3	147.9
6169.56	Ca I	2.52	-0.48	165.6	111.5	157.5	178.6	155.6	175.7	146.1	154.7	156.3	167.7	90.4	174.5	144.9	167.7	158.0	187.9
6439.08	Ca I	2.52	0.39	232.7	168.5	225.1	235.0	226.6	235.2	238.2	214.9	219.1	227.5	181.8	253.0	230.3	240.7	220.4	251.1
6455.60	Ca I	2.52	-1.29	155.8	85.6	106.2	92.6	172.9	192.2	134.1	135.9	159.0	155.3	...	178.6	...	194.4	177.9	149.0
6471.67	Ca I	2.52	-0.76	...	...	...	...	...	...	...	...	...	...	...	...	...	...	...	...
6493.79	Ca I	2.52	-0.32	195.3	139.0	193.3	213.1	187.8	174.8	196.5	176.7	192.2	186.3	134.8	205.0	188.9	199.2	183.4	193.1
6499.65	Ca I	2.52	-0.82	129.7	80.5	132.1	147.0	129.4	122.0	130.1	136.8	128.4	118.6	80.8	139.6	122.0	120.3	134.2	133.3
6508.84	Ca I	2.52	-2.41	42.4	...	26.8	43.2	27.7	17.6	33.6	19.8	21.9	20.8	...	46.0	22.3	33.2	29.5	51.5
6330.09	Cr I	0.94	-2.92	127.0	63.7	141.3	127.1	146.4	127.9	141.2	141.4	127.0	132.2	36.7	169.3	116.1	143.9	140.8	146.2
6645.13	Eu II	1.37	0.20	71.3	15.9	53.5	78.2	49.1	55.0	69.0	79.7	56.2	52.8	99.1	73.9	53.1	68.6	59.5	61.5
5399.96	Fe I	4.37	0.54	167.3	136.9	218.7	145.2	142.3	143.1	173.4	160.3	166.5	165.7	128.4	163.3	132.5	155.5	160.1	119.1
5383.37	Fe I	4.31	0.50	185.9	150.1	150.5	171.1	157.9	160.1	188.8	162.0	157.8	161.6	114.1	182.2	161.0	174.9	159.2	170.3
5386.34	Fe I	4.16	-1.74	53.4	...	...	...	38.8	57.5	62.9	...	44.6	51.8	...	61.2	27.4	33.5	45.2	53.9
5393.17	Fe I	3.24	-0.92	199.6	180.7	198.8	217.9	209.6	233.1	216.2	200.3	218.7	212.3	176.0	239.2	187.7	207.6	221.0	214.6
5395.22	Fe I	4.45	-1.73	29.4	...	29.8	30.2	23.3	30.1	31.4	29.3	23.1	...	...	34.6	34.9	...	30.1	31.4
5405.79	Fe I	0.99	-1.85	...	...	...	...	...	...	...	...	...	...	262.0	...	...	...	...	...
5415.19	Fe I	4.39	0.51	155.8	145.2	151.4	174.2	167.5	186.8	152.5	155.3	176.2	167.1	108.5	168.1	162.7	166.5	174.0	184.9
5417.04	Fe I	4.42	-1.42	58.4	26.7	38.4	48.0	39.8	51.5	37.4	40.4	34.9	66.0	...	53.7	28.8	52.4	35.7	71.3
5434.53	Fe I	1.01	-2.12	...	299.9	...	...	...	...	...	...	...	...	245.4	...	...	...	...	...
5436.30	Fe I	4.39	-1.35	...	...	...	...	...	...	...	...	...	...	...	...	...	...	...	...
5464.29	Fe I	4.14	-1.62	82.1	...	59.5	90.4	53.5	...	51.8	70.7	52.6	60.1	27.0	...	49.2	52.6	62.9	73.5
5470.09	Fe I	4.45	-1.60	15.1	...	28.2	24.7	25.2	17.5	25.4	24.2	33.7	21.2	16.8	...	26.5	22.1	27.1	27.7
5501.48	Fe I	0.96	-0.35	205.8	238.7	266.5	267.8	275.4	254.1	274.3	260.6	257.5	270.8	185.7	274.6	242.7	273.0	251.4	286.4
5506.79	Fe I	0.99	-2.79	...	234.7	...	...	...	...	...	...	...	...	214.3	...	279.6	...	...	...
5539.29	Fe I	3.64	-2.59	68.3	33.8	49.5	67.2	59.1	...	57.5	58.8	58.1	59.5	...	78.3	59.9	63.0	55.9	76.0
5586.77	Fe I	3.37	-0.10	235.9	177.8	206.8	244.4	239.6	245.6	243.9	225.7	228.8	224.0	143.4	248.2	227.3	245.4	228.6	250.2
6120.26	Fe I	0.91	-5.94	79.1	49.5	70.6	92.1	109.1	75.3	88.9	83.4	95.8	85.6	...	21.9	85.5	83.9	87.7	89.8
6136.62	Fe I	2.45	-1.50	...	206.5	...	...	...	...	...	...	...	...	217.6	...	...	...	...	...
6137.00	Fe I	2.20	-2.95	...	129.5	...	...	...	...	...	...	...	...	...	...	...	...	...	...
6151.62	Fe I	2.18	-3.37	140.1	95.0	138.2	142.5	147.0	125.3	137.1	138.8	125.4	134.2	80.9	147.5	135.1	128.9	134.2	137.7
6157.75	Fe I	4.07	-1.26	133.4	50.1	105.8	125.1	100.1	104.2	113.4	110.4	104.8	115.1	82.2	151.9	86.0	104.4	104.6	126.4
6159.38	Fe I	4.61	-1.97	...	...	...	23.5	26.4	...	...	18.7	19.1	...	...	65.3	...	...	16.9	34.5
6165.36	Fe I	4.14	-1.47	83.7	32.6	67.6	64.3	64.9	67.5	58.8	65.4	74.7	68.5	24.2	92.0	63.1	72.8	71.0	75.5
6173.34	Fe I	2.22	-2.85	162.7	113.0	156.6	171.8	169.0	156.1	171.4	167.6	157.9	158.9	121.6	176.5	156.0	158.8	157.1	154.5
6180.20	Fe I	2.73	-2.78	133.2	101.8	138.6	119.5	149.9	116.9	123.1	139.7	154.7	132.3	59.3	85.7	132.5	142.0	143.8	147.1
6187.99	Fe I	3.94	-1.58	84.5	43.5	75.3	79.9	84.2	75.2	67.6	81.8	72.9	80.1	40.8	...	63.7	86.5	76.2	69.4
6200.31	Fe I	2.61	-2.44	158.0	120.6	143.2	152.2	148.0	159.7	153.8	152.7	151.5	149.3	98.8	145.4	154.9	163.4	155.3	158.0
6213.43	Fe I	2.22	-2.66	210.8	147.0	194.4	200.8	184.6	189.0	192.7	183.8	181.6	211.8	143.0	199.2	194.4	183.9	187.4	187.5
6219.29	Fe I	2.20	-2.44	206.1	160.9	189.8	197.5	207.2	...	198.5	184.7	204.1	202.2	133.7	212.0	191.6	202.5	189.9	201.2
6226.74	Fe I	3.88	-2.20	68.4	32.8	52.3	65.2	55.6	57.7	52.5	57.2	64.5	53.7	29.7	110.4	46.9	70.8	60.1	67.6
6252.57	Fe I	2.40	-1.76	205.2	180.6	207.3	199.2	199.8	198.6	210.1	205.0	194.4	205.9	153.3	223.5	149.1	203.8	199.8	202.1
6265.13	Fe I	2.18	-2.55	178.4	137.1	186.1	173.1	196.7	169.8	190.6	185.0	167.5	195.1	125.9	195.1	176.7	189.2	182.5	199.8
6271.28	Fe I	3.32	-2.96	65.9	17.8	52.9	57.7	64.5	54.3	52.2	68.3	71.0	51.7	21.1	57.0	64.9	53.0	67.1	77.7
6297.80	Fe I	2.22	-2.74	...	...	...	...	...	...	...	...	...	...	...	...	...	...	...	...
6301.50	Fe I	3.65	-0.72	...	...	...	...	...	...	...	...	...	...	...	...	...	...	...	...
6307.85	Fe I	3.64	-3.27	16.1	...	...	24.0	...	...	...	...	...	...	...	...	...	...	...	23.3
6322.69	Fe I	2.59	-2.43	162.5	127.2	153.4	164.7	164.6	162.2	164.7	160.1	160.6	172.0	111.3	178.3	158.5	153.4	160.5	179.3
6330.85	Fe I	4.73	-1.22	42.9	...	31.3	48.0	34.2	41.5	37.2	43.4	31.8	27.0	18.2	48.2	39.8	42.7	39.1	37.6
6335.33	Fe I	2.20	-2.23	206.3	173.4	208.8	210.1	218.4	209.7	222.1	221.7	210.4	211.5	141.0	231.0	216.4	216.5	213.1	221.3
6336.82	Fe I	3.69	-1.05	152.0	126.2	141.9	143.0	139.4	138.7	144.1	144.5	170.1	141.9	98.9	163.1	135.3	141.4	136.1	163.9
6344.15	Fe I	2.43	-2.92	184.5	117.9	174.1	185.6	165.2	166.3	173.1	177.7	167.8	163.8	118.9	206.3	160.1	181.2	163.1	187.8
6355.04	Fe I	2.84	-2.29	165.2	116.7	170.7	164.0	159.6	157.0	165.8	163.6	154.9	168.7	87.9	172.1	143.3	172.9	166.7	174.6
6380.75	Fe I	4.19	-1.50	93.9	33.1	73.6	...	77.9	80.3	77.1	79.7	73.4	65.7	28.2	121.3	99.8	56.4	82.7</	

$\lambda(\text{\AA})$	elem	$\chi$	$g^f$	113	115	123	125	132	135	138	140	141	146	147	148	149	150	151	155
6318.72	Mg I	5.11	-1.97	...	16.2	34.9	49.1	34.8	...	35.6	46.7	39.3	30.9	18.4	49.4	...	48.0	35.6	...
6319.24	Mg I	5.11	-2.21	...	16.2	...	...	...	...	20.5	...	...	16.8	...	...	31.6	29.6	15.2	43.2
6319.49	Mg I	5.11	-2.43	...	...	...	...	17.4	...	...	29.5	...	...	...	30.2	...	...	...	...
5420.36	Mn I	2.14	-1.46	200.1	95.8	203.6	197.0	220.8	196.5	222.4	195.4	174.3	207.8	63.7	205.3	181.0	213.1	211.6	210.3
5432.55	Mn I	0.00	-3.80	263.5	179.6	254.6	266.5	291.7	262.1	...	262.5	255.0	255.6	124.9	...	241.8	293.8	261.2	294.8
5516.77	Mn I	2.18	-1.85	...	47.3	147.1	174.4	162.9	148.4	175.0	136.1	144.6	138.2	32.4	162.0	...	155.6	148.7	170.4
6154.23	Na I	2.10	-1.56	41.3	...	...	20.5	20.4	20.9	...	...	21.9	20.2	...	46.1	...	33.3	24.7	27.3
6160.75	Na I	2.10	-1.26	59.5	...	31.9	66.9	22.8	49.0	...	33.4	19.6	26.1	18.9	81.9	41.0	42.1	43.0	58.0
5416.38	Nd II	0.86	-0.98	27.2	19.7	19.3	41.2	34.4	28.6	16.4	...	27.1	38.4	16.3	50.2	...	35.8	38.9	59.2
5431.54	Nd II	1.12	-0.47	72.2	...	48.1	72.8	58.9	63.0	54.4	58.8	51.9	57.6	62.1	103.5	...	66.2	51.0	83.4
5485.71	Nd II	1.26	-0.12	44.5	...	37.1	47.6	33.0	37.2	36.3	33.1	32.1	41.4	58.7	50.5	29.4	32.4	36.1	26.9
5578.73	Ni I	1.68	-2.67	143.8	101.6	125.0	142.4	131.0	144.8	178.3	131.1	141.7	139.2	77.9	157.8	123.1	130.2	141.3	159.8
5587.87	Ni I	0.93	-2.37	178.7	110.3	160.3	167.9	174.8	168.4	160.2	154.8	155.5	164.5	77.3	177.3	146.9	165.8	164.0	161.1
5589.37	Ni I	3.90	-1.15	36.9	16.5	17.4	27.1	26.4	30.7	18.4	16.8	27.5	28.4	23.6	42.3	23.3	26.4	33.0	...
5593.75	Ni I	3.90	-0.79	39.5	24.1	32.6	32.6	30.3	36.5	50.2	40.1	38.7	47.1	21.4	56.9	22.9	30.6	34.2	57.4
6128.97	Ni I	1.68	-3.39	94.9	60.5	87.9	90.5	86.8	88.6	94.2	85.4	81.7	90.6	38.2	106.1	80.3	80.6	80.3	98.7
6130.14	Ni I	4.27	-0.98	...	...	...	15.2	16.4	...	...	27.6	19.6	...	...	28.5	...	...	...	18.3
6177.25	Ni I	1.83	-3.60	60.9	30.1	62.8	59.5	71.7	57.9	52.1	69.8	59.9	61.2	15.5	56.6	52.3	59.5	55.4	68.9
6186.72	Ni I	4.11	-0.90	33.4	...	30.8	39.1	...	18.6	28.9	20.7	20.9	18.1	...	63.2	22.5	...	24.1	46.1
6204.61	Ni I	4.09	-1.15	...	17.6	...	21.5	24.8	...	...	...	...	23.7	...	...	...	...	27.2	26.1
6223.99	Ni I	4.10	-0.97	26.4	...	28.9	33.5	34.3	39.7	37.0	...	32.9	26.1	...	61.9	...	36.7	37.2	34.1
6230.10	Ni I	4.11	-1.20	36.7	...	29.3	...	...	29.4	...	...	...	...	...	...	...	30.0	...	41.0
6322.17	Ni I	4.15	-1.21	...	...	15.2	23.0	...	...	...	...	...	15.4	...	...	23.1	...	...	40.0
6327.60	Ni I	1.68	-3.09	119.6	83.7	118.4	111.7	128.7	102.5	123.2	133.8	95.5	119.3	54.5	106.5	105.5	96.0	113.4	134.1
6378.26	Ni I	4.15	-0.82	33.2	...	27.8	44.3	33.8	...	32.9	35.4	32.5	23.6	...	66.8	...	...	27.1	...
6384.67	Ni I	4.15	-1.00	33.9	21.6	23.3	...	18.5	33.5	31.6	23.5	33.3	16.9	16.8	46.2	22.6	36.5	...	46.1
6482.80	Ni I	1.94	-2.85	101.1	66.4	107.9	114.1	126.7	119.3	111.3	116.9	98.8	108.5	62.4	97.0	95.9	105.9	114.7	115.1
6586.32	Ni I	1.95	-2.79	194.5	133.9	128.3	77.4	184.8	163.8	155.5	150.6	148.5	144.5	...	244.2	45.6	171.5	190.1	198.3
6598.61	Ni I	4.24	-0.93	...	...	...	...	32.1	21.3	30.7	22.5	...	...	...	28.0	27.6	...	...	20.3
6635.14	Ni I	4.42	-0.75	...	...	18.4	21.2	...	...	...	...	...	...	...	...	...	...	...	...
6300.31	O I	0.00	-9.75	...	...	...	60.9	...	...	...	...	...	...	...	...	...	...	49.7	...
6363.79	O I	0.02	-10.25	25.3	...	43.7	27.9	35.3	48.6	56.9	35.5	27.7	38.8	...	76.2	29.8	30.0	42.6	46.1
5526.82	Sc II	1.77	0.03	110.3	114.6	109.6	119.6	111.5	113.9	111.5	103.7	107.1	115.0	104.1	106.8	111.5	113.6	105.3	106.3
6245.62	Sc II	1.51	-0.97	79.5	48.8	86.4	77.6	69.4	69.4	60.4	62.7	59.3	67.5	41.8	95.9	52.3	80.3	67.5	64.6
6309.90	Sc II	1.50	-1.52	55.7	...	42.8	46.8	...	...	44.5	...	27.2	...	...	68.8	...	41.6	...	...
6604.60	Sc II	1.36	-1.31	105.8	63.6	99.6	97.4	82.0	93.5	78.6	83.5	73.7	90.6	80.8	109.0	90.8	77.5	92.9	98.3
6125.03	Si I	5.62	-1.57	...	...	...	...	20.1	20.8	...	...	...	...	...	...	31.7	...	...	...
6142.48	Si I	5.62	-1.51	...	...	...	...	...	...	...	...	...	...	...	...	...	...	...	...
6145.02	Si I	5.61	-1.37	25.9	...	19.3	15.4	...	...	...	...	21.0	16.3	...	...	21.8	25.1	...	...
6155.14	Si I	5.62	-0.80	58.8	...	42.5	46.5	38.9	40.0	50.4	35.3	30.6	52.0	24.6	59.3	47.5	52.5	31.9	49.2
6237.33	Si I	5.61	-1.02	38.7	16.0	20.6	31.0	21.7	18.8	...	20.6	...	24.1	16.8	31.6	21.1	25.6	...	24.1
6243.82	Si I	5.61	-1.27	...	...	...	37.4	...	...	...	22.8	...	22.0	18.5	59.8	...	...	29.3	...
5490.16	Ti I	1.46	-0.93	110.1	58.0	110.6	116.7	120.2	91.1	122.7	109.7	102.3	114.6	27.2	130.8	82.4	111.7	118.5	128.8
5503.90	Ti I	2.58	-0.19	67.9	37.5	58.1	69.5	68.6	61.1	78.3	68.4	48.9	52.4	17.1	101.7	31.1	60.6	65.1	98.4
6126.22	Ti I	1.07	-1.42	116.7	68.4	139.4	137.9	148.0	144.5	150.6	146.2	118.2	132.2	51.4	192.2	112.1	145.7	139.4	153.2
6220.50	Ti I	2.68	-0.14	...	...	64.9	...	76.8	...	...	...	...	...	27.1	...	...	...	91.7	...
6258.10	Ti I	1.44	-0.35	...	98.9	190.7	...	225.1	187.2	206.2	187.1	147.7	182.3	79.2	229.9	152.7	188.5	196.3	219.2
6303.77	Ti I	1.44	-1.57	93.2	42.4	80.8	107.9	91.6	91.4	104.1	86.3	79.1	85.1	...	137.0	61.7	102.3	91.0	106.3
6312.24	Ti I	1.46	-1.55	...	...	...	92.2	88.8	89.8	95.7	83.1	...	71.3	15.5	...	67.4	...	86.2	93.4
6336.10	Ti I	1.44	-1.74	68.1	26.4	74.0	76.7	79.4	76.6	90.5	68.3	65.0	73.7	...	104.9	...	84.8	78.0	86.6
6508.12	Ti I	1.43	-2.05	38.7	...	46.6	68.8	...	61.0	61.7	52.8	30.8	44.5	...	100.9	40.0	52.2	54.7	76.2
6556.08	Ti I	1.46	-1.07	...	...	63.2	143.9	...	...	...	...	111.7	...	...	...	...	139.5	...	...
6599.13	Ti I	0.90	-2.09	131.4	67.1	134.4	152.6	164.2	126.2	147.0	141.4	94.4	127.9	48.6	208.9	99.1	132.2	146.6	157.7
6666.53	Ti I	1.46	-1.62	...	...	16.4	34.4	...	27.9	27.4	16.3	...	...	...	39.6	...	15.5	28.1	32.9
5418.77	Ti II	1.58	-2.11	106.8	93.4	88.2	102.3	109.2	97.9	108.2	109.0	104.4	99.2	82.3	97.1	122.5	112.2	115.8	107.1
6219.94	Ti II	2.06	-2.82	...	...	27.4	...	...	...	...	...	32.2	...	...	60.9	...	29.2	32.8	...
6559.58	Ti II	2.05	-2.02	...	36.1	61.0	...	...	...	...	...	59.4	...	...	57.0	...	66.1	...	...
6606.95	Ti II	2.06	-2.79	50.9	28.4	44.2	54.1	32.3	31.4	31.2	36.8	29.3	...	61.6	37.6	50.0	33.7	35.9	28.7
6680.13	Ti II	3.09	-1.86	33.2	18.7	...	29.1	...	21.6	22.9	...	22.5	...	24.3	...	21.5	35.0	32.5	29.3
6119.53	V I	1.06	-0.32	82.3	...	...	...	...	...	...	...	...	...	...	...	...	...	...	...
6128.33	V I	1.05	-2.30	...	...	...	...	23.1	...	...	17.2	...	...	...	43.4	...	22.1	...	19.0
6135.37	V I	1.05	-0.75	100.8	25.1	100.6	108.0	123.9	100.8	105.6	95.6	93.4	88.5	...	153.8	75.9	90.9	97.9	122.4
6150.15	V I	0.30	-1.79	119.9	59.5	143.2	142.7	168.2	130.2	166.0	141.7	108.0	136.4	...	177.8	102.1	157.5	147.7	169.2
6190.19	V I	0.29	-1.29	171.2	95.8	171.8	180.1	194.0	165.2	199.6	182.2	152.7	161.8	36.4	207.4	139.5	181.2	187.1	213.4
6216.36	V I	0.28	-0.81	160.3	78.5	175.3	189.1	187.8	175.4	199.9	184.7	144.7	170.8	52.3	256.3	154.2	187.2	187.2	207.0
6224.51	V I	0.29	-2.01	120.1	...	121.9	128.5	137.2	113.9	145.1	123.8	103.5	122.7	21.9	177.8	103.8	119.4	132.3	153.6
6233.20	V I	0.28	-2.07	79.7	22.3	99.8	111.8	105.5	76.6	96.4	83.2	72.7	80.9	...	123.7	53.8	90.8	87.9	121.3
6243.11	V I	0.30	-0.98	...	124.7	...	...	...	...	...	...	...	...	...	58.6	...	...	...	...
6251.82	V I	0.29	-1.30	130.4	58.6	144.4	149.5	161.7	135.8	164.0	149.2	115.8	128.4	25.6	188.7	124.9	145.8	143.9	153.2
6274.66	V I	0.27	-1.67	...	...	...	...	133.2	126.7	142.6	114.0	...	113.2	19.0	...	77.9	...	122.1	148.4
6357.29	V I	1.85	-0.91	21.3	...	...	36.8	30.5	24.3	...	23.6	16.9	26.3	36.					

Table 6.A2: Complete line list with parameters and associated  $EW$ 's (in mÅ, measured by DAOSPEC) for all the stars. Part 3/5.

$\lambda(\text{\AA})$	elem	$\chi$	$gf$	156	158	160	163	166	168	171	173	180	185	190	195	196	197	203	204
6141.73	Ba II	0.70	-0.08	225.1	...	240.2	286.5	266.8	229.1	238.0	254.3	...	271.5	221.8	198.9	233.8	248.2	235.4	226.6
6496.91	Ba II	0.60	-0.38	244.0	250.3	248.0	...	...	254.1	238.6	221.7	265.0	290.5	279.9	230.2	229.5	231.6	294.5	293.4
6122.23	Ca I	1.89	-0.32	215.2	219.7	242.5	287.1	251.3	245.5	247.3	258.7	210.9	254.2	249.5	205.9	225.2	236.6	245.0	234.6
6156.03	Ca I	2.52	-2.39	...	22.1	32.8	40.5	...	...	...	...	29.0	30.0	44.3	20.5	...	20.3	37.2	...
6161.30	Ca I	2.52	-1.27	82.4	117.5	119.1	152.0	138.7	132.7	115.0	143.1	128.1	146.0	122.7	93.3	111.4	140.4	143.2	114.8
6162.17	Ca I	1.90	-0.32	236.3	240.9	261.9	299.6	263.2	271.3	268.3	285.0	256.5	294.3	254.4	238.4	251.0	253.5	251.8	270.0
6166.44	Ca I	2.52	-1.14	89.8	102.1	122.8	137.7	117.9	110.2	121.7	132.9	108.8	132.6	134.0	93.0	115.0	127.3	128.5	112.0
6169.04	Ca I	2.52	-0.80	128.6	116.8	136.9	160.1	143.0	154.3	147.0	145.1	101.7	154.0	145.7	108.5	128.6	124.5	148.2	140.9
6169.56	Ca I	2.52	-0.48	131.8	148.2	162.7	181.1	174.7	173.7	177.3	156.9	127.1	165.2	155.1	130.8	156.6	145.7	161.1	156.5
6439.08	Ca I	2.52	0.39	200.2	228.1	212.2	251.3	229.0	232.1	243.3	232.7	...	236.3	246.8	202.8	216.5	...	237.1	...
6455.60	Ca I	2.52	-1.29	81.4	127.6	154.4	225.1	178.2	184.1	163.1	198.1	...	171.9	166.4	124.8	110.0	...	106.9	...
6471.67	Ca I	2.52	-0.76	...	...	...	...	...	...	...	...	...	...	...	...	...	...	...	...
6493.79	Ca I	2.52	-0.32	168.5	163.9	179.8	198.6	192.5	186.1	199.3	193.7	185.8	182.5	192.0	152.5	182.4	207.2	192.7	208.7
6499.65	Ca I	2.52	-0.82	109.3	117.4	123.9	150.4	124.5	133.7	131.7	139.9	132.3	142.3	130.2	106.8	124.4	151.7	137.3	132.1
6508.84	Ca I	2.52	-2.41	...	16.5	32.7	42.6	23.9	24.2	26.2	20.6	24.7	45.6	25.6	18.7	21.1	43.6	38.5	...
6330.09	Cr I	0.94	-2.92	104.5	117.7	122.9	152.9	117.2	131.3	150.5	142.5	120.8	158.1	133.9	92.1	137.3	136.1	132.3	126.3
6645.13	Eu II	1.37	0.20	60.6	73.1	60.1	79.0	56.8	67.5	57.4	61.5	73.6	69.8	61.4	50.0	58.8	76.5	68.6	103.2
5369.96	Fe I	4.37	0.54	162.0	166.7	206.6	171.3	151.9	168.6	178.3	143.9	155.9	...	160.8	192.0	199.2	167.9	147.9	153.2
5383.37	Fe I	4.31	0.50	169.9	166.2	139.3	175.2	185.8	173.5	171.8	169.9	150.5	163.7	171.9	157.3	163.1	172.5	140.9	156.9
5386.34	Fe I	4.16	-1.74	53.6	53.1	54.8	47.3	38.5	...	54.9	56.4	54.0	67.3	62.0	25.5	44.7	37.7	48.4	58.9
5393.17	Fe I	3.24	-0.92	183.9	210.6	219.9	230.0	229.4	216.6	211.2	251.7	193.1	218.9	204.4	181.8	194.5	179.7	220.3	197.7
5395.22	Fe I	4.45	-1.73	20.7	...	...	...	34.8	35.1	22.3	16.2	24.3	...	26.4	42.7	...	19.6	21.3	...
5405.79	Fe I	0.99	-1.85	...	...	...	...	...	...	...	...	...	...	...	...	...	...	...	...
5415.19	Fe I	4.39	0.51	136.8	151.1	159.0	193.5	181.7	175.9	195.7	191.2	137.7	163.0	176.3	163.9	169.2	150.8	174.7	153.3
5417.04	Fe I	4.42	-1.42	47.1	40.0	70.3	49.3	52.3	53.5	43.0	57.7	...	53.1	48.2	46.1	46.2	...	19.9	33.8
5434.53	Fe I	1.01	-2.12	...	...	...	...	...	...	...	...	...	...	...	...	...	...	...	...
5436.30	Fe I	4.39	-1.35	...	101.2	...	...	...	...	...	...	...	...	...	...	...	...	...	...
5464.29	Fe I	4.14	-1.62	27.8	57.0	76.3	78.1	67.3	56.4	50.9	60.2	72.8	67.2	57.1	61.1	38.4	72.1	...	54.1
5470.09	Fe I	4.45	-1.60	...	25.4	28.3	42.6	22.5	16.5	...	40.6	38.9	32.0	21.5	21.8	19.7	30.1	18.4	17.6
5501.48	Fe I	0.96	-3.05	234.0	233.3	257.0	278.4	266.8	264.8	282.2	272.6	232.1	255.2	280.6	243.2	262.5	274.4	261.9	230.6
5506.79	Fe I	0.99	-2.79	262.4	295.6	...	...	...	...	...	...	290.0	...	...	274.6	...	...	...	295.9
5539.29	Fe I	3.64	-2.59	32.4	64.9	65.7	76.2	70.3	57.9	57.3	85.4	43.4	75.9	57.1	53.5	46.2	39.2	57.9	40.8
5586.77	Fe I	3.37	-0.10	227.9	246.8	223.8	250.6	246.9	237.1	230.5	256.1	168.4	232.4	238.7	221.8	220.4	202.2	243.4	195.1
6120.26	Fe I	0.91	-5.94	76.0	99.1	96.3	110.2	103.0	109.5	94.5	82.0	63.8	83.3	107.0	66.7	88.7	90.0	98.9	82.2
6136.62	Fe I	2.45	-1.50	...	...	...	...	...	...	...	...	...	...	...	227.1	261.7	281.1	...	...
6137.00	Fe I	2.20	-2.95	...	...	...	...	...	...	...	...	...	...	...	171.3	158.0	170.5	...	...
6151.62	Fe I	2.18	-3.37	113.5	140.1	130.2	133.1	138.0	122.9	129.2	143.7	122.6	144.0	143.0	126.9	128.2	129.0	133.4	126.1
6157.75	Fe I	4.07	-1.26	94.5	101.4	116.5	120.5	112.6	120.9	109.4	112.1	141.1	118.0	108.9	95.3	105.5	121.0	115.0	121.7
6159.38	Fe I	4.61	-1.97	20.1	...	...	28.6	...	...	...	20.8	...	38.7	17.0	...	...	24.3	20.3	18.5
6165.36	Fe I	4.14	-1.47	155.7	67.6	71.0	76.0	72.6	67.6	64.9	69.3	66.4	87.0	80.6	66.7	67.5	69.9	73.3	54.5
6173.34	Fe I	2.22	-2.85	142.5	142.6	173.1	169.8	155.6	157.9	153.4	165.3	160.6	162.6	182.1	155.7	154.8	163.1	163.9	162.8
6180.20	Fe I	2.73	-2.78	111.3	119.3	126.8	...	154.7	170.7	147.2	144.3	74.0	126.0	151.5	118.7	...	102.6	137.8	133.2
6187.99	Fe I	3.94	-1.58	64.3	64.9	82.2	85.5	83.3	79.1	68.8	82.8	73.2	81.0	79.5	64.7	77.8	81.6	74.0	71.1
6200.31	Fe I	2.61	-2.44	145.8	135.5	155.6	168.8	148.7	150.1	155.4	157.8	147.7	151.6	159.6	132.3	148.6	130.0	156.1	145.8
6213.43	Fe I	2.22	-2.66	171.7	193.8	185.5	195.0	192.3	181.1	201.0	191.1	187.4	203.5	205.5	164.8	190.2	193.6	184.3	190.5
6219.29	Fe I	2.20	-2.44	187.0	207.9	201.6	214.2	204.7	187.9	193.5	211.4	192.1	223.9	205.5	183.7	193.6	202.9	198.7	201.7
6226.74	Fe I	3.88	-2.20	33.5	58.5	59.9	71.2	59.1	59.8	54.7	45.7	58.4	60.0	72.2	68.3	55.5	60.3	72.0	68.6
6252.57	Fe I	2.40	-1.76	188.6	190.2	210.8	222.0	217.8	200.5	202.5	209.8	198.5	199.5	223.8	194.3	211.5	214.7	190.6	202.6
6265.13	Fe I	2.18	-2.55	174.0	168.5	192.2	193.1	192.4	185.9	188.1	170.4	173.1	185.7	196.2	162.4	184.3	187.6	176.2	182.3
6271.28	Fe I	3.32	-2.96	47.9	52.8	55.0	66.9	60.2	61.6	53.1	72.0	61.2	62.3	61.9	44.7	51.7	61.7	55.3	70.6
6297.80	Fe I	2.22	-2.74	...	...	...	...	...	...	...	...	...	...	...	...	...	...	...	...
6301.50	Fe I	3.65	-0.72	...	...	...	...	...	...	...	...	...	...	...	...	...	...	...	...
6307.85	Fe I	3.64	-3.27	...	...	...	23.2	...	...	...	33.5	...	...	...	...	...	18.3	...	...
6322.69	Fe I	2.59	-2.43	151.4	148.5	160.4	165.2	147.5	166.0	169.9	171.5	137.3	162.4	173.7	140.8	156.4	158.7	140.2	153.5
6330.85	Fe I	4.73	-1.22	22.6	31.5	39.7	38.0	38.9	36.2	26.2	38.3	35.7	43.1	37.8	25.8	25.2	34.7	28.5	50.5
6335.33	Fe I	2.20	-2.23	198.4	198.9	207.1	227.9	206.1	194.0	209.6	229.7	201.3	223.0	246.2	188.2	220.2	221.9	213.3	212.8
6336.82	Fe I	3.69	-1.05	153.7	138.2	142.5	153.3	138.0	154.9	144.5	164.3	144.8	144.1	154.6	137.6	149.2	144.0	134.1	140.9
6344.15	Fe I	2.43	-2.92	161.7	167.4	163.1	201.9	177.3	165.8	169.7	188.9	175.8	198.2	183.3	126.5	...	163.6	168.5	160.7
6355.04	Fe I	2.84	-2.29	131.6	154.5	151.7	158.8	158.5	147.6	153.7	165.2	165.5	174.2	160.0	139.9	163.1	161.3	155.1	138.5
6380.75	Fe I	4.19	-1.50	50.2	88.4	74.7	93.3	67.6	80.9	68.7	96.5	72.3	99.7	90.6	77.2	80.1	75.6	84.5	99.0
6392.54	Fe I	2.28	-3.95	82.1	91.4	87.2	90.5	...	76.7	88.9	116.1	75.4	93.4	97.6	66.6	88.9	91.1	98.1	94.1
6393.61	Fe I	2.43	-1.63	225.5	226.0	241.8	257.2	227.9	243.4	251.5	249.0	236.4	258.3	256.2	225.2	236.9	220.9	242.8	235.4
6408.03	Fe I	3.69	-1.00	124.1	126.1	145.9	177.4	151.3	144.5	165.7	152.3	...	169.4	150.4	138.7	159.9	...	128.7	...
6419.96	Fe I	4.73	-0.24	91.4	112.4	106.4	123.4	89.2	96.0	112.2	120.5	...	113.2	115.1	104.2	103.8	...	107.7	...
6421.36	Fe I	2.28	-2.01	209.8	226.0	215.6	242.9	231.2	194.9	223.8	255.2	...	232.8	241.4	185.8	220.4	...	222.5	...
6430.86	Fe I	2.18	-1.95	230.1	248.4	236.8	275.6	260.											

$\lambda(\text{\AA})$	elem	$\chi$	$g^f$	156	158	160	163	166	168	171	173	180	185	190	195	196	197	203	204
6318.72	Mg I	5.11	-1.97	...	37.4	29.8	41.1	37.8	32.0	38.7	36.9	33.1	47.8	29.6	32.7	...	40.3	37.3	...
6319.24	Mg I	5.11	-2.21	20.3	35.0	...	...	25.3	...	30.1	25.5	...	25.5	...	...	...	...	28.9	...
6319.49	Mg I	5.11	-2.43	...	...	...	...	...	...	...	...	...	...	...	...	...	31.2	...	...
5420.36	Mn I	2.14	-1.46	150.2	206.1	203.1	221.2	215.5	189.3	222.0	210.7	181.6	211.2	208.7	169.8	168.1	198.9	217.9	180.9
5432.55	Mn I	0.00	-3.80	214.4	255.9	264.5	...	269.7	274.6	...	...	241.8	272.8	287.4	191.7	258.7	297.8	297.4	254.9
5516.77	Mn I	2.18	-1.85	95.4	...	151.6	166.5	151.8	133.5	138.1	...	130.4	162.3	145.0	108.8	133.6	159.5	152.5	142.7
6154.23	Na I	2.10	-1.56	...	22.3	...	41.9	19.6	...	...	25.5	19.3	49.6	...	18.2	...	23.6	24.3	...
6160.75	Na I	2.10	-1.26	...	42.3	40.7	53.0	47.3	47.9	...	59.0	45.5	54.0	...	23.7	19.0	42.0	53.5	37.6
5416.38	Nd II	0.86	-0.98	35.7	35.1	43.2	54.3	38.9	29.1	30.3	28.6	...	...	...	16.6	28.8	...	...	...
5431.54	Nd II	1.12	-0.47	...	80.1	52.8	76.6	60.0	47.6	45.2	77.4	66.9	68.0	54.2	31.0	34.9	49.7	65.3	46.7
5485.71	Nd II	1.26	-0.12	19.8	33.2	42.0	53.0	43.5	35.4	17.7	30.8	61.9	51.3	26.4	18.0	40.2	43.7	40.8	...
5578.73	Ni I	1.68	-2.67	112.7	147.7	142.8	145.1	147.2	142.7	128.4	156.1	130.1	150.4	143.3	115.8	132.9	135.1	136.1	121.8
5587.87	Ni I	0.93	-2.37	136.7	147.5	163.4	191.0	175.0	167.2	154.0	169.1	146.5	176.9	161.7	153.4	150.3	143.2	153.9	137.3
5589.37	Ni I	3.90	-1.15	...	...	26.9	...	19.9	23.5	31.0	36.2	25.2	45.0	19.1	22.3	21.7	35.6	23.8	32.3
5593.75	Ni I	3.90	-0.79	...	23.7	49.4	47.4	45.0	43.7	34.6	41.7	54.7	34.6	40.8	40.3	39.4	27.0	32.1	40.5
6128.97	Ni I	1.68	-3.39	68.1	79.7	76.2	84.7	82.6	89.9	84.1	83.6	79.3	95.2	87.8	69.8	72.5	86.7	98.0	76.8
6130.14	Ni I	4.27	-0.98	...	...	16.4	23.1	...	...	...	...	...	...	...	...	29.0	...	...	...
6177.25	Ni I	1.83	-3.60	54.1	53.2	69.2	79.8	51.3	62.1	69.6	55.4	44.1	64.2	67.1	38.7	55.5	57.8	56.6	60.8
6186.72	Ni I	4.11	-0.90	18.1	20.5	35.0	39.3	28.1	42.4	24.0	33.1	23.7	32.2	35.7	23.5	16.5	23.8	32.3	20.9
6204.61	Ni I	4.09	-1.15	...	20.4	36.3	38.5	15.0	21.8	...	25.7	...	16.3	30.5	...	...	...	...	...
6223.99	Ni I	4.10	-0.97	...	...	20.6	47.2	...	22.3	...	33.9	18.6	41.4	...	...	21.7	36.9	38.3	...
6230.10	Ni I	4.11	-1.20	...	...	29.2	...	...	...	27.6	29.1	37.6	47.3	...	...	...	20.5	...	...
6322.17	Ni I	4.15	-1.21	...	30.6	...	...	...	...	32.4	20.6	46.5	...	26.7	...	...	...	...	...
6327.60	Ni I	1.68	-3.09	106.8	117.3	114.2	132.6	112.0	106.7	105.5	130.8	109.1	123.6	114.1	99.2	116.8	122.5	93.3	107.2
6378.26	Ni I	4.15	-0.82	20.6	33.7	28.8	33.4	44.1	27.9	38.4	...	32.6	23.7	15.5	...	27.7	...	34.5	...
6384.67	Ni I	4.15	-1.00	...	...	26.3	41.4	31.7	26.6	28.4	...	...	42.2	...	...	...	22.3	...	...
6482.80	Ni I	1.94	-2.85	105.1	116.7	109.1	120.5	106.3	97.9	101.4	113.7	104.0	113.9	106.0	96.5	102.1	131.1	111.4	109.4
6586.32	Ni I	1.95	-2.79	57.5	84.8	133.6	210.7	143.3	217.8	183.8	192.6	...	176.2	185.4	109.3	179.5	...	92.3	...
6598.61	Ni I	4.24	-0.93	...	...	17.0	...	30.3	...	34.6	...	...	...	...	...	...	...	...	...
6635.14	Ni I	4.42	-0.75	29.3	...	...	...	...	...	...	...	25.1	...	...	...	...	38.8	25.7	...
6300.31	O I	0.00	-9.75	...	66.7	...	...	...	...	...	...	...	...	...	...	...	...	...	...
6363.79	O I	0.02	-10.25	...	43.1	...	46.5	32.7	33.3	41.0	82.8	33.3	43.3	35.4	22.6	...	42.8	34.7	38.5
5526.82	Sc II	1.77	0.03	116.2	104.1	119.5	105.9	110.4	99.2	130.1	95.1	123.1	118.7	99.5	99.6	124.8	115.6	129.0	112.1
6245.62	Sc II	1.51	-0.97	74.3	73.9	75.9	61.7	65.2	65.3	78.0	72.4	82.5	64.3	...	62.0	71.6	57.8	82.2	65.5
6309.90	Sc II	1.50	-1.52	...	...	38.9	...	41.7	41.5	39.1	...	40.4	...	29.6	...	30.4	...	47.4	46.8
6604.60	Sc II	1.36	-1.31	79.4	96.7	80.9	105.7	58.9	84.3	102.2	88.2	101.6	74.8	76.6	89.8	81.3	112.3	101.7	130.0
6125.03	Si I	5.62	-1.57	...	...	...	...	...	...	...	...	...	...	...	...	...	...	...	...
6142.48	Si I	5.62	-1.51	...	...	...	...	...	...	...	...	...	18.4	...	...	...	...	...	...
6145.02	Si I	5.61	-1.37	20.6	17.7	21.8	...	...	...	...	...	...	22.4	...	...	...	...	...	...
6155.14	Si I	5.62	-0.80	...	38.4	36.0	45.6	29.4	32.6	...	55.7	54.0	53.8	35.9	46.7	38.5	44.0	34.2	47.1
6237.33	Si I	5.61	-1.02	18.4	...	31.0	26.0	...	17.4	...	...	31.4	...	15.2	15.8	...	24.4	19.9	...
6243.82	Si I	5.61	-1.27	15.7	31.6	33.4	...	36.7	33.6	...	...	...	43.3	...	...	23.6	...	43.2	...
5490.16	Ti I	1.46	-0.93	70.3	98.8	124.8	133.6	109.2	111.7	104.3	130.2	84.2	114.5	118.2	68.1	88.1	108.5	126.7	111.7
5503.90	Ti I	2.58	-0.19	23.3	49.9	71.0	87.9	64.4	66.8	51.1	76.5	45.1	73.1	68.1	25.3	47.4	58.7	62.7	41.7
6126.22	Ti I	1.07	-1.42	113.8	119.7	138.8	153.9	132.6	132.0	132.4	152.3	124.4	149.9	147.5	101.3	120.6	145.1	154.4	126.1
6220.50	Ti I	2.68	-0.14	...	80.5	...	69.0	...	...	72.4	...	90.4	...	...	...	...	...	...	...
6258.10	Ti I	1.44	-0.35	138.9	157.8	186.4	219.4	176.7	206.5	...	207.7	149.3	197.1	191.4	117.3	158.3	205.0	185.6	178.4
6303.77	Ti I	1.44	-1.57	33.8	60.0	...	86.3	87.1	98.3	71.8	105.4	78.6	105.8	79.9	44.6	79.1	90.3	80.7	78.9
6312.24	Ti I	1.46	-1.55	37.9	60.4	81.1	97.8	72.4	...	68.2	88.5	...	87.9	84.4	44.5	...	89.6	89.7	75.1
6336.10	Ti I	1.44	-1.74	36.1	54.6	73.5	102.5	75.8	68.5	83.5	100.7	54.6	97.4	64.3	36.0	62.0	79.5	73.6	82.2
6508.12	Ti I	1.43	-2.05	...	24.8	62.3	...	56.1	42.3	42.8	59.6	33.9	64.9	45.2	22.9	33.8	65.3	54.9	57.5
6556.08	Ti I	1.46	-1.07	...	...	...	...	...	133.3	...	126.7	...	...	...	...	123.4	...	...	...
6599.13	Ti I	0.90	-2.09	72.4	93.8	141.2	166.2	117.3	136.8	144.5	178.2	...	154.9	138.3	75.9	119.3	...	115.4	...
6666.53	Ti I	1.46	-1.62	...	29.9	...	19.5	...	18.8	...	22.5	24.3	42.7	...	16.2	...	30.3	20.7	...
5418.77	Ti I	1.58	-2.11	95.7	108.8	110.7	113.7	102.1	112.0	124.6	113.1	89.6	101.4	107.3	94.0	94.2	104.3	100.3	97.9
6219.94	Ti I	2.06	-2.82	...	36.6	...	...	...	24.0	...	29.5	...	31.7	29.9	19.0	20.8	...	...	...
6559.58	Ti I	2.05	-2.02	...	...	...	...	...	...	...	...	66.8	...	...	...	50.8	...	...	...
6606.95	Ti I	2.06	-2.79	36.6	43.4	43.2	59.3	41.4	21.7	30.1	49.3	62.8	41.2	...	41.6	34.3	61.9	...	116.7
6680.13	Ti I	3.09	-1.86	...	30.1	...	41.2	35.1	...	33.8	46.0	27.6	18.9	24.0	27.8	23.6	42.1	29.4	41.7
6119.53	Vi I	1.06	-0.32	...	...	...	95.2	...	85.0	83.8	...	...	...	71.8	...	...	...	...	...
6128.33	Vi I	1.05	-2.30	...	...	...	28.4	...	...	...	...	...	...	...	...	...	...	...	...
6135.37	Vi I	1.05	-0.75	59.0	74.2	98.4	125.6	94.6	92.1	90.6	120.3	88.8	120.2	98.7	44.8	76.0	116.9	107.6	79.7
6150.15	Vi I	0.30	-1.79	96.1	122.6	143.3	167.4	136.1	150.2	144.5	172.1	95.1	165.9	131.1	69.0	123.5	153.3	143.5	140.1
6199.19	Vi I	0.29	-1.29	111.7	150.8	204.2	202.9	166.0	178.2	177.3	214.4	144.4	195.4	186.9	101.1	155.0	180.9	193.7	...
6216.36	Vi I	0.28	-0.81	128.8	168.3	182.5	194.6	176.4	177.0	164.9	199.8	166.2	203.9	184.0	119.0	150.0	196.7	182.8	178.4
6224.51	Vi I	0.29	-2.01	73.1	101.4	134.9	147.3	121.0	142.6	130.0	147.7	101.6	150.4	120.1	72.8	99.1	136.0	136.8	108.5
6233.20	Vi I	0.28	-2.07	39.5	73.3	100.9	96.7	81.9	93.7	88.3	100.8	66.8	108.1	91.8	29.3	72.9	104.0	100.5	72.9
6243.11	Vi I	0.30	-0.98	...	234.4	...	...	...	284.4	...	...	...	...	...	177.1	...	...	...	...
6251.82	Vi I	0.29	-1.30	97.9	116.9	144.0	149.8	144.7	144.5	135.5	158.8	128.1	172.4	147.0	83.6	130.8	161.6	151.6	134.5
6274.66	Vi I	0.27	-1.67	65.1	108.5	133.7	132.8	...	...	...	134.1	...	127.4	...	57.2	...	128.9	119.2	...
6357.29	Vi I	1.85	-0.91	...	23.3	25.5	30.9	31.4	...	...	35.0	...	35.2	20.4	19.6	...	...	26.4	...
6452.32	Vi I	1.19																	

Table 6.A2: Complete line list with parameters and associated  $EW$ 's (in mÅ, measured by DAOSPEC) for all the stars. Part 4/5.

				Equivalent width, one star per column, BLxxx															
$\lambda(\text{\AA})$	elem	$\chi$	$gf$	205	208	210	211	213	216	218	221	227	228	229	233	239	242	247	250
6141.73	Ba II	0.70	-0.08	267.8	259.2	265.1	271.8	252.9	282.6	...	251.0	244.0	215.3	275.9	261.5	228.5	226.7	250.1	...
6496.91	Ba II	0.60	-0.38	243.1	270.3	284.0	297.9	235.1	281.4	280.7	256.7	268.8	232.7	284.4	247.9	258.8	250.3	246.8	...
6122.23	Ca I	1.89	-0.32	244.8	250.7	233.3	279.0	246.7	276.6	...	247.1	230.7	248.7	267.5	242.6	228.3	213.3	250.5	...
6156.03	Ca I	2.52	-2.39	...	26.0	25.6	36.6	24.6	42.3	39.8	25.7	26.1	35.5	42.9	26.5	20.7	28.5	36.9	38.6
6161.30	Ca I	2.52	-1.27	150.3	142.6	145.4	155.4	137.5	160.3	163.3	127.7	136.1	129.6	143.4	141.2	108.0	106.0	145.6	167.0
6162.17	Ca I	1.90	-0.32	261.5	273.6	274.5	...	268.1	...	...	255.5	266.5	269.6	289.8	285.5	249.2	237.1	279.7	...
6166.44	Ca I	2.52	-1.14	133.0	132.0	119.9	146.1	117.2	136.1	148.2	117.9	117.6	123.8	158.7	121.9	118.0	96.5	133.1	174.5
6169.04	Ca I	2.52	-0.80	144.1	155.5	133.2	156.5	152.7	149.2	148.9	144.0	126.5	150.0	146.1	147.2	150.0	95.7	147.2	170.9
6169.56	Ca I	2.52	-0.48	164.3	170.2	176.8	167.0	159.8	171.8	183.3	167.8	169.8	153.2	176.3	164.3	146.0	117.5	169.5	210.3
6439.08	Ca I	2.52	0.39	225.4	228.8	231.7	234.7	227.2	...	243.2	205.2	210.7	231.2	235.4	235.6	224.7	200.1	237.1	243.9
6455.00	Ca I	2.52	-1.29	192.1	161.5	184.7	113.3	117.5	...	...	57.1	102.5	133.8	175.2	185.3	175.1	123.0	163.5	222.9
6471.67	Ca I	2.52	-0.76	...	...	...	...	...	...	...	...	...	...	...	...	...	...	...	...
6493.79	Ca I	2.52	-0.32	195.2	181.3	191.7	191.3	182.7	222.4	223.7	179.6	178.8	189.8	208.7	196.6	180.4	160.4	163.1	190.3
6499.65	Ca I	2.52	-0.82	111.5	122.6	135.9	140.6	124.9	153.6	145.6	115.7	124.0	116.1	137.1	126.6	126.6	125.1	121.6	159.1
6508.84	Ca I	2.52	-2.41	31.7	36.6	32.1	50.9	25.0	67.1	58.0	36.9	24.0	18.6	41.6	33.1	22.5	16.0	25.5	67.4
6330.09	Cr II	0.94	-2.92	122.0	122.3	132.8	160.3	130.2	161.8	160.6	133.3	138.7	150.4	142.5	132.2	116.1	120.3	147.0	178.8
6645.13	Eu I	1.37	0.20	57.2	52.8	72.2	74.0	68.7	86.3	68.4	83.5	76.2	50.7	80.2	65.1	40.1	47.2	66.4	62.5
5369.96	Fe I	4.37	0.54	167.4	163.5	164.9	168.3	147.9	175.4	146.3	201.7	148.9	217.2	...	152.5	148.5	134.5	194.3	199.0
5383.37	Fe I	4.31	0.50	181.5	162.1	170.0	164.5	169.7	172.1	204.0	171.3	166.6	166.8	165.7	169.5	145.3	155.0	182.6	177.1
5386.34	Fe I	4.16	-1.74	60.5	52.5	53.0	...	53.7	55.1	59.5	...	22.1	46.8	51.8	61.5	72.8	25.3	60.5	...
5393.17	Fe I	3.24	-0.92	221.4	227.6	200.5	209.7	222.4	226.2	211.3	211.4	210.9	209.1	231.5	230.0	224.4	201.2	222.3	246.8
5395.22	Fe I	4.45	-1.73	25.6	24.3	24.7	37.6	...	31.9	36.1	...	44.0	35.6	19.7	40.2	...	...	...	36.0
5405.79	Fe I	0.99	-1.85	...	...	...	...	...	...	...	...	...	...	...	...	...	...	...	...
5415.19	Fe I	4.39	0.51	188.5	163.3	179.9	185.6	175.6	172.9	163.6	144.5	153.8	173.8	172.0	164.7	179.3	133.7	189.9	170.1
5417.04	Fe I	4.42	-1.42	47.8	44.0	45.5	36.5	28.8	40.2	49.6	32.7	49.8	44.8	34.4	46.3	67.8	27.4	58.3	42.6
5434.53	Fe I	1.01	-2.12	...	...	...	...	...	...	...	...	...	...	...	...	...	...	...	...
5436.30	Fe I	4.39	-1.35	...	...	...	...	...	...	...	...	...	...	...	...	...	...	...	...
5464.29	Fe I	4.14	-1.62	78.2	81.2	59.0	...	56.1	88.6	89.9	62.3	61.6	54.0	81.9	85.5	55.0	61.4	52.1	...
5470.09	Fe I	4.45	-1.60	24.2	28.7	...	51.0	29.4	55.1	32.4	20.7	39.1	16.2	...	30.9	22.1	...	26.7	57.7
5501.48	Fe I	0.96	-3.05	250.9	257.7	261.3	265.2	254.2	274.4	297.6	242.7	230.1	273.8	279.0	263.5	260.7	238.4	274.6	...
5506.79	Fe I	0.99	-2.79	...	...	...	...	...	...	...	275.1	...	...	...	...	297.8	282.4	...	...
5539.29	Fe I	3.64	-2.59	75.1	72.4	73.9	82.0	61.6	74.2	95.8	58.1	60.1	54.3	78.0	71.8	56.2	36.9	78.9	86.2
5586.77	Fe I	3.37	-0.10	299.6	237.1	247.2	236.5	236.5	222.0	249.5	214.1	192.1	235.0	242.8	238.3	231.8	192.0	279.5	288.0
6120.26	Fe I	0.91	-5.94	78.6	78.7	89.7	107.2	105.7	96.8	113.2	88.6	75.8	100.8	97.2	82.1	82.5	63.2	87.8	112.1
6136.62	Fe I	2.45	-1.50	...	...	...	288.4	...	...	...	...	...	...	...	...	...	255.6	...	...
6137.00	Fe I	2.20	-2.95	...	...	...	164.4	...	...	174.1	...	...	...	...	...	...	164.9	...	...
6151.62	Fe I	2.18	-3.37	134.8	134.6	126.9	147.0	136.5	142.0	141.4	124.7	137.7	139.2	133.4	150.7	125.6	115.7	147.1	146.2
6157.75	Fe I	4.07	-1.26	122.8	123.1	115.8	127.0	118.0	124.3	132.6	108.9	116.6	102.5	125.4	134.5	109.0	103.9	121.7	109.4
6159.38	Fe I	4.61	-1.97	16.6	...	16.8	34.0	...	...	40.8	19.3	...	26.7	...	16.9	...	...	...	...
6165.36	Fe I	4.14	-1.47	65.1	72.9	73.8	76.1	68.3	70.3	74.1	68.4	64.8	78.8	77.9	80.4	58.5	52.3	68.7	97.4
6173.34	Fe I	2.22	-2.85	167.9	171.2	159.8	156.2	160.9	166.2	179.1	166.7	159.6	165.3	179.0	179.5	150.8	156.8	177.6	175.4
6180.20	Fe I	2.73	-2.78	142.3	135.5	158.9	133.2	137.1	131.0	141.5	122.1	107.0	133.3	143.2	139.8	138.4	87.1	141.0	144.5
6187.99	Fe I	3.94	-1.58	80.3	86.8	97.2	85.8	78.7	80.5	85.4	77.2	66.0	78.5	77.8	70.5	78.7	60.8	92.8	94.0
6200.31	Fe I	2.61	-2.44	157.3	150.8	157.3	150.1	148.1	152.8	147.3	154.7	129.6	156.9	159.5	155.7	159.0	141.7	175.0	138.3
6213.43	Fe I	2.22	-2.66	179.4	184.1	192.5	182.8	191.9	187.1	183.4	196.9	200.1	189.3	198.5	198.0	168.8	177.8	200.1	184.1
6219.29	Fe I	2.20	-2.44	201.7	204.1	198.7	203.1	192.4	204.3	190.6	194.0	198.8	208.5	200.7	198.6	195.0	191.2	223.6	198.7
6226.74	Fe I	3.88	-2.20	71.7	72.4	49.0	70.7	75.1	69.2	70.5	49.4	53.9	59.6	76.6	69.8	53.1	47.5	51.8	87.6
6252.57	Fe I	2.40	-1.76	202.2	196.9	204.6	200.4	200.6	217.1	189.9	193.4	207.3	206.2	203.2	200.5	208.4	189.7	205.0	196.3
6265.13	Fe I	2.18	-2.55	181.0	179.9	199.6	183.7	167.1	189.0	201.1	177.6	181.4	192.7	182.8	173.4	175.5	171.9	188.3	213.4
6271.28	Fe I	3.32	-2.96	71.3	59.8	84.7	81.2	68.9	73.8	71.0	...	56.2	58.1	55.0	63.8	60.7	50.9	51.9	65.4
6297.80	Fe I	2.22	-2.74	...	...	...	...	...	...	...	...	...	...	...	...	...	...	...	...
6301.50	Fe I	3.65	-0.72	...	...	...	...	...	...	...	...	...	...	...	...	...	...	...	...
6307.85	Fe I	3.64	-3.27	...	...	26.1	26.6	...	...	...	...	...	...	...	18.2	...	...	...	...
6322.69	Fe I	2.59	-2.43	152.4	155.6	162.8	151.3	156.4	173.8	168.2	154.4	153.9	179.7	156.8	162.6	153.0	142.6	172.5	170.5
6330.85	Fe I	4.73	-1.22	51.9	63.2	45.0	54.3	37.3	49.6	43.7	35.7	34.3	33.5	52.2	...	39.5	29.9	52.5	26.0
6335.33	Fe I	2.20	-2.23	196.9	216.0	218.7	213.1	216.5	233.3	228.9	206.0	211.5	208.0	226.1	201.3	203.5	202.1	209.1	233.0
6336.82	Fe I	3.69	-1.05	161.6	143.0	160.9	147.3	143.2	155.8	149.3	141.8	143.2	149.9	155.6	142.5	142.7	128.4	158.8	145.1
6344.15	Fe I	2.43	-2.92	187.9	191.9	179.6	195.9	185.9	191.7	200.8	170.1	170.1	174.4	189.4	196.4	159.6	145.3	191.2	204.8
6355.04	Fe I	2.84	-2.29	162.9	164.4	151.7	171.9	170.8	178.9	171.9	152.1	150.7	163.7	139.8	169.0	146.2	136.6	158.0	168.8
6380.75	Fe I	4.19	-1.50	97.3	102.2	89.6	77.1	87.3	90.2	103.2	85.2	83.9	89.3	75.3	9				

$\lambda(\text{\AA})$	elem	$\chi$	$g^f$	205	208	210	211	213	216	218	221	227	228	229	233	239	242	247	250
6318.72	Mg I	5.11	-1.97	46.5	41.8	55.4	46.9	39.1	51.1	47.3	...	...	31.8	35.8	44.6	...	41.6	...	58.6
6319.24	Mg I	5.11	-2.21	...	36.2	...	23.7	...	25.3	33.9	19.2	29.8	...	...	...	19.4	...	43.4	34.6
6319.49	Mg I	5.11	-2.43	...	...	35.7	...	...	...	...	...	...	...	...	24.0	...	36.0	...	...
5420.36	Mn I	2.14	-1.46	222.1	201.1	213.4	230.0	191.8	206.6	221.1	185.9	155.9	217.5	222.2	204.7	224.6	180.7	226.2	211.8
5432.55	Mn I	0.00	-3.80	248.6	272.1	276.2	294.5	270.2	297.9	...	237.3	266.0	278.9	274.8	271.8	257.9	239.2	281.5	...
5516.77	Mn I	2.18	-1.85	158.4	...	175.1	172.6	141.3	191.9	182.3	140.3	160.1	...	178.1	160.3	126.4	131.3	...	157.8
6154.23	Na I	2.10	-1.56	37.4	38.0	36.5	40.5	...	42.5	27.2	...	33.8	16.6	29.5	37.6	16.8	...	24.6	44.5
6160.75	Na I	2.10	-1.26	50.6	51.6	51.1	57.3	40.1	65.8	60.3	27.5	48.6	29.5	51.5	63.1	...	28.9	54.0	88.7
5416.38	Nd II	0.86	-0.98	...	38.9	50.4	43.3	36.4	40.5	40.0	...	34.3	...	21.4	22.1	22.8	...	57.5	65.4
5431.54	Nd II	1.12	-0.47	65.2	60.6	57.3	68.0	...	66.6	73.5	69.4	90.6	47.5	64.9	52.6	30.8	66.1	86.5	66.9
5485.71	Nd II	1.26	-0.12	37.2	40.6	45.4	54.2	41.9	58.1	54.4	50.7	36.4	...	53.4	51.7	25.4	34.8	...	36.7
5578.73	Ni I	1.68	-2.67	142.9	143.8	160.6	142.6	142.5	148.6	164.2	121.6	123.3	150.8	145.0	142.7	129.9	129.3	135.9	184.6
5587.87	Ni I	0.93	-2.37	171.5	168.7	191.9	154.0	154.7	177.2	172.2	131.3	166.7	165.8	184.2	168.3	163.9	121.0	180.6	177.0
5589.37	Ni I	3.90	-1.15	27.6	35.4	31.8	32.0	26.8	28.3	37.3	...	26.3	20.2	20.1	26.7	19.7	17.8	...	...
5593.75	Ni I	3.90	-0.79	51.5	56.2	59.7	43.0	35.4	39.2	43.3	32.4	45.5	35.0	38.1	51.7	29.4	38.9	45.0	49.4
6128.97	Ni I	1.68	-3.39	78.6	85.2	93.6	97.5	93.8	106.0	104.8	90.8	71.8	92.9	90.9	99.0	78.8	79.3	90.2	93.8
6130.14	Ni I	4.27	-0.98	17.0	19.7	...	19.2	...	33.2	...	...	...	...	...	...	...	25.6	...	...
6177.25	Ni I	1.83	-3.60	57.7	68.3	77.5	73.0	58.1	79.0	61.1	54.6	55.8	61.7	76.6	66.2	60.1	45.9	78.2	63.9
6186.72	Ni I	4.11	-0.90	33.5	33.6	40.0	39.3	38.9	50.3	52.2	29.5	22.0	30.9	32.3	30.2	25.1	25.5	41.4	86.0
6204.61	Ni I	4.09	-1.15	28.4	23.7	...	20.2	25.2	...	22.5	16.8	23.9	...	25.1	27.2	27.4	...	30.5	...
6223.99	Ni I	4.10	-0.97	45.0	44.0	41.2	44.4	34.7	28.8	44.0	39.0	...	25.2	40.3	32.3	26.2	31.1	48.3	61.9
6230.10	Ni I	4.11	-1.20	26.8	30.5	39.3	...	26.7	45.1	...	15.2	...	28.3	...	32.0	...	24.3	27.2	46.6
6322.17	Ni I	4.15	-1.21	23.4	26.4	16.4	29.0	21.4	...	...	...	...	...	...	15.2	...	...	...	...
6327.60	Ni I	1.68	-3.09	121.5	118.8	124.0	125.6	103.0	131.3	129.8	116.6	109.6	112.7	116.5	109.8	110.1	97.3	129.5	130.5
6378.26	Ni I	4.15	-0.82	33.2	25.4	23.3	40.5	33.4	32.9	50.0	30.1	31.3	30.8	32.5	34.2	22.8	...	38.5	47.2
6384.67	Ni I	4.15	-1.00	...	...	29.8	47.9	...	38.7	45.6	...	38.8	...	37.7	47.0	...	33.3	58.1	43.2
6482.80	Ni I	1.94	-2.85	103.8	99.7	121.0	116.2	86.2	127.1	117.2	104.6	101.6	105.6	97.7	113.8	103.5	100.4	110.0	125.8
6586.32	Ni I	1.95	-2.79	142.5	165.3	179.6	139.6	154.3	...	157.2	80.0	58.3	150.4	174.5	155.2	154.8	120.3	185.7	185.8
6598.61	Ni I	4.24	-0.93	...	30.9	...	...	...	33.8	17.0	...	17.8	...	...	...	...	42.1	...	...
6635.14	Ni I	4.42	-0.75	...	17.0	...	...	...	36.7	...	31.8	23.1	...	...	...	...	...	20.1	...
6300.31	O I	0.00	-9.75	...	...	...	...	...	...	...	...	...	...	...	...	...	64.4	...	65.4
6363.79	O I	0.02	-10.25	...	39.7	39.4	47.0	44.8	51.8	51.7	34.5	39.3	42.8	50.7	31.8	27.7	37.2	41.5	54.8
5526.82	Sc II	1.77	0.03	112.9	110.3	103.8	104.6	115.0	123.4	99.0	108.6	113.0	100.1	117.8	102.3	118.4	101.7	114.5	103.8
6245.62	Sc II	1.51	-0.97	80.1	72.5	64.2	69.6	77.7	...	69.7	67.1	76.2	64.0	67.8	65.6	61.8	65.4	74.5	69.5
6309.90	Sc II	1.50	-1.52	33.8	...	...	...	46.4	58.7	57.0	...	57.1	22.3	44.7	47.9	...	...	...	...
6604.60	Sc II	1.36	-1.31	87.2	98.9	97.4	100.1	93.4	111.0	98.2	109.9	84.6	92.1	85.0	89.8	87.5	78.4	75.7	95.7
6125.03	Si I	5.62	-1.57	41.7	...	...	48.4	...	...	...	...	16.4	...	...	...	...	...	...	...
6142.48	Si I	5.62	-1.51	...	...	...	...	...	...	...	...	18.5	...	21.8	...	...	...	...	...
6145.02	Si I	5.61	-1.37	...	...	...	...	27.6	19.2	...	...	...	23.1	34.5	...	...	...	...	...
6155.14	Si I	5.62	-0.80	57.4	45.8	40.5	45.3	43.8	51.5	50.1	43.2	54.9	31.3	42.5	45.8	32.7	45.0	42.3	33.1
6237.33	Si I	5.61	-1.02	32.5	28.2	18.4	23.9	21.0	24.3	18.1	23.3	25.5	...	27.3	19.1	23.2	23.2	...	37.4
6243.82	Si I	5.61	-1.27	41.7	47.4	35.3	56.3	29.1	...	...	...	29.2	26.3	46.1	33.8	23.5	...	37.5	40.2
5490.16	Ti I	1.46	-0.93	100.1	107.3	122.6	134.3	112.7	135.9	148.3	109.9	112.4	105.2	123.3	134.1	93.7	95.3	133.0	140.3
5503.90	Ti I	2.58	-0.19	67.3	70.1	71.8	83.0	68.6	88.7	89.3	57.4	44.5	58.7	83.7	79.9	43.2	39.5	71.4	109.5
6126.22	Ti I	1.07	-1.42	122.8	150.5	134.6	164.4	145.3	169.4	170.1	134.9	130.7	143.2	151.8	140.1	118.9	117.5	159.2	189.2
6220.50	Ti I	2.68	-0.14	...	...	...	87.8	...	86.3	...	...	52.1	...	...	...	...	...	65.2	...
6258.10	Ti I	1.44	-0.35	151.1	182.8	187.5	207.9	184.1	228.0	232.0	170.1	199.9	212.6	206.9	178.7	150.3	142.5	153.9	297.9
6303.77	Ti I	1.44	-1.57	77.5	89.4	88.6	118.9	93.1	118.0	115.2	76.7	78.8	86.2	112.3	91.1	80.3	67.8	91.0	122.5
6312.24	Ti I	1.46	-1.55	...	87.6	93.7	109.2	...	...	...	73.4	76.1	92.9	...	91.8	61.6	66.7	74.4	130.0
6336.10	Ti I	1.44	-1.74	67.5	80.4	76.9	94.4	80.4	96.4	98.4	69.0	79.1	77.2	84.1	84.7	55.2	40.0	84.6	128.3
6508.12	Ti I	1.43	-2.05	31.5	45.7	59.1	81.0	57.5	86.4	84.7	45.7	66.1	52.5	66.3	65.7	26.5	...	46.9	110.6
6556.08	Ti I	1.46	-1.07	...	...	...	133.0	...	...	...	...	...	...	...	...	...	...	...	...
6599.13	Ti I	0.90	-2.09	111.3	120.8	153.8	181.9	142.2	...	186.1	101.0	113.8	148.0	156.7	132.8	110.5	99.0	149.9	221.2
6666.53	Ti I	1.46	-1.62	19.2	34.5	34.7	36.1	...	41.7	38.9	...	...	...	35.8	18.4	15.1	...	37.9	59.0
5418.77	Ti II	1.58	-2.11	111.5	96.6	114.0	97.2	111.6	101.5	97.4	103.3	95.0	100.9	109.3	104.3	82.5	80.7	98.5	99.3
6219.94	Ti II	2.06	-2.82	36.1	...	...	...	...	...	...	...	...	...	41.7	37.2	...	28.1	40.3	...
6559.58	Ti II	2.05	-2.02	...	...	...	...	49.2	72.9	54.2	...	...	...	...	...	...	...	...	...
6606.95	Ti II	2.06	-2.79	45.7	49.4	43.0	52.7	40.4	67.7	35.3	55.5	45.0	40.3	25.8	51.0	34.4	48.0	27.7	23.8
6680.13	Ti II	3.09	-1.86	36.3	...	29.2	19.9	22.4	25.4	18.2	26.7	...	28.0	21.7	27.1	...	...	31.5	...
6119.53	VI	1.06	-0.32	...	...	96.7	...	...	...	...	...	...	...	...	...	...	...	...	...
6128.33	VI	1.05	-2.30	...	...	...	...	...	...	...	...	...	...	...	17.8	...	...	...	41.6
6135.37	VI	1.05	-0.75	80.7	100.2	104.6	133.1	102.6	136.0	140.1	89.2	106.0	114.3	122.1	104.1	...	87.5	89.4	150.5
6150.15	VI	0.30	-1.79	120.7	126.9	138.9	158.2	148.7	173.3	182.5	122.2	151.2	162.3	152.9	149.4	112.1	106.3	147.3	198.5
6190.19	VI	0.29	-1.29	155.0	166.1	195.5	221.2	177.2	217.9	212.1	154.2	177.1	186.7	215.9	196.5	144.0	141.5	186.4	232.6
6216.36	VI	0.28	-0.81	150.6	174.7	188.8	200.7	183.0	219.5	213.9	166.7	204.3	195.9	198.9	195.9	152.6	162.2	180.1	225.7
6224.51	VI	0.29	-2.01	177.7	122.9	132.0	159.3	142.3	154.2	161.2	120.2	...	130.9	148.4	140.2	91.9	111.0	141.8	196.7
6233.20	VI	0.28	-2.07	66.4	91.8	95.3	108.2	88.2	128.0	134.0	94.6	99.7	101.9	112.8	94.1	63.2	69.7	81.0	130.6
6243.11	VI	0.30	-0.98	...	...	...	...	...	...	...	...	...	...	...	281.0	...	...	...	...
6251.82	VI	0.29	-1.30	112.2	139.4	140.5	169.3	140.3	177.0	160.9	137.1	155.4	156.3	161.9	141.1	116.6	117.8	135.5	164.7
6274.66	VI	0.27	-1.67	...	111.8	126.9	142.9	...	...	...	109.8	118.2	130.0	...	...</				

Table 6.A2: Complete line list with parameters and associated  $EW$ 's (in mÅ, measured by DAOSPEC) for all the stars. Part 5/5.

$\lambda$ (Å)	elem	$\chi$	$g_f$	Equivalent width, one star per column, BLxxx																
				253	257	258	260	261	262	266	267	269	278	279	295	300	304	311	315	323
6141.73	BaII	0.70	-0.08	287.8	...	297.3	232.5	218.4	230.4	173.6	248.7	246.2	...	167.2	...	293.7	261.3	253.0	215.4	260.3
6496.91	BaII	0.60	-0.38	282.5	290.1	...	228.3	202.2	266.1	185.8	237.1	273.8	...	160.6	...	265.7	244.0	...	193.9	264.9
6122.23	CaI	1.89	-0.32	279.3	291.0	281.2	242.9	236.3	...	182.2	223.9	258.7	...	174.8	...	275.1	271.8	247.5	201.6	252.6
6156.03	CaI	2.52	-2.39	38.4	46.8	43.7	32.1	20.5	...	...	32.0	28.5	45.4	...	...	17.5	15.6	36.5	...	...
6161.30	CaI	2.52	-1.27	163.2	166.7	180.6	127.1	127.9	113.3	50.6	132.8	132.2	177.4	47.0	161.4	145.4	143.2	138.3	87.7	148.1
6162.17	CaI	1.90	-0.32	...	...	...	278.8	266.5	256.1	196.0	270.4	282.6	...	184.9	...	291.6	288.4	277.4	221.8	282.1
6166.44	CaI	2.52	-1.14	148.6	150.4	150.5	136.3	125.4	121.0	64.0	146.7	124.0	147.9	37.8	157.0	135.9	130.7	128.6	103.2	113.8
6169.04	CaI	2.52	-0.80	163.3	169.7	161.6	145.9	135.6	129.1	94.4	148.5	144.6	159.9	64.5	154.9	152.0	149.4	133.3	123.6	105.8
6169.56	CaI	2.52	-0.48	170.4	196.1	182.1	165.5	140.1	154.1	112.4	168.4	151.7	177.3	86.8	196.2	176.1	171.7	171.3	156.6	146.5
6439.08	CaI	2.52	0.39	236.5	223.4	247.4	213.6	209.2	230.1	183.4	225.8	215.5	238.4	155.1	260.0	224.0	228.4	...	207.2	235.2
6455.60	CaI	2.52	-1.29	84.2	113.4	187.4	152.1	...	...	29.3	153.2	75.5	170.9	...	192.0	...	130.8	...	155.9	60.6
6471.67	CaI	2.52	-0.76	...	...	...	...	...	...	...	...	...	...	...	...	...	...	...	...	...
6493.79	CaI	2.52	-0.32	209.7	223.2	189.5	187.3	182.2	181.5	139.8	196.4	194.6	211.4	126.6	199.2	210.3	205.2	204.5	156.9	195.8
6499.65	CaI	2.52	-0.82	144.6	159.2	138.6	118.5	121.0	133.3	77.6	106.5	138.1	151.2	45.9	141.8	127.3	131.3	125.9	105.2	126.8
6508.84	CaI	2.52	-2.41	45.2	57.3	55.8	38.7	32.4	43.9	...	37.1	46.5	61.5	...	57.0	29.9	28.7	38.6	...	41.5
6330.09	CrI	0.94	-2.92	152.8	162.8	163.2	142.5	123.5	130.7	64.1	132.6	130.4	172.1	35.2	159.7	150.2	140.8	137.0	106.9	158.7
6445.13	EuII	1.37	0.20	75.8	74.3	90.6	51.4	62.8	54.1	30.6	64.9	82.4	78.2	34.6	82.9	61.2	59.4	131.1	75.5	70.1
5369.96	FeI	3.37	0.54	171.7	171.0	180.1	182.4	172.0	179.4	112.4	164.9	141.9	247.5	101.7	208.0	164.4	158.8	238.5	145.2	165.1
5383.37	FeI	4.31	0.50	153.4	169.7	181.0	171.1	145.9	149.5	130.6	135.1	153.1	182.5	93.5	173.8	187.3	160.0	139.8	129.9	162.6
5386.34	FeI	4.16	-1.74	...	...	...	...	45.7	33.1	...	56.6	55.8	...	17.7	57.3	...	35.6	39.6	58.9	35.8
5393.17	FeI	3.24	-0.92	226.5	248.5	235.0	210.7	213.9	192.2	169.3	229.2	204.2	235.2	125.3	246.4	218.6	224.3	198.2	210.6	178.5
5395.22	FeI	4.45	-1.73	37.3	39.0	43.7	...	...	17.1	...	31.1	27.5	31.5	...	36.2	...	31.6	29.1	31.2	22.2
5405.79	FeI	0.99	-1.85	...	...	...	...	...	...	283.9	...	...	...	...	284.6	...	...	...	...	...
5415.19	FeI	4.39	0.51	177.9	181.1	190.1	182.6	159.5	166.7	145.1	161.7	146.3	173.3	110.4	178.1	163.2	166.8	141.8	150.5	151.3
5417.04	FeI	4.42	-1.42	65.8	47.7	43.5	36.1	39.1	43.0	19.2	77.1	23.1	33.3	...	46.4	35.3	32.4	...	40.8	23.0
5434.53	FeI	1.01	-2.12	...	...	...	...	...	...	271.4	...	...	...	...	259.8	...	...	...	...	...
5436.30	FeI	4.39	-1.35	...	...	...	...	...	...	...	...	...	...	...	...	...	...	...	...	...
5464.29	FeI	4.14	-1.62	92.2	...	90.0	56.4	59.3	56.0	...	...	74.2	...	...	108.1	71.5	58.9	62.9	19.7	67.0
5470.09	FeI	4.45	-1.60	34.5	46.1	...	28.5	33.1	23.5	...	29.9	31.6	43.6	...	35.5	33.3	29.8	40.3	...	39.2
5501.48	FeI	0.96	-3.05	277.6	268.8	274.5	250.1	264.8	245.2	207.2	250.1	234.0	279.6	185.4	278.9	277.9	241.0	237.5	285.3	...
5506.79	FeI	0.99	-2.79	...	...	...	...	...	290.9	212.0	...	...	...	...	204.9	...	...	294.6	271.7	...
5539.29	FeI	3.64	-2.59	78.5	95.8	83.4	71.9	61.5	55.6	26.6	87.2	52.8	86.6	21.8	84.0	...	57.8	48.2	48.9	61.5
5586.77	FeI	3.37	-0.10	252.5	248.6	278.2	246.4	225.6	213.5	171.9	224.0	199.3	243.8	149.2	274.9	225.7	221.1	190.1	212.5	211.9
6120.26	FeI	0.91	-5.94	101.4	111.6	106.3	102.5	97.4	72.3	28.4	93.0	83.3	96.8	36.1	102.3	94.0	107.8	106.2	76.8	82.3
6136.62	FeI	2.45	-1.50	...	...	...	254.6	...	237.6	274.3	282.0	...	...	159.6	...	...	...	222.3	...	...
6137.00	FeI	2.20	-2.95	...	...	...	172.1	...	...	158.3	163.6	195.8	85.9	...	...	...	...	139.1	...	...
6151.62	FeI	2.18	-3.37	148.8	136.1	144.6	122.5	127.2	128.9	90.8	124.8	122.8	137.6	76.5	149.9	124.0	140.5	128.3	119.4	134.3
6157.75	FeI	4.07	-1.26	129.7	142.4	139.5	102.0	100.3	125.4	59.8	125.9	107.2	143.3	43.0	146.4	127.3	109.5	119.9	127.2	130.0
6159.38	FeI	4.61	-1.97	27.0	41.7	37.7	20.1	...	29.4	...	30.5	25.2	52.9	...	45.3	...	22.7	...	...	...
6165.36	FeI	4.14	-1.47	82.7	87.5	86.5	59.3	65.0	67.8	39.1	75.4	60.6	84.0	28.0	76.3	65.3	68.5	72.3	80.4	72.8
6173.34	FeI	2.22	-2.85	183.2	186.7	180.4	163.0	161.3	156.7	100.5	170.7	148.2	171.0	99.7	184.4	179.6	176.4	169.7	143.7	190.2
6180.20	FeI	2.73	-2.78	...	148.7	168.4	147.2	165.3	100.1	98.9	146.3	125.3	134.8	84.8	157.8	140.4	138.1	131.9	125.8	76.9
6187.99	FeI	3.94	-1.58	87.3	108.2	97.1	96.2	67.7	81.1	42.9	85.6	75.3	94.7	36.8	78.5	78.1	88.2	80.3	78.4	77.8
6200.31	FeI	2.61	-2.44	171.8	164.5	170.2	165.1	151.3	147.9	114.6	166.8	145.1	149.0	104.1	165.9	163.2	161.1	157.6	139.1	146.9
6213.43	FeI	2.22	-2.66	196.8	195.7	192.3	193.3	161.9	200.9	140.1	184.5	185.9	204.3	134.1	197.2	188.4	201.4	183.5	151.7	206.2
6219.29	FeI	2.20	-2.44	215.8	211.3	206.0	214.4	173.8	206.8	154.0	197.0	189.1	201.4	132.3	200.5	189.8	202.1	192.9	179.9	213.1
6226.74	FeI	3.88	-2.20	67.3	78.6	72.2	63.4	...	61.1	22.7	63.5	46.8	...	...	80.6	52.6	60.6	54.8	57.7	69.8
6252.57	FeI	2.40	-1.76	217.6	211.9	205.2	197.7	199.2	202.1	168.2	189.9	189.2	213.3	135.4	221.5	196.8	218.8	205.8	173.9	217.1
6265.13	FeI	2.18	-2.55	195.3	207.8	209.4	188.2	163.6	180.2	107.0	180.3	187.9	208.3	120.1	206.1	191.0	195.1	193.5	160.3	175.7
6271.28	FeI	3.32	-2.96	66.5	82.4	59.1	64.5	52.9	55.9	29.5	59.5	57.6	70.0	37.0	75.4	44.6	57.2	65.8	47.7	51.9
6297.80	FeI	2.22	-2.74	...	...	...	...	...	...	...	...	...	...	...	...	...	...	...	...	...
6301.50	FeI	3.65	-0.72	...	...	...	...	...	...	...	...	...	...	...	...	...	...	...	...	...
6307.85	FeI	3.64	-3.27	...	25.0	...	...	...	19.5	...	21.4	...	27.9	...	...	...	...	...	...	...
6322.69	FeI	2.59	-2.43	176.2	160.4	163.1	176.9	148.3	153.4	124.0	153.4	155.5	167.8	99.6	169.0	144.1	158.5	165.5	142.7	166.6
6330.85	FeI	4.73	-1.22	35.3	...	50.8	42.8	...	49.4	...	41.6	36.5	54.1	...	50.0	37.7	28.8	...	27.6	40.7
6335.33	FeI	2.20	-2.23	235.2	224.2	214.1	221.1	207.0	213.7	161.9	201.8	201.1	225.6	151.8	230.9	213.8	237.8	206.4	180.8	234.2
6336.82	FeI	3.69	-1.05	157.5	150.6	146.2	153.3	144.4	134.0	122.5	162.7	140.0	156.0	80.9	161.6	152.4	155.2	146.1	92.0	148.4
6344.15	FeI	2.43	-2.92	206.9	188.4	191.4	183.1	161.7	208.7	109.6	165.4	193.5	209.6	82.6	217.8	189.7	184.2	175.9	153.5	176.2
6355.04	FeI	2.84	-2.29	189.5	177.7	174.5	181.2	136.5	149.6	96.0	159.7	152.6	186.8	100.9	183.4	144.1	166.6	154.4	144.1	162.0
6380.75	FeI	4.19	-1.50	106.5	99.1	89.6	81.8	94.7	77.4	38.4	99.5	76.0	98.8	34.6	93.0	78.3	83.4	93.6	59.7	87.2
6392.54	FeI	2.28	-3.95	93.9	98.2	104.3	108.8	100.9	87.8	30.4	99.3	85.8	101.4	36.9	113.5	87.1	106.7	96.7	67.5	86.1
6393.61	FeI	2.43	-1.63	263.2	261.0	261.7	246.0	246.5	249.8	169.9	240.0	240.2	250.0	161.7	273.4	256.6	252.2	253.5	198.7	243.8

$\lambda(\text{\AA})$	elem	$\chi$	g <sup>f</sup>	253	257	258	260	261	262	266	267	269	278	279	295	300	304	311	315	323
6318.72	Mg I	5.11	-1.97	44.0	64.6	47.2	32.4	25.6	50.3	27.4	43.6	28.3	...	...	49.7	42.8	...	41.7	...	30.7
6319.24	Mg I	5.11	-2.21	26.0	25.8	...	...	...	20.5	...	...	26.4	38.8	...	41.9	...	...	25.7	...	...
6319.49	Mg I	5.11	-2.43	...	...	...	...	...	...	...	28.2	...	...	...	...	31.0	18.5	...	...	15.2
5420.36	Mn I	2.14	-1.46	203.5	220.4	238.5	190.0	185.7	193.4	71.1	201.4	204.6	222.2	57.3	229.3	196.5	217.0	172.2	199.3	192.7
5432.55	Mn I	0.00	-3.80	292.1	...	283.8	268.2	...	271.9	156.3	236.9	254.0	...	111.4	...	281.0	270.9	284.1	220.5	291.9
5516.77	Mn I	2.18	-1.85	167.7	174.7	179.1	146.2	156.5	142.5	49.9	139.3	164.4	210.9	...	211.2	158.8	161.1	154.3	108.0	144.2
6154.23	Na I	2.10	-1.56	41.9	37.6	45.3	...	25.0	...	...	31.7	24.5	52.8	16.2	48.8	33.4	17.0	24.3	...	...
6160.75	Na I	2.10	-1.26	68.6	62.1	63.6	34.0	32.5	25.2	...	58.8	51.6	96.0	...	70.2	52.3	38.9	47.2	26.3	44.3
5416.38	Nd II	0.86	-0.98	19.8	36.1	54.3	40.6	48.5	...	...	37.3	18.9	32.6	...	69.6	35.0	33.4	...	...	...
5431.54	Nd II	1.12	-0.47	70.6	75.9	121.6	50.1	40.4	59.3	...	56.7	61.9	74.7	27.7	91.0	60.1	35.5	...	38.3	58.7
5485.71	Nd II	1.26	-0.12	55.3	60.8	59.8	31.8	46.5	37.0	...	23.3	35.6	66.5	...	50.6	59.8	43.1	34.8	...	33.9
5578.73	Ni II	1.68	-2.67	147.4	165.4	161.2	125.8	121.5	121.0	96.1	148.4	141.2	174.5	81.1	161.9	143.0	152.3	131.7	128.5	140.8
5587.87	Ni I	1.93	-2.37	171.3	204.0	176.8	159.7	138.7	142.1	79.7	164.8	145.6	188.1	73.0	191.4	161.9	177.5	131.3	148.8	146.6
5589.37	Ni I	3.90	-1.15	37.4	25.3	25.2	38.7	28.7	22.6	...	...	40.2	99.9	...	36.7	...	24.5	31.2	28.5	25.9
5593.75	Ni I	3.90	-0.79	39.7	53.6	47.5	38.2	45.3	42.2	...	28.6	30.1	54.8	39.7	43.5	35.9	35.2	19.7	49.5	24.3
6128.97	Ni II	1.68	-3.39	105.2	96.0	99.1	93.3	86.7	94.7	48.8	92.7	86.6	108.3	34.0	99.2	99.3	95.3	77.0	42.2	93.8
6130.14	Ni II	4.27	-0.98	16.7	27.5	...	...	25.4	...	...	26.6	...	...	...	22.4	...	...	25.1	17.2	...
6177.25	Ni II	1.83	-3.60	82.2	80.4	76.0	62.4	69.3	61.0	39.8	69.0	56.1	66.7	31.7	78.2	72.8	67.1	67.9	66.2	62.4
6186.72	Ni II	4.11	-0.90	37.1	52.5	52.6	37.1	...	20.1	...	27.4	25.2	44.9	23.9	37.3	39.8	...	33.6	32.3	30.7
6204.61	Ni II	4.09	-1.15	40.7	...	...	15.4	...	17.3	16.5	16.9	...	26.0	15.8	20.8	...	...	21.7	31.3	15.0
6223.99	Ni II	4.11	-0.97	37.8	45.9	49.3	23.0	39.9	...	...	...	25.7	46.1	...	31.2	28.4	30.1	42.3	42.0	...
6230.10	Ni II	4.11	-1.20	35.0	46.7	43.8	...	...	...	...	36.6	29.1	70.0	...	44.2	31.1	31.5	...	21.9	47.8
6322.17	Ni II	4.15	-1.21	...	32.3	...	...	...	...	23.1	...	...	...	...	...	20.4	24.4	...	...	...
6327.60	Ni II	1.68	-3.09	125.6	135.2	130.8	115.7	115.6	117.1	71.5	113.1	110.2	130.9	43.0	133.5	116.1	121.3	118.2	92.1	114.8
6378.26	Ni II	4.15	-0.82	40.4	46.7	35.4	30.4	18.4	32.6	21.6	23.9	29.3	46.1	...	41.6	26.0	20.4	40.0	41.3	31.9
6384.67	Ni II	1.15	-1.00	38.5	49.3	60.2	...	...	20.0	18.8	46.5	47.6	50.0	30.6	54.0	44.0	28.1	38.4	...	34.2
6482.80	Ni II	1.94	-0.85	113.7	115.3	110.1	98.6	93.3	118.0	66.3	110.8	136.0	134.6	57.3	110.1	102.2	96.2	136.9	93.3	105.5
6586.32	Ni II	1.95	-2.79	122.2	133.4	148.7	158.1	136.6	46.1	59.8	164.4	41.4	116.8	41.1	162.2	164.2	157.8	...	150.0	135.1
6598.61	Ni II	4.24	-0.93	27.1	...	...	...	...	...	...	...	...	...	...	...	...	...	...	...	26.3
6635.14	Ni II	4.42	-0.75	25.1	...	23.9	...	...	36.9	...	...	...	45.6	23.9	21.6	...	...	68.7	...	18.4
6300.31	O I	0.00	-9.75	...	...	...	...	...	...	...	...	...	...	...	...	...	...	...	...	...
6363.79	O I	0.02	-10.25	45.8	54.1	40.5	42.5	27.0	33.2	23.4	41.1	48.6	46.6	...	31.9	37.8	46.1	38.9	41.9	55.7
5526.82	Sc II	1.77	-0.07	71.9	110.3	110.1	91.8	111.6	119.5	96.0	107.6	107.9	115.4	115.7	96.4	122.6	109.3	112.3	131.2	105.6
6245.62	Sc II	1.51	-0.97	19.7	67.0	77.7	71.9	65.9	66.6	68.4	61.3	69.2	...	52.8	78.5	54.1	61.2	82.8	54.5	60.6
6309.90	Sc II	1.50	-1.52	58.0	54.7	...	34.7	37.1	...	18.7	39.9	...	...	...	30.6	...	54.7	43.5	...	...
6604.60	Sc II	1.36	-1.31	101.0	88.9	94.8	82.7	84.2	98.3	58.4	83.7	113.2	93.9	54.5	102.4	87.0	82.5	126.4	71.7	82.6
6125.03	Si II	5.62	-1.57	...	...	...	31.7	...	...	...	32.3	38.8	...	...	56.2	...	...	...	17.4	...
6142.48	Si II	5.62	-1.51	...	...	...	...	...	...	...	26.0	...	...	...	16.5	...	...	...	16.9	...
6145.02	Si II	5.61	-1.37	15.4	22.7	...	...	...	...	...	22.1	...	21.2	...	...	...	...	19.3	...	21.7
6155.14	Si II	5.62	-0.80	47.6	55.8	39.1	42.8	27.6	45.5	...	41.0	38.9	51.2	34.6	49.0	40.0	39.0	43.5	47.9	45.0
6237.33	Si II	5.61	-1.02	26.6	23.7	32.1	16.0	...	30.2	...	33.6	23.4	43.1	22.3	31.0	26.8	...	21.6	31.4	...
6243.82	Si II	5.61	-1.27	...	53.1	44.0	...	...	...	22.5	28.0	33.8	46.9	...	...	...	29.3	17.0	23.1	...
5490.16	Ti II	1.46	-0.93	132.3	158.9	148.0	98.6	116.9	97.2	50.8	87.2	113.2	143.2	32.3	152.3	123.0	132.5	106.5	92.5	117.3
5503.90	Ti II	2.58	-0.19	76.8	94.2	125.2	66.3	65.9	56.5	23.4	53.6	52.8	107.6	...	103.1	86.6	67.2	53.2	40.6	71.7
6126.22	Ti II	1.07	-1.42	167.5	167.6	172.5	130.1	130.7	127.2	56.8	138.8	148.4	182.3	32.4	172.4	162.0	159.6	138.8	119.0	160.5
6220.50	Ti II	2.68	-0.14	...	...	...	...	...	...	24.1	...	56.6	94.0	...	81.3	80.0	...	...	...	...
6258.10	Ti II	1.44	-0.35	223.9	231.1	232.3	195.2	160.5	181.7	83.5	165.8	209.4	258.2	72.4	243.1	216.5	223.1	181.3	138.1	204.8
6303.77	Ti II	1.44	-1.57	121.7	117.2	115.7	91.1	79.0	87.1	41.0	77.9	87.3	121.2	...	115.6	96.2	100.3	87.9	68.3	97.9
6312.24	Ti II	1.46	-1.55	...	114.7	107.9	...	...	79.2	20.6	78.5	91.3	113.1	...	100.9	...	...	88.7	45.6	86.3
6336.10	Ti II	1.44	-1.74	103.0	101.2	115.0	90.8	66.1	63.6	26.0	77.7	90.6	120.9	25.3	97.7	90.7	89.7	73.6	68.5	103.8
6508.12	Ti II	1.43	-2.05	69.8	90.0	72.0	56.9	45.3	53.3	...	38.1	71.5	94.2	...	90.2	58.0	54.3	63.9	31.0	63.5
6556.08	Ti II	1.46	-1.07	...	...	...	...	138.0	...	...	...	...	...	...	...	...	139.8	...	...	...
6599.13	Ti II	0.90	-2.09	153.9	186.8	181.3	147.5	111.3	136.9	46.9	109.4	167.9	173.1	24.5	194.5	159.1	174.3	...	78.9	164.2
6666.53	Ti II	1.46	-1.62	41.8	50.1	59.5	...	...	...	...	39.7	39.2	...	...	...	29.8	33.9	46.2	...	...
5418.77	Ti III	1.58	-2.11	111.2	97.0	96.3	99.6	115.3	93.2	97.6	116.2	83.3	109.4	122.1	92.7	109.8	102.2	83.0	110.0	96.5
6219.94	Ti III	2.06	-2.82	...	...	28.0	31.3	28.1	...	21.6	48.8	...	...	33.9	27.4	...	40.7	...	21.8	...
6559.58	Ti III	2.05	-2.02	67.8	...	...	...	72.9	...	...	...	...	...	...	...	57.7	61.8	...	...	...
6606.95	Ti III	2.06	-2.79	43.8	40.7	46.2	24.6	34.4	47.6	39.3	34.1	59.6	49.2	31.7	49.9	33.7	...	88.0	27.1	31.1
6680.13	Ti III	3.09	-1.86	23.1	29.5	33.0	17.5	27.9	...	26.5	41.5	29.1	21.4	26.1	36.4	25.1	17.9	36.6	30.7	19.9
6119.53	Vi	1.06	-0.32	...	...	...	...	...	...	...	...	...	97.4	...	...	...	...	74.5	...	79.1
6128.33	Vi	1.05	-2.30	...	...	...	...	18.8	...	...	...	...	30.5	...	...	...	...	...	...	...
6135.37	Vi	1.05	-0.75	139.1	151.3	...	88.9	103.1	102.4	23.7	97.8	113.4	145.4	18.9	145.0	114.8	116.7	109.2	53.5	116.8
6150.15	Vi	0.30	-1.79	166.8	178.6	152.7	148.5	140.0	128.8	39.7	123.6	147.8	181.6	23.9	181.2	170.7	172.2	148.8	95.5	150.0
6199.19	Vi	0.29	-1.29	222.5	220.2	219.8	188.6	170.3	182.9	80.9	185.5	188.0	224.1	44.0	216.4	206.0	200.3	177.1	122.5	176.8
6216.36	Vi	0.28	-0.81	198.5	213.6	215.0	183.8	172.5	178.3	76.9	161.4	197.1	220.1	46.5	199.8	186.6	200.0	187.5	164.8	221.4
6224.51	Vi	0.29	-2.01	146.9	157.1	166.9	131.9	119.3	125.7	31.5	117.9	141.9	170.8	...	156.3	142.7	150.1	119.8	85.1	153.5
6233.20	Vi	0.28	-2.07	106.0	107.5	117.6	111.4	80.0	87.4	...	73.4	107.9	130.9	...	130.1	109.1	119.3	95.1	54	



**Table 6.A3:** Abundance ratio of the Fornax Field stars, where we list the abundance, its associated error ( $\sigma$ ) and the number of lines used (n). The quoted error is the error on [element/H], not [X/Fe]. Part 1

Star	[Fe I/H] $\sigma$ n	[Fe II/H] $\sigma$ (n)	[Ba II/Fe] $\sigma$ n	[Ca I/Fe] $\sigma$ (n)	[Cr I/Fe] $\sigma$ n	[Eu II/Fe] $\sigma$ (n)	[La II/Fe] $\sigma$ n	[Mg I/Fe] $\sigma$ (n)
BL038	-0.88 $\pm$ 0.07 (43)	-0.70 $\pm$ 0.09 (4)	0.80 $\pm$ 0.16 (2)	-0.25 $\pm$ 0.11 (8)	-0.31 $\pm$ 0.23 (1)	0.62 $\pm$ 0.23 (1)	0.43 $\pm$ 0.16 (2)	0.03 $\pm$ 0.16 (2)
BL045	-1.09 $\pm$ 0.05 (48)	-0.78 $\pm$ 0.08 (5)	-0.05 $\pm$ 0.21 (2)	-0.33 $\pm$ 0.06 (8)	-0.36 $\pm$ 0.16 (1)	0.19 $\pm$ 0.16 (1)	0.17 $\pm$ 0.16 (1)	0.02 $\pm$ 0.18 (2)
BL052	-1.02 $\pm$ 0.06 (37)	-0.52 $\pm$ 0.25 (2)	0.57 $\pm$ 0.39 (2)	-0.42 $\pm$ 0.12 (8)	-0.51 $\pm$ 0.34 (1)	0.67 $\pm$ 0.34 (1)	0.25 $\pm$ 0.34 (1)	0.07 $\pm$ 0.24 (2)
BL065	-1.43 $\pm$ 0.07 (42)	-1.06 $\pm$ 0.17 (5)	0.19 $\pm$ 0.13 (2)	-0.09 $\pm$ 0.12 (9)	-0.51 $\pm$ 0.18 (1)	0.35 $\pm$ 0.18 (1)	... $\pm$ ... (0)	0.00 $\pm$ 0.18 (1)
BL076	-0.85 $\pm$ 0.06 (43)	-0.43 $\pm$ 0.14 (4)	0.49 $\pm$ 0.16 (2)	-0.21 $\pm$ 0.06 (9)	-0.42 $\pm$ 0.19 (1)	0.34 $\pm$ 0.19 (1)	0.21 $\pm$ 0.19 (1)	-0.15 $\pm$ 0.13 (2)
BL077	-0.79 $\pm$ 0.06 (40)	-0.38 $\pm$ 0.24 (4)	0.29 $\pm$ 0.13 (2)	-0.46 $\pm$ 0.06 (8)	-0.62 $\pm$ 0.15 (1)	0.29 $\pm$ 0.15 (1)	-0.01 $\pm$ 0.11 (2)	-0.27 $\pm$ 0.09 (3)
BL079	-0.52 $\pm$ 0.08 (39)	-0.16 $\pm$ 0.42 (2)	0.98 $\pm$ 0.44 (1)	-0.26 $\pm$ 0.17 (7)	-0.30 $\pm$ 0.44 (1)	0.45 $\pm$ 0.44 (1)	0.44 $\pm$ 0.31 (2)	-0.06 $\pm$ 0.31 (2)
BL081	-0.62 $\pm$ 0.06 (40)	-0.44 $\pm$ 0.20 (4)	0.91 $\pm$ 0.13 (2)	-0.34 $\pm$ 0.07 (9)	-0.52 $\pm$ 0.19 (1)	0.26 $\pm$ 0.19 (1)	0.36 $\pm$ 0.13 (2)	-0.32 $\pm$ 0.13 (2)
BL084	-0.82 $\pm$ 0.05 (39)	-0.59 $\pm$ 0.10 (4)	0.66 $\pm$ 0.21 (2)	-0.30 $\pm$ 0.06 (9)	-0.57 $\pm$ 0.19 (1)	0.44 $\pm$ 0.19 (1)	0.24 $\pm$ 0.13 (2)	-0.12 $\pm$ 0.19 (1)
BL085	-2.58 $\pm$ 0.05 (31)	-1.99 $\pm$ 0.10 (4)	0.12 $\pm$ 0.11 (2)	0.33 $\pm$ 0.06 (9)	... $\pm$ ... (0)	... $\pm$ ... (0)	0.75 $\pm$ 0.15 (1)	0.35 $\pm$ 0.15 (1)
BL091	-0.96 $\pm$ 0.06 (46)	-0.60 $\pm$ 0.21 (5)	0.56 $\pm$ 0.12 (2)	-0.15 $\pm$ 0.07 (7)	-0.34 $\pm$ 0.17 (1)	0.52 $\pm$ 0.17 (1)	0.32 $\pm$ 0.12 (2)	-0.04 $\pm$ 0.12 (2)
BL092	-0.95 $\pm$ 0.08 (45)	-0.57 $\pm$ 0.10 (3)	0.66 $\pm$ 0.16 (2)	-0.23 $\pm$ 0.08 (9)	-0.45 $\pm$ 0.23 (1)	0.53 $\pm$ 0.23 (1)	0.30 $\pm$ 0.16 (2)	0.04 $\pm$ 0.13 (3)
BL096	-0.75 $\pm$ 0.08 (42)	-0.95 $\pm$ 0.18 (4)	0.70 $\pm$ 0.18 (2)	-0.18 $\pm$ 0.10 (6)	-0.53 $\pm$ 0.25 (1)	0.53 $\pm$ 0.25 (1)	0.36 $\pm$ 0.25 (1)	0.02 $\pm$ 0.14 (3)
BL097	-0.92 $\pm$ 0.05 (43)	-0.53 $\pm$ 0.24 (5)	0.56 $\pm$ 0.20 (2)	-0.18 $\pm$ 0.09 (9)	-0.54 $\pm$ 0.17 (1)	0.48 $\pm$ 0.17 (1)	0.25 $\pm$ 0.12 (2)	0.06 $\pm$ 0.17 (1)
BL100	-0.93 $\pm$ 0.06 (48)	-0.67 $\pm$ 0.13 (5)	0.20 $\pm$ 0.25 (2)	-0.48 $\pm$ 0.08 (8)	-0.50 $\pm$ 0.19 (1)	... $\pm$ ... (0)	0.15 $\pm$ 0.13 (2)	0.00 $\pm$ 0.17 (3)
BL104	-0.96 $\pm$ 0.06 (43)	-0.33 $\pm$ 0.23 (4)	0.58 $\pm$ 0.15 (2)	-0.20 $\pm$ 0.07 (9)	-0.75 $\pm$ 0.21 (1)	0.64 $\pm$ 0.21 (1)	0.45 $\pm$ 0.21 (1)	-0.01 $\pm$ 0.15 (2)
BL113	-0.75 $\pm$ 0.06 (42)	-0.65 $\pm$ 0.10 (5)	0.94 $\pm$ 0.21 (1)	-0.08 $\pm$ 0.09 (9)	-0.42 $\pm$ 0.21 (1)	0.45 $\pm$ 0.21 (1)	0.40 $\pm$ 0.15 (2)	-0.03 $\pm$ 0.21 (1)
BL115	-1.44 $\pm$ 0.06 (40)	-0.85 $\pm$ 0.12 (4)	0.07 $\pm$ 0.11 (2)	-0.28 $\pm$ 0.06 (8)	-0.55 $\pm$ 0.16 (1)	0.12 $\pm$ 0.16 (1)	0.11 $\pm$ 0.11 (2)	0.01 $\pm$ 0.13 (3)
BL123	-0.97 $\pm$ 0.05 (41)	-0.78 $\pm$ 0.07 (4)	0.40 $\pm$ 0.12 (2)	-0.30 $\pm$ 0.06 (8)	-0.40 $\pm$ 0.17 (1)	0.40 $\pm$ 0.17 (1)	0.38 $\pm$ 0.12 (2)	-0.04 $\pm$ 0.12 (2)
BL125	-0.73 $\pm$ 0.07 (44)	-0.61 $\pm$ 0.13 (3)	0.87 $\pm$ 0.18 (2)	-0.21 $\pm$ 0.09 (8)	-0.57 $\pm$ 0.25 (1)	0.51 $\pm$ 0.25 (1)	0.58 $\pm$ 0.25 (2)	0.02 $\pm$ 0.18 (2)
BL132	-0.85 $\pm$ 0.06 (43)	-0.61 $\pm$ 0.12 (4)	0.23 $\pm$ 0.21 (2)	-0.45 $\pm$ 0.07 (8)	-0.50 $\pm$ 0.20 (1)	0.24 $\pm$ 0.20 (1)	0.01 $\pm$ 0.14 (2)	-0.13 $\pm$ 0.12 (3)
BL135	-0.95 $\pm$ 0.07 (39)	-0.69 $\pm$ 0.17 (4)	0.62 $\pm$ 0.15 (2)	-0.30 $\pm$ 0.08 (7)	-0.41 $\pm$ 0.21 (1)	0.47 $\pm$ 0.21 (1)	0.29 $\pm$ 0.15 (2)	-0.02 $\pm$ 0.21 (1)
BL138	-1.01 $\pm$ 0.06 (43)	-0.58 $\pm$ 0.13 (5)	0.47 $\pm$ 0.21 (2)	-0.18 $\pm$ 0.09 (9)	-0.47 $\pm$ 0.17 (1)	0.55 $\pm$ 0.17 (1)	0.40 $\pm$ 0.12 (2)	-0.08 $\pm$ 0.10 (3)
BL140	-0.86 $\pm$ 0.07 (41)	0.22 $\pm$ 0.27 (5)	0.69 $\pm$ 0.13 (2)	-0.30 $\pm$ 0.06 (9)	-0.39 $\pm$ 0.18 (1)	0.62 $\pm$ 0.18 (1)	0.45 $\pm$ 0.13 (2)	0.04 $\pm$ 0.15 (3)
BL141	-0.82 $\pm$ 0.06 (46)	-0.42 $\pm$ 0.12 (5)	0.28 $\pm$ 0.15 (2)	-0.33 $\pm$ 0.08 (7)	-0.47 $\pm$ 0.21 (1)	0.39 $\pm$ 0.21 (1)	0.28 $\pm$ 0.15 (2)	-0.11 $\pm$ 0.15 (2)
BL146	-0.92 $\pm$ 0.06 (39)	-0.64 $\pm$ 0.07 (5)	0.58 $\pm$ 0.20 (2)	-0.36 $\pm$ 0.10 (8)	-0.40 $\pm$ 0.16 (1)	0.41 $\pm$ 0.16 (1)	0.49 $\pm$ 0.11 (2)	-0.14 $\pm$ 0.09 (3)
BL147	-1.37 $\pm$ 0.07 (47)	-0.87 $\pm$ 0.10 (4)	1.27 $\pm$ 0.23 (2)	-0.30 $\pm$ 0.11 (9)	-0.80 $\pm$ 0.32 (1)	1.38 $\pm$ 0.32 (1)	1.09 $\pm$ 0.23 (2)	0.43 $\pm$ 0.24 (3)
BL148	-0.63 $\pm$ 0.11 (37)	-0.56 $\pm$ 0.15 (4)	0.09 $\pm$ 0.33 (1)	-0.29 $\pm$ 0.14 (8)	-0.23 $\pm$ 0.33 (1)	0.35 $\pm$ 0.33 (1)	0.54 $\pm$ 0.23 (2)	-0.13 $\pm$ 0.19 (3)
BL149	-0.91 $\pm$ 0.07 (45)	-0.83 $\pm$ 0.17 (5)	0.57 $\pm$ 0.18 (2)	-0.30 $\pm$ 0.09 (8)	-0.52 $\pm$ 0.25 (1)	0.43 $\pm$ 0.25 (1)	0.31 $\pm$ 0.18 (2)	-0.06 $\pm$ 0.18 (2)
BL150	-0.83 $\pm$ 0.06 (42)	-0.41 $\pm$ 0.15 (4)	0.36 $\pm$ 0.16 (2)	-0.18 $\pm$ 0.08 (7)	-0.38 $\pm$ 0.22 (1)	0.50 $\pm$ 0.22 (1)	0.37 $\pm$ 0.16 (2)	0.01 $\pm$ 0.16 (2)
BL151	-0.86 $\pm$ 0.07 (45)	-0.60 $\pm$ 0.10 (3)	0.74 $\pm$ 0.13 (2)	-0.25 $\pm$ 0.07 (8)	-0.33 $\pm$ 0.18 (1)	0.46 $\pm$ 0.18 (1)	0.42 $\pm$ 0.13 (2)	-0.06 $\pm$ 0.10 (3)
BL155	-0.75 $\pm$ 0.07 (40)	-0.52 $\pm$ 0.21 (3)	0.76 $\pm$ 0.20 (2)	-0.17 $\pm$ 0.08 (9)	-0.40 $\pm$ 0.22 (1)	0.39 $\pm$ 0.22 (1)	0.34 $\pm$ 0.16 (2)	-0.03 $\pm$ 0.31 (2)
BL156	-1.13 $\pm$ 0.07 (45)	-0.62 $\pm$ 0.19 (5)	0.51 $\pm$ 0.13 (2)	-0.28 $\pm$ 0.07 (7)	-0.44 $\pm$ 0.19 (1)	0.65 $\pm$ 0.19 (1)	0.54 $\pm$ 0.13 (2)	-0.01 $\pm$ 0.13 (2)
BL158	-0.87 $\pm$ 0.07 (43)	-0.40 $\pm$ 0.15 (4)	0.95 $\pm$ 0.23 (1)	-0.38 $\pm$ 0.08 (9)	-0.49 $\pm$ 0.23 (1)	0.64 $\pm$ 0.23 (1)	0.58 $\pm$ 0.16 (2)	0.06 $\pm$ 0.13 (3)
BL160	-0.87 $\pm$ 0.06 (37)	-0.52 $\pm$ 0.08 (5)	0.55 $\pm$ 0.12 (2)	-0.31 $\pm$ 0.08 (9)	-0.60 $\pm$ 0.15 (1)	0.47 $\pm$ 0.15 (1)	0.46 $\pm$ 0.15 (1)	-0.20 $\pm$ 0.11 (2)
BL163	-0.74 $\pm$ 0.07 (41)	-0.52 $\pm$ 0.14 (4)	0.95 $\pm$ 0.20 (1)	-0.08 $\pm$ 0.07 (8)	-0.23 $\pm$ 0.20 (1)	0.51 $\pm$ 0.20 (1)	0.62 $\pm$ 0.14 (2)	-0.16 $\pm$ 0.14 (2)
BL166	-0.89 $\pm$ 0.07 (42)	-0.54 $\pm$ 0.24 (4)	0.74 $\pm$ 0.16 (2)	-0.23 $\pm$ 0.08 (7)	-0.59 $\pm$ 0.22 (1)	0.42 $\pm$ 0.22 (1)	0.36 $\pm$ 0.16 (2)	-0.07 $\pm$ 0.13 (3)
BL168	-0.88 $\pm$ 0.08 (41)	-0.57 $\pm$ 0.20 (4)	0.55 $\pm$ 0.13 (2)	-0.12 $\pm$ 0.07 (7)	-0.30 $\pm$ 0.18 (1)	0.54 $\pm$ 0.18 (1)	0.53 $\pm$ 0.13 (2)	-0.11 $\pm$ 0.13 (2)
BL171	-0.90 $\pm$ 0.06 (40)	-0.19 $\pm$ 0.14 (4)	0.18 $\pm$ 0.13 (2)	-0.26 $\pm$ 0.07 (7)	-0.28 $\pm$ 0.18 (1)	0.44 $\pm$ 0.18 (1)	0.33 $\pm$ 0.13 (2)	-0.03 $\pm$ 0.11 (3)
BL173	-0.78 $\pm$ 0.07 (41)	-0.55 $\pm$ 0.14 (5)	0.54 $\pm$ 0.15 (2)	-0.36 $\pm$ 0.08 (8)	-0.54 $\pm$ 0.21 (1)	0.40 $\pm$ 0.21 (1)	0.47 $\pm$ 0.15 (2)	-0.12 $\pm$ 0.12 (3)
BL180	-0.91 $\pm$ 0.07 (38)	-0.68 $\pm$ 0.06 (1)	1.22 $\pm$ 0.34 (1)	-0.25 $\pm$ 0.12 (8)	-0.46 $\pm$ 0.34 (1)	0.58 $\pm$ 0.34 (1)	0.76 $\pm$ 0.24 (2)	-0.08 $\pm$ 0.24 (2)
BL185	-0.71 $\pm$ 0.07 (39)	-0.78 $\pm$ 0.14 (4)	0.96 $\pm$ 0.16 (2)	-0.06 $\pm$ 0.10 (9)	-0.15 $\pm$ 0.22 (1)	0.37 $\pm$ 0.22 (1)	0.43 $\pm$ 0.18 (2)	-0.07 $\pm$ 0.13 (3)

*Continued on next page*

Star	[Fe I/H] $\sigma$ n	[Fe II/H] $\sigma$ (n)	[Ba II/Fe] $\sigma$ n	[Ca I/Fe] $\sigma$ (n)	[Cr I/Fe] $\sigma$ n	[Eu II/Fe] $\sigma$ (n)	[La II/Fe] $\sigma$ n	[Mg I/Fe] $\sigma$ (n)
BL190	-0.79 $\pm$ 0.05 (43)	-0.60 $\pm$ 0.12 (4)	0.06 $\pm$ 0.13 (2)	-0.43 $\pm$ 0.06 (8)	-0.67 $\pm$ 0.18 (1)	0.39 $\pm$ 0.18 (1)	0.01 $\pm$ 0.15 (2)	-0.32 $\pm$ 0.13 (2)
BL195	-0.97 $\pm$ 0.06 (48)	-0.77 $\pm$ 0.09 (4)	0.17 $\pm$ 0.25 (2)	-0.20 $\pm$ 0.08 (8)	-0.43 $\pm$ 0.19 (1)	0.43 $\pm$ 0.19 (1)	0.10 $\pm$ 0.19 (1)	-0.07 $\pm$ 0.13 (2)
BL196	-1.02 $\pm$ 0.06 (43)	-0.76 $\pm$ 0.10 (5)	0.22 $\pm$ 0.13 (2)	-0.34 $\pm$ 0.06 (9)	-0.40 $\pm$ 0.18 (1)	0.50 $\pm$ 0.18 (1)	0.40 $\pm$ 0.13 (2)	-0.22 $\pm$ 0.18 (1)
BL197	-0.89 $\pm$ 0.07 (39)	-0.79 $\pm$ 0.13 (2)	0.79 $\pm$ 0.30 (2)	-0.42 $\pm$ 0.10 (7)	-0.57 $\pm$ 0.24 (1)	0.54 $\pm$ 0.24 (1)	0.37 $\pm$ 0.17 (2)	0.05 $\pm$ 0.16 (3)
BL203	-0.83 $\pm$ 0.07 (43)	-0.55 $\pm$ 0.12 (3)	0.58 $\pm$ 0.19 (2)	-0.19 $\pm$ 0.09 (9)	-0.47 $\pm$ 0.27 (1)	0.51 $\pm$ 0.27 (1)	0.36 $\pm$ 0.19 (2)	-0.07 $\pm$ 0.16 (3)
BL204	-1.00 $\pm$ 0.07 (33)	-0.74 $\pm$ 0.16 (2)	0.46 $\pm$ 0.47 (2)	-0.15 $\pm$ 0.15 (5)	-0.30 $\pm$ 0.34 (1)	0.92 $\pm$ 0.34 (1)	0.53 $\pm$ 0.24 (2)	-0.10 $\pm$ 0.34 (1)
BL205	-0.69 $\pm$ 0.07 (43)	-0.63 $\pm$ 0.08 (5)	0.76 $\pm$ 0.16 (2)	-0.21 $\pm$ 0.12 (7)	-0.42 $\pm$ 0.19 (1)	0.31 $\pm$ 0.19 (1)	0.41 $\pm$ 0.13 (2)	-0.07 $\pm$ 0.13 (2)
BL208	-0.66 $\pm$ 0.06 (43)	-0.73 $\pm$ 0.06 (3)	0.86 $\pm$ 0.16 (2)	-0.07 $\pm$ 0.10 (9)	-0.56 $\pm$ 0.22 (1)	0.24 $\pm$ 0.22 (1)	0.44 $\pm$ 0.16 (2)	-0.08 $\pm$ 0.13 (3)
BL210	-0.76 $\pm$ 0.07 (42)	-0.37 $\pm$ 0.22 (5)	0.90 $\pm$ 0.15 (2)	-0.32 $\pm$ 0.07 (8)	-0.53 $\pm$ 0.21 (1)	0.47 $\pm$ 0.21 (1)	0.52 $\pm$ 0.15 (2)	0.06 $\pm$ 0.18 (3)
BL211	-0.67 $\pm$ 0.07 (43)	-0.95 $\pm$ 0.14 (4)	0.98 $\pm$ 0.16 (2)	-0.20 $\pm$ 0.07 (9)	-0.21 $\pm$ 0.22 (1)	0.40 $\pm$ 0.22 (1)	0.45 $\pm$ 0.16 (2)	-0.15 $\pm$ 0.13 (3)
BL213	-0.87 $\pm$ 0.06 (42)	-0.63 $\pm$ 0.10 (5)	0.65 $\pm$ 0.15 (2)	-0.32 $\pm$ 0.07 (9)	-0.51 $\pm$ 0.21 (1)	0.52 $\pm$ 0.21 (1)	0.47 $\pm$ 0.15 (2)	-0.19 $\pm$ 0.16 (2)
BL216	-0.72 $\pm$ 0.07 (35)	-0.93 $\pm$ 0.19 (2)	0.96 $\pm$ 0.18 (2)	-0.18 $\pm$ 0.10 (7)	-0.28 $\pm$ 0.25 (1)	0.55 $\pm$ 0.25 (1)	0.62 $\pm$ 0.18 (2)	-0.03 $\pm$ 0.14 (3)
BL218	-0.60 $\pm$ 0.09 (41)	-0.60 $\pm$ 0.23 (3)	1.02 $\pm$ 0.26 (1)	-0.26 $\pm$ 0.10 (7)	-0.38 $\pm$ 0.26 (1)	0.29 $\pm$ 0.26 (1)	0.48 $\pm$ 0.18 (2)	-0.09 $\pm$ 0.15 (3)
BL221	-0.86 $\pm$ 0.06 (43)	-0.75 $\pm$ 0.20 (5)	0.80 $\pm$ 0.15 (2)	-0.27 $\pm$ 0.10 (9)	-0.39 $\pm$ 0.21 (1)	0.68 $\pm$ 0.21 (1)	0.61 $\pm$ 0.15 (2)	-0.11 $\pm$ 0.15 (2)
BL227	-0.91 $\pm$ 0.08 (43)	-0.65 $\pm$ 0.14 (3)	0.94 $\pm$ 0.18 (2)	-0.21 $\pm$ 0.08 (9)	-0.21 $\pm$ 0.25 (1)	0.70 $\pm$ 0.25 (1)	0.47 $\pm$ 0.18 (2)	-0.05 $\pm$ 0.18 (2)
BL228	-0.88 $\pm$ 0.05 (42)	-0.49 $\pm$ 0.17 (4)	-0.05 $\pm$ 0.13 (2)	-0.45 $\pm$ 0.08 (9)	-0.37 $\pm$ 0.16 (1)	0.31 $\pm$ 0.16 (1)	0.08 $\pm$ 0.11 (2)	-0.16 $\pm$ 0.11 (2)
BL229	-0.71 $\pm$ 0.06 (39)	-0.48 $\pm$ 0.14 (4)	0.79 $\pm$ 0.17 (2)	-0.25 $\pm$ 0.11 (8)	-0.58 $\pm$ 0.24 (1)	0.48 $\pm$ 0.24 (1)	0.46 $\pm$ 0.17 (2)	-0.16 $\pm$ 0.17 (2)
BL233	-0.68 $\pm$ 0.07 (44)	-0.46 $\pm$ 0.12 (4)	0.66 $\pm$ 0.16 (2)	-0.47 $\pm$ 0.08 (8)	-0.64 $\pm$ 0.22 (1)	0.36 $\pm$ 0.22 (1)	0.33 $\pm$ 0.16 (2)	-0.13 $\pm$ 0.13 (3)
BL239	-0.88 $\pm$ 0.07 (43)	-0.67 $\pm$ 0.12 (4)	0.67 $\pm$ 0.21 (2)	-0.21 $\pm$ 0.08 (8)	-0.47 $\pm$ 0.22 (1)	0.26 $\pm$ 0.22 (1)	0.14 $\pm$ 0.16 (2)	-0.15 $\pm$ 0.16 (2)
BL242	-1.04 $\pm$ 0.07 (43)	-0.73 $\pm$ 0.23 (3)	0.64 $\pm$ 0.16 (2)	-0.45 $\pm$ 0.09 (9)	-0.37 $\pm$ 0.21 (1)	0.47 $\pm$ 0.21 (1)	0.27 $\pm$ 0.16 (2)	0.15 $\pm$ 0.17 (3)
BL247	-0.82 $\pm$ 0.09 (37)	-0.61 $\pm$ 0.12 (5)	0.49 $\pm$ 0.11 (2)	-0.30 $\pm$ 0.11 (9)	-0.38 $\pm$ 0.15 (1)	0.47 $\pm$ 0.15 (1)	0.50 $\pm$ 0.11 (2)	0.10 $\pm$ 0.23 (2)
BL250	-0.68 $\pm$ 0.09 (38)	-0.51 $\pm$ 0.34 (4)	... $\pm$ ... (0)	-0.06 $\pm$ 0.11 (7)	-0.17 $\pm$ 0.26 (1)	0.26 $\pm$ 0.26 (1)	0.43 $\pm$ 0.18 (2)	-0.03 $\pm$ 0.15 (3)
BL253	-0.66 $\pm$ 0.06 (39)	-0.61 $\pm$ 0.12 (4)	0.88 $\pm$ 0.14 (2)	-0.32 $\pm$ 0.11 (8)	-0.50 $\pm$ 0.20 (1)	0.42 $\pm$ 0.20 (1)	0.53 $\pm$ 0.14 (2)	-0.20 $\pm$ 0.12 (3)
BL257	-0.58 $\pm$ 0.07 (41)	-1.09 $\pm$ 0.15 (3)	0.91 $\pm$ 0.24 (1)	-0.30 $\pm$ 0.08 (8)	-0.47 $\pm$ 0.24 (1)	0.32 $\pm$ 0.24 (1)	0.62 $\pm$ 0.17 (2)	-0.11 $\pm$ 0.14 (3)
BL258	-0.56 $\pm$ 0.08 (39)	-0.53 $\pm$ 0.08 (4)	1.01 $\pm$ 0.23 (1)	-0.16 $\pm$ 0.13 (9)	-0.35 $\pm$ 0.23 (1)	0.49 $\pm$ 0.23 (1)	0.56 $\pm$ 0.16 (2)	-0.29 $\pm$ 0.16 (2)
BL260	-0.86 $\pm$ 0.06 (39)	-0.36 $\pm$ 0.11 (3)	0.07 $\pm$ 0.13 (2)	-0.30 $\pm$ 0.08 (9)	-0.49 $\pm$ 0.19 (1)	0.32 $\pm$ 0.19 (1)	0.26 $\pm$ 0.13 (2)	-0.27 $\pm$ 0.13 (2)
BL261	-0.79 $\pm$ 0.09 (43)	-0.37 $\pm$ 0.24 (4)	0.40 $\pm$ 0.15 (2)	-0.36 $\pm$ 0.08 (8)	-0.55 $\pm$ 0.21 (1)	0.46 $\pm$ 0.21 (1)	0.30 $\pm$ 0.15 (2)	-0.13 $\pm$ 0.15 (2)
BL262	-0.78 $\pm$ 0.07 (44)	-0.44 $\pm$ 0.15 (5)	0.59 $\pm$ 0.25 (2)	-0.19 $\pm$ 0.10 (7)	-0.38 $\pm$ 0.27 (1)	0.33 $\pm$ 0.27 (1)	0.25 $\pm$ 0.19 (2)	-0.01 $\pm$ 0.16 (3)
BL266	-1.44 $\pm$ 0.06 (43)	-1.16 $\pm$ 0.21 (4)	0.18 $\pm$ 0.14 (2)	-0.18 $\pm$ 0.09 (10)	-0.36 $\pm$ 0.20 (1)	0.45 $\pm$ 0.20 (1)	0.18 $\pm$ 0.14 (2)	0.04 $\pm$ 0.23 (2)
BL267	-0.72 $\pm$ 0.08 (46)	-0.64 $\pm$ 0.11 (5)	0.65 $\pm$ 0.14 (2)	-0.16 $\pm$ 0.10 (9)	-0.32 $\pm$ 0.20 (1)	0.37 $\pm$ 0.20 (1)	0.47 $\pm$ 0.14 (2)	0.00 $\pm$ 0.12 (3)
BL269	-0.81 $\pm$ 0.08 (44)	-0.47 $\pm$ 0.40 (2)	0.89 $\pm$ 0.20 (2)	-0.22 $\pm$ 0.09 (9)	-0.54 $\pm$ 0.28 (1)	0.64 $\pm$ 0.28 (1)	0.40 $\pm$ 0.20 (2)	-0.06 $\pm$ 0.16 (3)
BL278	-0.73 $\pm$ 0.07 (38)	-0.87 $\pm$ 0.16 (3)	... $\pm$ ... (0)	0.04 $\pm$ 0.11 (8)	-0.11 $\pm$ 0.25 (1)	0.40 $\pm$ 0.25 (1)	0.60 $\pm$ 0.18 (2)	0.00 $\pm$ 0.18 (2)
BL279	-1.51 $\pm$ 0.08 (44)	-1.31 $\pm$ 0.20 (3)	0.46 $\pm$ 0.15 (2)	-0.03 $\pm$ 0.11 (9)	-0.51 $\pm$ 0.21 (1)	0.64 $\pm$ 0.21 (1)	0.23 $\pm$ 0.15 (2)	0.18 $\pm$ 0.21 (1)
BL295	-0.69 $\pm$ 0.08 (38)	-0.25 $\pm$ 0.27 (3)	... $\pm$ ... (0)	-0.07 $\pm$ 0.13 (8)	-0.45 $\pm$ 0.25 (1)	0.44 $\pm$ 0.25 (1)	0.67 $\pm$ 0.18 (2)	-0.04 $\pm$ 0.14 (3)
BL300	-0.92 $\pm$ 0.07 (40)	-0.60 $\pm$ 0.09 (4)	1.08 $\pm$ 0.13 (2)	-0.16 $\pm$ 0.09 (7)	-0.28 $\pm$ 0.19 (1)	0.46 $\pm$ 0.19 (1)	0.74 $\pm$ 0.13 (2)	0.18 $\pm$ 0.11 (3)
BL304	-0.89 $\pm$ 0.06 (42)	-0.68 $\pm$ 0.12 (4)	0.56 $\pm$ 0.14 (2)	-0.34 $\pm$ 0.08 (8)	-0.57 $\pm$ 0.20 (1)	0.38 $\pm$ 0.20 (1)	0.36 $\pm$ 0.20 (1)	-0.09 $\pm$ 0.16 (2)
BL311	-0.78 $\pm$ 0.06 (34)	-1.00 $\pm$ 0.40 (2)	0.63 $\pm$ 0.34 (1)	-0.25 $\pm$ 0.13 (7)	-0.52 $\pm$ 0.34 (1)	0.85 $\pm$ 0.34 (1)	0.36 $\pm$ 0.24 (2)	-0.17 $\pm$ 0.20 (3)
BL315	-0.82 $\pm$ 0.10 (45)	-0.62 $\pm$ 0.18 (4)	0.66 $\pm$ 0.18 (2)	-0.34 $\pm$ 0.09 (6)	-0.51 $\pm$ 0.21 (1)	0.69 $\pm$ 0.21 (1)	0.49 $\pm$ 0.15 (2)	-0.01 $\pm$ 0.21 (1)
BL323	-0.88 $\pm$ 0.06 (42)	-0.69 $\pm$ 0.19 (3)	0.53 $\pm$ 0.18 (2)	-0.56 $\pm$ 0.14 (8)	-0.48 $\pm$ 0.26 (1)	0.43 $\pm$ 0.26 (1)	0.18 $\pm$ 0.18 (2)	-0.18 $\pm$ 0.15 (3)

**Table 6.A3:** Abundance ratio of the Fornax Field stars, where we list the abundance, its associated error ( $\sigma$ ) and the number of lines used (n). The quoted error is the error on [element/H], not [X/Fe]. Part 2

Star	[Na I/Fe] $\sigma$ n	[Nd II/Fe] $\sigma$ (n)	[Ni I/Fe] $\sigma$ n	[O I/Fe] $\sigma$ (n)	[Si I/Fe] $\sigma$ n	[Ti I/Fe] $\sigma$ (n)	[Ti II/Fe] $\sigma$ n	[Y II/Fe] $\sigma$ (n)
BL038	-0.46 $\pm$ 0.16 (2)	0.22 $\pm$ 0.21 (3)	-0.13 $\pm$ 0.06 (15)	0.34 $\pm$ 0.23 (1)	0.35 $\pm$ 0.17 (4)	-0.16 $\pm$ 0.14 (7)	0.18 $\pm$ 0.13 (3)	0.10 $\pm$ 0.23 (1)
BL045	... $\pm$ ... (0)	-0.06 $\pm$ 0.16 (1)	-0.22 $\pm$ 0.07 (11)	0.22 $\pm$ 0.16 (1)	0.25 $\pm$ 0.24 (2)	-0.23 $\pm$ 0.05 (10)	0.03 $\pm$ 0.12 (4)	... $\pm$ ... (0)
BL052	-0.85 $\pm$ 0.34 (1)	0.22 $\pm$ 0.24 (2)	-0.28 $\pm$ 0.10 (11)	0.28 $\pm$ 0.34 (1)	0.16 $\pm$ 0.34 (1)	-0.37 $\pm$ 0.13 (7)	-0.12 $\pm$ 0.49 (2)	-0.16 $\pm$ 0.34 (1)
BL065	... $\pm$ ... (0)	0.49 $\pm$ 0.18 (1)	-0.15 $\pm$ 0.08 (8)	0.56 $\pm$ 0.18 (1)	0.32 $\pm$ 0.21 (2)	-0.18 $\pm$ 0.08 (7)	0.28 $\pm$ 0.13 (4)	... $\pm$ ... (0)
BL076	-0.67 $\pm$ 0.13 (2)	0.20 $\pm$ 0.15 (3)	-0.26 $\pm$ 0.08 (13)	0.20 $\pm$ 0.19 (1)	-0.16 $\pm$ 0.11 (3)	-0.21 $\pm$ 0.06 (9)	0.09 $\pm$ 0.18 (3)	... $\pm$ ... (0)
BL077	-0.78 $\pm$ 0.15 (1)	0.23 $\pm$ 0.14 (3)	-0.23 $\pm$ 0.06 (14)	0.25 $\pm$ 0.15 (1)	-0.09 $\pm$ 0.11 (2)	-0.38 $\pm$ 0.06 (10)	-0.01 $\pm$ 0.15 (2)	... $\pm$ ... (0)
BL079	-0.70 $\pm$ 0.31 (2)	0.36 $\pm$ 0.25 (3)	-0.24 $\pm$ 0.12 (14)	0.12 $\pm$ 0.44 (1)	-0.18 $\pm$ 0.31 (2)	-0.05 $\pm$ 0.16 (8)	-0.11 $\pm$ 0.45 (2)	0.08 $\pm$ 0.44 (1)
BL081	-0.70 $\pm$ 0.13 (2)	0.21 $\pm$ 0.17 (3)	-0.24 $\pm$ 0.06 (14)	0.14 $\pm$ 0.19 (1)	-0.45 $\pm$ 0.13 (2)	-0.19 $\pm$ 0.07 (10)	-0.05 $\pm$ 0.16 (3)	-0.34 $\pm$ 0.19 (1)
BL084	... $\pm$ ... (0)	0.21 $\pm$ 0.18 (3)	-0.22 $\pm$ 0.07 (13)	0.05 $\pm$ 0.19 (1)	-0.10 $\pm$ 0.24 (2)	-0.38 $\pm$ 0.06 (9)	0.27 $\pm$ 0.23 (2)	-0.40 $\pm$ 0.19 (1)
BL085	... $\pm$ ... (0)	1.53 $\pm$ 0.15 (1)	0.29 $\pm$ 0.15 (4)	... $\pm$ ... (0)	0.84 $\pm$ 0.15 (1)	0.56 $\pm$ 0.15 (1)	0.45 $\pm$ 0.26 (4)	... $\pm$ ... (0)
BL091	-0.47 $\pm$ 0.12 (2)	0.42 $\pm$ 0.10 (3)	-0.09 $\pm$ 0.07 (13)	0.10 $\pm$ 0.17 (1)	-0.07 $\pm$ 0.18 (3)	-0.25 $\pm$ 0.06 (9)	0.27 $\pm$ 0.21 (3)	-0.31 $\pm$ 0.17 (1)
BL092	-0.95 $\pm$ 0.16 (2)	0.30 $\pm$ 0.13 (3)	-0.20 $\pm$ 0.09 (11)	0.14 $\pm$ 0.23 (1)	-0.08 $\pm$ 0.12 (4)	-0.23 $\pm$ 0.09 (9)	0.33 $\pm$ 0.20 (3)	0.20 $\pm$ 0.23 (1)
BL096	-0.77 $\pm$ 0.18 (2)	0.27 $\pm$ 0.21 (3)	-0.29 $\pm$ 0.08 (12)	0.34 $\pm$ 0.25 (1)	-0.07 $\pm$ 0.18 (2)	-0.19 $\pm$ 0.09 (8)	0.10 $\pm$ 0.14 (3)	-0.32 $\pm$ 0.25 (1)
BL097	-0.63 $\pm$ 0.12 (2)	0.30 $\pm$ 0.10 (3)	-0.10 $\pm$ 0.07 (16)	0.28 $\pm$ 0.17 (1)	-0.08 $\pm$ 0.13 (3)	-0.19 $\pm$ 0.05 (10)	0.21 $\pm$ 0.11 (3)	-0.06 $\pm$ 0.17 (1)
BL100	... $\pm$ ... (0)	0.30 $\pm$ 0.18 (2)	-0.27 $\pm$ 0.07 (15)	0.16 $\pm$ 0.19 (1)	-0.08 $\pm$ 0.16 (2)	-0.41 $\pm$ 0.07 (8)	0.30 $\pm$ 0.21 (2)	-0.41 $\pm$ 0.19 (1)
BL104	-0.79 $\pm$ 0.21 (1)	0.34 $\pm$ 0.13 (3)	-0.15 $\pm$ 0.07 (12)	0.37 $\pm$ 0.21 (1)	0.48 $\pm$ 0.23 (3)	-0.13 $\pm$ 0.07 (9)	0.21 $\pm$ 0.12 (3)	0.05 $\pm$ 0.21 (1)
BL113	-0.36 $\pm$ 0.15 (2)	0.25 $\pm$ 0.18 (3)	-0.24 $\pm$ 0.06 (12)	-0.05 $\pm$ 0.21 (1)	0.00 $\pm$ 0.10 (4)	-0.18 $\pm$ 0.08 (7)	0.24 $\pm$ 0.18 (3)	-0.19 $\pm$ 0.21 (1)
BL115	... $\pm$ ... (0)	0.48 $\pm$ 0.16 (1)	-0.12 $\pm$ 0.07 (10)	... $\pm$ ... (0)	0.00 $\pm$ 0.16 (1)	-0.25 $\pm$ 0.08 (8)	0.11 $\pm$ 0.14 (5)	... $\pm$ ... (0)
BL123	-0.74 $\pm$ 0.17 (1)	0.34 $\pm$ 0.12 (3)	-0.16 $\pm$ 0.05 (16)	0.30 $\pm$ 0.17 (1)	0.03 $\pm$ 0.10 (3)	-0.19 $\pm$ 0.06 (9)	-0.10 $\pm$ 0.21 (3)	-0.09 $\pm$ 0.17 (1)
BL125	-0.56 $\pm$ 0.21 (2)	0.39 $\pm$ 0.16 (3)	-0.33 $\pm$ 0.06 (15)	-0.05 $\pm$ 0.25 (1)	-0.15 $\pm$ 0.12 (4)	-0.09 $\pm$ 0.08 (9)	0.36 $\pm$ 0.20 (3)	-0.01 $\pm$ 0.25 (1)
BL132	-0.98 $\pm$ 0.14 (2)	0.14 $\pm$ 0.17 (3)	-0.19 $\pm$ 0.07 (12)	-0.11 $\pm$ 0.14 (2)	0.00 $\pm$ 0.15 (3)	-0.38 $\pm$ 0.08 (7)	0.07 $\pm$ 0.14 (2)	... $\pm$ ... (0)
BL135	-0.51 $\pm$ 0.15 (2)	0.37 $\pm$ 0.17 (3)	-0.05 $\pm$ 0.08 (14)	0.43 $\pm$ 0.21 (1)	0.04 $\pm$ 0.18 (3)	-0.02 $\pm$ 0.07 (9)	0.14 $\pm$ 0.15 (3)	-0.10 $\pm$ 0.21 (1)
BL138	... $\pm$ ... (0)	0.23 $\pm$ 0.17 (3)	-0.10 $\pm$ 0.08 (14)	0.44 $\pm$ 0.17 (1)	0.29 $\pm$ 0.17 (1)	-0.10 $\pm$ 0.06 (8)	0.15 $\pm$ 0.14 (3)	-0.15 $\pm$ 0.17 (1)
BL140	-0.82 $\pm$ 0.18 (1)	0.32 $\pm$ 0.28 (2)	-0.15 $\pm$ 0.08 (14)	0.13 $\pm$ 0.18 (1)	-0.15 $\pm$ 0.10 (3)	-0.24 $\pm$ 0.06 (9)	0.17 $\pm$ 0.13 (2)	0.06 $\pm$ 0.18 (1)
BL141	-0.91 $\pm$ 0.18 (2)	0.25 $\pm$ 0.14 (3)	-0.24 $\pm$ 0.06 (15)	0.03 $\pm$ 0.21 (1)	-0.21 $\pm$ 0.16 (2)	-0.38 $\pm$ 0.07 (9)	-0.08 $\pm$ 0.09 (5)	-0.45 $\pm$ 0.21 (1)
BL146	-0.72 $\pm$ 0.11 (2)	0.27 $\pm$ 0.12 (3)	-0.19 $\pm$ 0.06 (13)	0.28 $\pm$ 0.16 (1)	0.04 $\pm$ 0.08 (4)	-0.16 $\pm$ 0.05 (9)	-0.15 $\pm$ 0.16 (1)	-0.08 $\pm$ 0.16 (1)
BL147	-0.40 $\pm$ 0.32 (1)	0.88 $\pm$ 0.23 (3)	-0.34 $\pm$ 0.11 (9)	... $\pm$ ... (0)	0.10 $\pm$ 0.18 (3)	-0.32 $\pm$ 0.12 (7)	0.60 $\pm$ 0.27 (3)	-0.04 $\pm$ 0.32 (1)
BL148	-0.47 $\pm$ 0.23 (2)	0.73 $\pm$ 0.27 (3)	-0.16 $\pm$ 0.09 (14)	0.44 $\pm$ 0.33 (1)	0.03 $\pm$ 0.23 (3)	0.06 $\pm$ 0.13 (6)	-0.19 $\pm$ 0.20 (4)	-0.19 $\pm$ 0.33 (1)
BL149	-0.55 $\pm$ 0.25 (1)	0.05 $\pm$ 0.25 (1)	-0.26 $\pm$ 0.08 (13)	0.16 $\pm$ 0.25 (1)	0.23 $\pm$ 0.17 (4)	-0.40 $\pm$ 0.09 (8)	0.41 $\pm$ 0.14 (3)	0.03 $\pm$ 0.25 (1)
BL150	-0.60 $\pm$ 0.16 (2)	0.41 $\pm$ 0.20 (3)	-0.22 $\pm$ 0.11 (12)	0.05 $\pm$ 0.22 (1)	0.04 $\pm$ 0.13 (3)	-0.15 $\pm$ 0.08 (8)	0.02 $\pm$ 0.17 (4)	... $\pm$ ... (0)
BL151	-0.64 $\pm$ 0.13 (2)	0.31 $\pm$ 0.13 (3)	-0.20 $\pm$ 0.06 (11)	-0.04 $\pm$ 0.21 (2)	-0.02 $\pm$ 0.20 (2)	-0.12 $\pm$ 0.06 (9)	0.26 $\pm$ 0.12 (4)	... $\pm$ ... (0)
BL155	-0.57 $\pm$ 0.16 (2)	0.64 $\pm$ 0.31 (3)	-0.12 $\pm$ 0.09 (15)	0.27 $\pm$ 0.22 (1)	-0.06 $\pm$ 0.13 (3)	-0.07 $\pm$ 0.10 (10)	0.15 $\pm$ 0.13 (4)	0.16 $\pm$ 0.22 (1)
BL156	... $\pm$ ... (0)	0.35 $\pm$ 0.33 (2)	-0.11 $\pm$ 0.08 (11)	... $\pm$ ... (0)	0.04 $\pm$ 0.12 (3)	-0.43 $\pm$ 0.07 (8)	0.33 $\pm$ 0.20 (2)	... $\pm$ ... (0)
BL158	-0.60 $\pm$ 0.16 (2)	0.51 $\pm$ 0.27 (3)	-0.15 $\pm$ 0.08 (12)	0.17 $\pm$ 0.16 (2)	0.07 $\pm$ 0.12 (4)	-0.40 $\pm$ 0.08 (11)	0.35 $\pm$ 0.12 (4)	-0.13 $\pm$ 0.23 (1)
BL160	-0.67 $\pm$ 0.15 (1)	0.46 $\pm$ 0.11 (3)	-0.19 $\pm$ 0.06 (16)	... $\pm$ ... (0)	0.01 $\pm$ 0.09 (4)	-0.11 $\pm$ 0.06 (8)	0.31 $\pm$ 0.16 (2)	-0.05 $\pm$ 0.15 (1)
BL163	-0.46 $\pm$ 0.14 (2)	0.50 $\pm$ 0.14 (3)	-0.13 $\pm$ 0.06 (12)	0.28 $\pm$ 0.20 (1)	-0.18 $\pm$ 0.14 (2)	-0.05 $\pm$ 0.15 (8)	0.45 $\pm$ 0.21 (3)	0.01 $\pm$ 0.20 (1)
BL166	-0.57 $\pm$ 0.16 (2)	0.49 $\pm$ 0.13 (3)	-0.18 $\pm$ 0.07 (13)	0.17 $\pm$ 0.22 (1)	-0.08 $\pm$ 0.18 (3)	-0.11 $\pm$ 0.07 (10)	0.28 $\pm$ 0.23 (3)	0.00 $\pm$ 0.22 (1)
BL168	-0.47 $\pm$ 0.18 (1)	0.29 $\pm$ 0.11 (3)	-0.16 $\pm$ 0.06 (13)	0.17 $\pm$ 0.18 (1)	-0.02 $\pm$ 0.20 (3)	0.00 $\pm$ 0.06 (8)	0.01 $\pm$ 0.10 (3)	-0.32 $\pm$ 0.18 (1)
BL171	... $\pm$ ... (0)	0.30 $\pm$ 0.22 (3)	-0.20 $\pm$ 0.07 (14)	0.30 $\pm$ 0.18 (1)	... $\pm$ ... (0)	-0.23 $\pm$ 0.07 (8)	0.37 $\pm$ 0.17 (3)	-0.25 $\pm$ 0.18 (1)
BL173	-0.61 $\pm$ 0.15 (2)	0.46 $\pm$ 0.25 (3)	-0.14 $\pm$ 0.08 (13)	0.65 $\pm$ 0.21 (1)	0.18 $\pm$ 0.21 (1)	-0.19 $\pm$ 0.07 (9)	0.40 $\pm$ 0.19 (4)	-0.21 $\pm$ 0.21 (1)
BL180	-0.50 $\pm$ 0.24 (2)	0.65 $\pm$ 0.24 (2)	-0.27 $\pm$ 0.09 (13)	0.17 $\pm$ 0.34 (1)	0.06 $\pm$ 0.20 (3)	-0.18 $\pm$ 0.11 (9)	-0.01 $\pm$ 0.22 (4)	0.22 $\pm$ 0.34 (1)
BL185	-0.49 $\pm$ 0.16 (2)	0.41 $\pm$ 0.21 (2)	-0.24 $\pm$ 0.09 (16)	0.13 $\pm$ 0.22 (1)	-0.02 $\pm$ 0.11 (4)	-0.08 $\pm$ 0.08 (10)	0.01 $\pm$ 0.11 (4)	-0.12 $\pm$ 0.22 (1)

*Continued on next page*

Star	[Na I/Fe] $\sigma$ n	[Nd II/Fe] $\sigma$ (n)	[Ni I/Fe] $\sigma$ n	[O I/Fe] $\sigma$ (n)	[Si I/Fe] $\sigma$ n	[Ti I/Fe] $\sigma$ (n)	[Ti II/Fe] $\sigma$ n	[Y II/Fe] $\sigma$ (n)
BL190	... $\pm$ ... (0)	0.27 $\pm$ 0.31 (2)	-0.31 $\pm$ 0.07 (11)	0.09 $\pm$ 0.18 (1)	-0.22 $\pm$ 0.16 (2)	-0.40 $\pm$ 0.06 (9)	0.11 $\pm$ 0.14 (3)	-0.50 $\pm$ 0.23 (1)
BL195	-0.61 $\pm$ 0.13 (2)	0.03 $\pm$ 0.14 (3)	-0.21 $\pm$ 0.07 (8)	0.10 $\pm$ 0.19 (1)	-0.02 $\pm$ 0.16 (3)	-0.17 $\pm$ 0.06 (9)	0.23 $\pm$ 0.15 (4)	... $\pm$ ... (0)
BL196	-0.94 $\pm$ 0.18 (1)	0.31 $\pm$ 0.10 (3)	-0.27 $\pm$ 0.06 (11)	... $\pm$ ... (0)	0.03 $\pm$ 0.18 (1)	-0.28 $\pm$ 0.06 (9)	-0.04 $\pm$ 0.14 (5)	-0.05 $\pm$ 0.18 (1)
BL197	-0.70 $\pm$ 0.17 (2)	0.24 $\pm$ 0.17 (2)	-0.16 $\pm$ 0.07 (13)	0.19 $\pm$ 0.24 (1)	-0.03 $\pm$ 0.17 (2)	-0.30 $\pm$ 0.09 (7)	0.32 $\pm$ 0.28 (3)	0.13 $\pm$ 0.24 (1)
BL203	-0.56 $\pm$ 0.19 (2)	0.30 $\pm$ 0.27 (2)	-0.21 $\pm$ 0.08 (14)	0.13 $\pm$ 0.27 (1)	-0.05 $\pm$ 0.24 (3)	-0.19 $\pm$ 0.09 (9)	0.23 $\pm$ 0.32 (2)	-0.28 $\pm$ 0.27 (1)
BL204	-0.48 $\pm$ 0.34 (1)	0.60 $\pm$ 0.34 (1)	-0.24 $\pm$ 0.11 (9)	0.40 $\pm$ 0.34 (1)	0.11 $\pm$ 0.34 (1)	0.01 $\pm$ 0.12 (8)	0.36 $\pm$ 0.44 (3)	-0.20 $\pm$ 0.34 (1)
BL205	-0.48 $\pm$ 0.13 (2)	0.42 $\pm$ 0.30 (2)	-0.23 $\pm$ 0.06 (14)	... $\pm$ ... (0)	-0.02 $\pm$ 0.13 (5)	-0.20 $\pm$ 0.10 (9)	0.17 $\pm$ 0.12 (4)	-0.14 $\pm$ 0.19 (1)
BL208	-0.55 $\pm$ 0.16 (2)	0.36 $\pm$ 0.14 (3)	-0.31 $\pm$ 0.06 (16)	0.15 $\pm$ 0.22 (1)	-0.16 $\pm$ 0.14 (4)	-0.13 $\pm$ 0.07 (9)	0.05 $\pm$ 0.29 (2)	-0.54 $\pm$ 0.22 (1)
BL210	-0.60 $\pm$ 0.15 (2)	0.50 $\pm$ 0.12 (3)	-0.12 $\pm$ 0.07 (13)	0.16 $\pm$ 0.21 (1)	-0.20 $\pm$ 0.19 (3)	-0.19 $\pm$ 0.08 (10)	0.16 $\pm$ 0.13 (3)	-0.08 $\pm$ 0.21 (1)
BL211	-0.60 $\pm$ 0.16 (2)	0.32 $\pm$ 0.13 (3)	-0.17 $\pm$ 0.07 (16)	0.15 $\pm$ 0.22 (1)	0.38 $\pm$ 0.26 (4)	-0.03 $\pm$ 0.08 (8)	0.08 $\pm$ 0.19 (3)	0.04 $\pm$ 0.22 (1)
BL213	-0.67 $\pm$ 0.21 (1)	0.36 $\pm$ 0.15 (2)	-0.25 $\pm$ 0.06 (15)	0.29 $\pm$ 0.21 (1)	0.01 $\pm$ 0.10 (5)	-0.14 $\pm$ 0.07 (9)	-0.03 $\pm$ 0.17 (4)	0.15 $\pm$ 0.21 (1)
BL216	-0.52 $\pm$ 0.18 (2)	0.36 $\pm$ 0.14 (3)	-0.10 $\pm$ 0.08 (14)	0.24 $\pm$ 0.25 (1)	-0.10 $\pm$ 0.14 (3)	-0.02 $\pm$ 0.10 (6)	-0.10 $\pm$ 0.20 (4)	0.06 $\pm$ 0.25 (1)
BL218	-0.81 $\pm$ 0.18 (2)	0.26 $\pm$ 0.15 (3)	-0.19 $\pm$ 0.08 (16)	0.09 $\pm$ 0.26 (1)	-0.08 $\pm$ 0.26 (2)	-0.15 $\pm$ 0.09 (8)	-0.38 $\pm$ 0.13 (4)	-0.05 $\pm$ 0.26 (1)
BL221	-0.87 $\pm$ 0.21 (1)	0.51 $\pm$ 0.21 (2)	-0.25 $\pm$ 0.07 (15)	0.16 $\pm$ 0.21 (1)	-0.13 $\pm$ 0.15 (2)	-0.26 $\pm$ 0.07 (9)	0.47 $\pm$ 0.18 (3)	-0.06 $\pm$ 0.21 (1)
BL227	-0.46 $\pm$ 0.18 (2)	0.44 $\pm$ 0.31 (3)	-0.19 $\pm$ 0.07 (12)	0.29 $\pm$ 0.25 (1)	0.16 $\pm$ 0.10 (6)	-0.12 $\pm$ 0.09 (8)	0.23 $\pm$ 0.26 (2)	0.19 $\pm$ 0.25 (1)
BL228	-0.86 $\pm$ 0.11 (2)	0.41 $\pm$ 0.16 (1)	-0.25 $\pm$ 0.07 (14)	0.22 $\pm$ 0.16 (1)	-0.05 $\pm$ 0.12 (3)	-0.19 $\pm$ 0.05 (9)	0.16 $\pm$ 0.20 (3)	-0.30 $\pm$ 0.17 (1)
BL229	-0.71 $\pm$ 0.17 (2)	0.40 $\pm$ 0.17 (3)	-0.27 $\pm$ 0.09 (14)	0.24 $\pm$ 0.24 (1)	-0.03 $\pm$ 0.10 (6)	-0.24 $\pm$ 0.09 (7)	0.05 $\pm$ 0.12 (4)	-0.46 $\pm$ 0.24 (1)
BL233	-0.56 $\pm$ 0.16 (2)	0.25 $\pm$ 0.13 (3)	-0.24 $\pm$ 0.08 (15)	-0.01 $\pm$ 0.22 (1)	-0.18 $\pm$ 0.12 (4)	-0.21 $\pm$ 0.07 (9)	0.19 $\pm$ 0.13 (4)	0.11 $\pm$ 0.22 (1)
BL239	-0.74 $\pm$ 0.22 (1)	0.14 $\pm$ 0.13 (3)	-0.22 $\pm$ 0.08 (14)	0.11 $\pm$ 0.22 (1)	-0.21 $\pm$ 0.13 (3)	-0.29 $\pm$ 0.07 (9)	-0.08 $\pm$ 0.27 (2)	... $\pm$ ... (0)
BL242	-0.65 $\pm$ 0.21 (1)	0.32 $\pm$ 0.33 (2)	-0.13 $\pm$ 0.06 (13)	0.19 $\pm$ 0.15 (2)	0.09 $\pm$ 0.15 (2)	-0.23 $\pm$ 0.07 (8)	0.16 $\pm$ 0.24 (3)	-0.07 $\pm$ 0.21 (1)
BL247	-0.56 $\pm$ 0.11 (2)	0.94 $\pm$ 0.13 (2)	-0.07 $\pm$ 0.08 (15)	0.23 $\pm$ 0.15 (1)	0.15 $\pm$ 0.18 (2)	-0.23 $\pm$ 0.09 (10)	0.18 $\pm$ 0.17 (4)	0.43 $\pm$ 0.15 (1)
BL250	-0.37 $\pm$ 0.18 (2)	0.39 $\pm$ 0.23 (3)	-0.16 $\pm$ 0.10 (14)	0.05 $\pm$ 0.21 (2)	0.18 $\pm$ 0.18 (3)	-0.04 $\pm$ 0.11 (9)	-0.25 $\pm$ 0.18 (2)	-0.12 $\pm$ 0.26 (1)
BL253	-0.58 $\pm$ 0.14 (2)	0.36 $\pm$ 0.20 (3)	-0.19 $\pm$ 0.07 (17)	0.15 $\pm$ 0.20 (1)	-0.13 $\pm$ 0.11 (4)	-0.21 $\pm$ 0.08 (7)	-0.05 $\pm$ 0.12 (4)	-0.17 $\pm$ 0.20 (1)
BL257	-0.73 $\pm$ 0.17 (2)	0.31 $\pm$ 0.14 (3)	-0.20 $\pm$ 0.07 (15)	0.17 $\pm$ 0.24 (1)	-0.03 $\pm$ 0.14 (5)	-0.19 $\pm$ 0.11 (9)	0.03 $\pm$ 0.23 (3)	0.04 $\pm$ 0.24 (1)
BL258	-0.66 $\pm$ 0.16 (2)	0.50 $\pm$ 0.33 (3)	-0.20 $\pm$ 0.07 (15)	0.03 $\pm$ 0.23 (1)	-0.20 $\pm$ 0.18 (3)	-0.22 $\pm$ 0.11 (9)	0.16 $\pm$ 0.18 (4)	0.10 $\pm$ 0.23 (1)
BL260	-0.80 $\pm$ 0.19 (1)	0.36 $\pm$ 0.15 (3)	-0.26 $\pm$ 0.07 (12)	0.25 $\pm$ 0.19 (1)	0.30 $\pm$ 0.28 (3)	-0.19 $\pm$ 0.08 (8)	-0.06 $\pm$ 0.10 (4)	-0.21 $\pm$ 0.19 (1)
BL261	-0.78 $\pm$ 0.15 (2)	0.45 $\pm$ 0.12 (3)	-0.28 $\pm$ 0.10 (12)	-0.02 $\pm$ 0.21 (1)	-0.39 $\pm$ 0.21 (1)	-0.27 $\pm$ 0.07 (9)	0.11 $\pm$ 0.09 (5)	-0.03 $\pm$ 0.21 (1)
BL262	-0.93 $\pm$ 0.27 (1)	0.26 $\pm$ 0.26 (2)	-0.26 $\pm$ 0.08 (13)	0.11 $\pm$ 0.27 (1)	-0.13 $\pm$ 0.16 (3)	-0.12 $\pm$ 0.09 (9)	0.11 $\pm$ 0.30 (2)	... $\pm$ ... (0)
BL266	... $\pm$ ... (0)	... $\pm$ ... (0)	-0.18 $\pm$ 0.07 (10)	0.38 $\pm$ 0.20 (1)	0.39 $\pm$ 0.20 (1)	-0.13 $\pm$ 0.08 (9)	0.50 $\pm$ 0.12 (4)	0.07 $\pm$ 0.20 (1)
BL267	-0.43 $\pm$ 0.14 (2)	0.12 $\pm$ 0.23 (3)	-0.19 $\pm$ 0.09 (14)	0.18 $\pm$ 0.20 (1)	-0.10 $\pm$ 0.10 (7)	-0.16 $\pm$ 0.07 (8)	0.31 $\pm$ 0.13 (4)	-0.06 $\pm$ 0.20 (1)
BL269	-0.62 $\pm$ 0.20 (2)	0.27 $\pm$ 0.21 (3)	-0.22 $\pm$ 0.10 (15)	0.27 $\pm$ 0.28 (1)	0.27 $\pm$ 0.20 (4)	-0.13 $\pm$ 0.10 (10)	0.05 $\pm$ 0.31 (3)	-0.25 $\pm$ 0.28 (1)
BL278	-0.17 $\pm$ 0.18 (2)	0.50 $\pm$ 0.14 (3)	-0.13 $\pm$ 0.07 (14)	0.16 $\pm$ 0.25 (1)	-0.04 $\pm$ 0.12 (4)	0.16 $\pm$ 0.08 (9)	0.10 $\pm$ 0.12 (4)	0.10 $\pm$ 0.25 (1)
BL279	0.04 $\pm$ 0.21 (1)	0.66 $\pm$ 0.21 (1)	-0.03 $\pm$ 0.10 (12)	... $\pm$ ... (0)	0.34 $\pm$ 0.12 (3)	-0.23 $\pm$ 0.13 (5)	0.67 $\pm$ 0.14 (4)	... $\pm$ ... (0)
BL295	-0.50 $\pm$ 0.18 (2)	0.32 $\pm$ 0.21 (3)	-0.19 $\pm$ 0.07 (15)	-0.09 $\pm$ 0.25 (1)	0.04 $\pm$ 0.32 (3)	-0.10 $\pm$ 0.08 (9)	0.21 $\pm$ 0.29 (3)	0.08 $\pm$ 0.25 (1)
BL300	-0.47 $\pm$ 0.13 (2)	0.49 $\pm$ 0.11 (3)	-0.22 $\pm$ 0.07 (14)	0.18 $\pm$ 0.19 (1)	-0.02 $\pm$ 0.11 (3)	-0.04 $\pm$ 0.07 (8)	0.09 $\pm$ 0.12 (5)	-0.03 $\pm$ 0.19 (1)
BL304	-0.79 $\pm$ 0.14 (2)	0.21 $\pm$ 0.12 (3)	-0.19 $\pm$ 0.08 (14)	0.23 $\pm$ 0.20 (1)	0.11 $\pm$ 0.14 (2)	-0.27 $\pm$ 0.10 (9)	-0.12 $\pm$ 0.14 (3)	-0.33 $\pm$ 0.20 (1)
BL311	-0.68 $\pm$ 0.24 (2)	0.02 $\pm$ 0.34 (1)	-0.16 $\pm$ 0.10 (12)	0.15 $\pm$ 0.34 (1)	-0.12 $\pm$ 0.15 (5)	-0.33 $\pm$ 0.11 (9)	0.47 $\pm$ 0.42 (3)	0.24 $\pm$ 0.34 (1)
BL315	-0.85 $\pm$ 0.21 (1)	0.34 $\pm$ 0.21 (1)	-0.32 $\pm$ 0.11 (15)	0.29 $\pm$ 0.21 (1)	-0.04 $\pm$ 0.11 (6)	-0.33 $\pm$ 0.07 (9)	0.33 $\pm$ 0.14 (4)	... $\pm$ ... (0)
BL323	-0.76 $\pm$ 0.26 (1)	0.16 $\pm$ 0.26 (2)	-0.23 $\pm$ 0.08 (15)	0.26 $\pm$ 0.26 (1)	0.12 $\pm$ 0.18 (2)	-0.34 $\pm$ 0.09 (8)	0.07 $\pm$ 0.17 (3)	0.06 $\pm$ 0.26 (1)

